STABILITY AND CONTROL EVALUATION OF THE PILATUS "HELI-PORTER" MODEL PC-6 / 350 AIRPLANE

LT. MARTIN L. McCULLOUGH, USN
LT. MAURICE H. MANAHAN, USN

DEPARTMENT OF AEROSPACE AND MECHANICAL SCIENCES
PRINCETON UNIVERSITY

STABILITY AND CONTROL EVALUATION OF THE PILATUS "HELI-PORTER" MODEL PC-6/350 AIRPLANE

by

Lt. Martin L. McCullough, USN

Lt. Maurice H. Manahan, USN

Department of Aerospace and Mechanical Sciences

Report No. 779

Submitted in partial fulfillment of the requirements for the Degree of Master of Science in Engineering from Princeton University, June 1966.

ACKNOWLEDGEMENTS

The authors wish to express their appreciation and gratitude to Mr. Thomas E. Sweeney for his guidance and supervision during this investigation.

We are indebted to the United States Navy for providing this opportunity for post graduate study and to the Fairchild Hiller Corporation for furnishing the test aircraft.

Further appreciation is extended to the hangar staff, especially to Messrs. G. Reinecke and S. A. Weissenburger, for their cooperation and assistance in installing the test instrumentation and for providing excellent maintenance of the test aircraft.

The authors also wish to thank Mr. Andrew Rostas of the Forrestal Center Photo Laboratory for his rapid processing of the flight test films.

A special thanks to Mrs. Grace Arnesen who typed this manuscript.

TABLE OF CONTENTS

LIST OF TABLES

LIST OF FIGURES

LIST OF FIGURES (continued)

LIST OF FIGURES (continued)

LIST OF SYMBOLS

Capital Letters

AR	Aspect ratio
Bhp	Brake horsepower, hp.
CAS	Calibrated airspeed, mph
C_D	Drag coefficient
C_h	Hinge moment coefficient
C_{h_α}	$(d C_h / d \alpha)_\delta$
$C_{h_{\dot{\delta}}}$	$(d C_h / d \delta)_\alpha$
C_{l_p}	Rolling moment damping derivative
$C_{l_{\delta_a}}$	Rolling moment derivative due to aileron deflection
C_L	Lift coefficient
C_m	Pitching moment coefficient
C_{N_A}	Normal force coefficient
dC_m / dC_L	Static margin
D_p	Propeller diameter, ft.
F_s	Stick force, lbs.
IAS	Indicated airspeed, mph
K	Aileron multipling factor
K_f	Fuselage emperical factor
L_f	Fuselage overall length, ft.
M.A.C.	Mean aerodynamic chord, ft.
N	Number of propellers
N_m	Stick-fixed maneuver point, % MAC
N_m'	Stick-free maneuver point, % MAC

LIST OF SYMBOLS (continued)

N_o	Stick-fixed neutral point, % MAC
N_o'	Stick-free neutral point, % MAC
S	Area, sq. ft.
T_c	Thrust coefficient
V	Velocity, fps
$\overline{V}$	Tail volume
W	Weight, lbs.

Small Letters

a	Lift curve slope, per deg. or rad.
a.c.	Aerodynamic center
b	Span, ft.
c	Chord, ft.
c.g.	Center of gravity
e	Oswald efficiency factor
g	Acceleration of gravity, ft./sec.^{2}
h	Height of thrust line above c.g., ft.
l_p	Horizontal distance from c.g. to propeller, ft.
l_t	Horizontal distance from c.g. to tail a.c., ft.
n	Normal load factor
p	Roll rate, degs. per sec.
r	Tip plate correction factor
w_f	Maximum width of fuselage, ft.
x_a	Horizontal distance from c.g. to wing a.c., ft.
$x_{c.g.}$	Horizontal distance from MAC leading edge to c.g., ft.
z_a	Vertical distance from c.g. to wing a.c., ft.

LIST OF SYMBOLS (continued)

Subscripts

a	Ailerons
a.c.	Aerodynamic center
c.g.	Center of gravity
e	Elevator
f	Fuselage
o	Two dimensional
p	Propeller
t	Tail
s	Stick
w	Wing

Greek Symbols

α	Angle of attack, degs. or rads.
δ	Control deflections, degs.
$\frac{d\beta}{d\alpha}$	Wing upwash derivative, rads.
$\frac{d\epsilon}{d\alpha}$	Wing downwash derivative, rads.
$\frac{d\epsilon_p}{d\alpha}$	Propeller downwash derivative, rads.
η_p	Propeller efficiency
η_t	Tail efficiency
ρ	Density, slugs/cu. ft.
τ	Relative control effectiveness

STABILITY AND CONTROL EVALUATION OF THE PILATUS "HELI-PORTER" MODEL PC-6/350 AIRPLANE

SUMMARY

An analysis of the static longitudinal and maneuvering stability and lateral controllability characteristics of the Pilatus "Heli-Porter" Model PC-6/350-H-1 Airplane was conducted during the months of February, March, and April of 1966. This analysis was conducted at the Forrestal Airport, Princeton, New Jersey by graduate students of the Department of Aerospace and Mechanical Sciences of Princeton University.

The "Heli-Porter" was tested at 8,000 feet in the cruise and approach configurations both for power-on and power-off conditions to determine its stick fixed and stick free static stability characteristics. The maneuvering stability and stick forces per "g" gradient of the aircraft were evaluated for the power-on cruise condition; while its lateral performance was determined for the power-on cruise and approach configurations.

From these evaluations, the "Heli-Porter" was found to have adequate stick fixed and stick free stability in the cruise and approach configurations both for the power-on and the power-off conditions. The aircraft also has excellent roll performance and a high level of maneuvering stability. However, its stick force per "g" and control forces in general are considered to be excessive if prolonged periods of maneuvering flight are anticipated.

It was found that the c.g. limits set by the manufacturer were well forward of any neutral and maneuver points determined during this test. An analytical study was also conducted and showed very close agreement with flight test results.

STABILITY AND CONTROL EVALUATION OF THE PILATUS "HELI-PORTER" MODEL PC-6/350 AIRPLANE

INTRODUCTION

This study is an investigation of the static longitudinal stability, maneuverability, and lateral controllability characteristics of the Pilatus "Heli-Porter" aircraft.

The "Heli-Porter" is an all-purpose small transporter type aircraft with excellent short field take-off and landing (STOL) characteristics. Previous to this investigation, no flight testing had been conducted with the "Heli-Porter" to determine its static longitudinal stability, although, the U. S. Army had conducted flight tests on a turbine powered version of the aircraft to determine its take-off and landing performance. From these tests the Army concluded that the "Turbo-Porter" aircraft had excellent STOL characteristics, but was unsatisfactory for maneuvering flight due to excessive stick forces. This report, Ref. 1, recommended that the aircraft's stick force per "g" and control forces in general be reduced.

In February of 1966 the Department of Aerospace and Mechanical Sciences of Princeton University obtained a "Heli-Porter" aircraft on loan from the Fairchild Hiller Corporation. With the above recommendations in mind, an investigation of the "Heli-Porter's" basic longitudinal stability, stick force gradient, and lateral controllability was undertaken.

The necessary flight test data was gathered to determine the stick fixed and stick free neutral points for both power-on and power-off configurations. These neutral points represent the static longitudinal stability of the aircraft.

The maneuvering stability of the aircraft was evaluated by determination of the stick fixed and stick free maneuver points and the stick force per "g" gradients for the power-on cruise configuration.

The lateral controllability was studied by determining the aircraft's rolling rate and helix angle, $pb/2V$, for varying aileron deflections in the power-on cruise and approach configurations.

The neutral points, maneuver points, and the helix angle were derived analytically for the power-on and power-off cruise configuration. These values were used as checks of the flight test results.

Flight testing began on March 10, 1966 and continued until March 28, 1966.

DESCRIPTION OF EQUIPMENT

TEST AIRCRAFT

The Pilatus "Heli-Porter" is an all-metal, single-engine, strut-braced, high-wing monoplane with a fixed conventional landing gear. It is powered by a LYCOMING IGO-540-A1A engine rated at 325 horsepower at 3000 RPM, driving a full-feathering constant speed 3 bladed HARTZELL propeller. The "Heli-Porter" was designed as an all-purpose small transporter with excellent short field take-off and landing characteristics. It has a maximum authorized gross weight of 4320 pounds and a large center-of-gravity range (11% to 33% M.A.C.).

The "Heli-Porter" has conventional stick and rudder bar controls operating its primary flight control surfaces. Horizontal stabilizer adjustment, rudder trim, and landing flaps are operated by means of hand cranks located in the cockpit. The ailerons are trimmed by means of a bendable fixed trim tab located on the right aileron.

The "Heli-Porter" was manufactured by the Pilatus Aircraft Works, Ltd., of Stans, Switzerland and is owned by the Fairchild Hiller Corporation, Hagerstown, Maryland. Identification photographs, three view drawings, and station diagrams for the aircraft are presented in Figs. 1, 2, and 3. The general aircraft specifications and limitations, found in Tables I and II, were compiled from manuals and reports published by Pilatus and the Fairchild Hiller Corporation.

FLIGHT TEST INSTRUMENTATION

GENERAL

Flight test instrumentation of the "Heli-Porter" was necessary to the extent that the neutral points, the maneuver points, and the rolling performance could be determined. To determine these parameters, it was necessary to measure elevator and aileron deflections, stick forces, normal acceleration, and airspeed. The rudder, horizontal stabilizer, and flaps were also instrumented to observe their floating tendencies.

PHOTO-PANEL

Since there were many variables to be recorded, it became evident at the outset of the investigation that an efficient and accurate recording system was necessary. To record the above variables a photo-panel system was chosen. This system provides permanent records for rechecking and further evaluation of flight test data.

The photo-panel consisted of a display board upon which the flight test remote indicators were mounted. The display board was mounted on a photo-panel box, equipped with an offset lighting system, with the meters facing a rear surfaced mirror. A surplus 16 mm gun camera equipped with a 15 mm wide angle lens was positioned behind the display panel for taking pictures of the reflected meter images. Standard Kodak 16 mm black and white Plus X and Tri X movie film were used. The electrical power for the metering system was obtained from four 6 volt dry cell batteries, delivering ± 12 volts, mounted on the rear of the display board. The camera and photo-panel lighting system were powered from the aircraft's 24 volt d.c. system. Control switches for the power to the meters and camera were located in the cockpit and were operated by the pilot flying the test. In this manner the drain on the ± 12 volt power supply and film waste were minimized.

Mounted on the side of the display board were potentiometers for zeroing and setting the gain of each meter. The photo-panel installation and display board layout can be seen in Fig. 4.

CONTROL DEFLECTIONS

The elevator, aileron, rudder, stabilizer, and flap deflections were measured with OHMITE AB Potentiometers (maximum resistance 3500 ohms) which were mounted on each control surface. The potentiometer locations and mounting brackets can be seen in Fig. 5.

The output of the potentiometers were brought to a common cannon plug located on the side of the photo-panel display board. The outputs were then connected to Simpson microammeters, model 25, having a 50-0-50 amp range. All control surfaces were calibrated for potentiometer output, in microamps, versus control deflections, in degrees. Calibration curves for each control surface can be found in Figs. 9 through 13.

STICK FORCES

In order to measure the control forces, the co-pilot's control stick was replaced by a specially designed force stick. The control forces were measured by means of four Baldwin SR-4 strain gages mounted on a flexing member atop the force stick. The strain gage outputs were fed into a wheatstone bridge whose output was then displayed upon a microammeter. The system received its electrical power from four $22\frac{1}{2}$ volt dry cell batteries connected in parallel. A complete description and wiring diagram of the wheatstone bridge and recording instrumentation can be found in Ref. 2. The output from the force stick was not displayed upon the photo-panel because of a last minute change in the stick's design. Also, due to the manner in which the strain gages were mounted, only forces in two directions, forward and aft, could be measured at one time. Lateral forces could be measured by rotating the force stick 90 degrees. The force stick and recording instrumentation can be seen in Fig. 6. Force stick calibration curves in pounds of stick force versus microamps can be found in Fig. 14.

NORMAL ACCELERATION

The aircraft's normal acceleration was measured by means of a Bourn Model 602A Accelerometer, having a ± 2.5 "g" range. The accelerometer was mounted under the co-pilot's seat, see Fig. 7. It received electrical power from the aircraft's 24 volt d.c. system and its output was displayed upon the photo-panel in microamps. The accelerometer was calibrated in microamps versus normal acceleration from 0 to 1.0 "g". A linear extrapolation from 1.0 to 2.0 "g" was then made. The normal acceleration calibration curve is found in Fig. 15.

STANDARD AIRCRAFT FLIGHT INSTRUMENTS

Standard aircraft instruments were used on the photo-panel to record airspeed, altitude, and rate of climb. The static and dynamic pressure necessary to operate these instruments was obtained directly from the aircraft's pressure system. The aircraft's static and dynamic pressure lines were tapped at a point just forward of the main fuel shut-off valve and were run to the instruments on the photo-panel.

Airspeed calibration was accomplished by the speed-course method which consisted of making timed runs at constant indicated airspeed and pressure altitude over a predetermined distance. Two runs were made in each direction to compensate for the wind and to aid in minimizing of timing errors. Airspeed calibration curves of calibrated airspeed versus indicated airspeed in mph for the cruise and landing configurations are found in Fig. 16.

ANGLES OF SIDESLIP MEASUREMENT

With the idea of investigating a "suspected" rudder lock tendency in the "Heli-Porter," an angle of sideslip measuring boom was constructed and mounted on the starboard wing of the aircraft, Figs. 1 and 8. The angle of sideslip vane received its electrical power from the aircraft's 24 volt system

and a 24 volt a.c. inverter which had been mounted in the aircraft. The system was instrumented for the display of angle of sideslip information upon the photo-panel; but, due to a last minute acceleration in the flight test program, the rudder study could not be conducted.

CENTER OF GRAVITY DETERMINATION

The determination of the c.g. required weighing the aircraft. Since the "Heli-Porter" has a conventional landing gear, it was necessary to level the aircraft (i.e., cabin floor level with the ground) before weighing. The basic weight of the aircraft was considered to be the weight of the aircraft less fuel, but with test instrumentation installed. The c.g. location was calculated by summation of moments and converted to c.g. position in percent M.A.C. This c.g. position was then compared with a c.g. position determined from the weight and balance charts of Ref. 3 for the same aircraft configuration. These two independent calculations of c.g. position were in very close agreement. Therefore, subsequent c.g. positions were determined from the charts in Ref. 3.

Since the flight tests were to be conducted at four different c.g. positions, a maximum c.g. shift, coincident with safe operations, was desired. A c.g. shift of approximately 14% M.A.C., from 16% to 30% M.A.C., was obtained by shifting of pilots, flying at different fuel loads, and carrying ballast. The two forward c.g. positions at 16% M.A.C. and 18% M.A.C., respectively, were achieved by having both pilots in the cockpit, hereafter called station I, and flying with different fuel loads. The most forward c.g. position was obtained by flying the aircraft with a partial fuel load, approximately 25 gallons. A full fuel load placed the c.g. at 18% M.A.C. A 25% M.A.C. c.g. position was achieved by shifting one pilot and two parachutes from station I to the rearmost seats in the cabin, identified hereafter as station IV. The most aft c.g. position, 30% M.A.C., required not only the shifting of one pilot and parachutes, but also the addition of 200 lbs. of ballast at station IV.

The basic weight and balance information is summarized below:

Basic aircraft weight, less fuel, but including test instrumentation	2771 lbs.
Basic aircraft moment	30,190 ft. lbs.
Station I moment arm	9 ft. 10.4 in.
Station IV moment arm	17 ft. 4.0 in.
Fuel moment arm	12 ft. 3.4 in.
Datum to leading edge of wing	9 ft. 10.0 in.
Mean aerodynamic chord	6 ft. 2.8 in.
Basic aircraft c.g.	16.84% M.A.C.

PROCEDURE

NEUTRAL POINTS

The static longitudinal stability of an aircraft is felt by the pilot as the amount of elevator deflection and stick force required to change speed about a trim point. The magnitudes of these elevator deflections and stick forces when expressed as stick fixed and stick free neutral points are a measure of static longitudinal stability. Theoretically, the neutral points can be found by testing at only two c.g. positions. However, for this investigation a total of four c.g. positions were used to minimize experimental error. The neutral points were found for two flight configurations, the cruise configuration and the landing approach configuration. Both configurations were tested with power-on and power-off in order to determine the effects of power on static stability.

The cruise configuration was flown with flaps up at a trim speed of 108 mph. Approximately 60% power was required for level flight at this trim speed at an altitude of 8,000 feet. All power-off flight conditions were flown as near as possible to a zero thrust condition.

The landing approach configuration was flown at an airspeed of 65 mph with flaps full down. The power for this configuration was determined as that necessary for level flight, normally 55-60% rated power, at an altitude of 8,000 feet.

The "Heli-Porter" aircraft uses a variable incidence horizontal tail for trim rather than a conventional trim tab. This difference, however, did not cause any problems in the determination of the static longitudinal stability. As explained in Ref. 4, the pitching moment curve is only shifted and its slope is not changed for variations in the tail lift resulting from changing stabilizer setting.

There are several flight test methods used at the present time to determine the stick fixed and stick free neutral points. The three most commonly used methods are: "Tab Angle" method, "Effective Weight Moment" method, and "Elevator Angle and Stick Force versus Airspeed" method, all of which are described in Ref. 5. For the "Heli-Porter" investigation, the "Elevator Angle and Stick Force versus Airspeed" method was selected. This method is easier to instrument than the "Effective Weight Moment" and requires less flight test data than the "Tab Angle" method.

NEUTRAL POINT: Flight test.

The same flight test procedure was used to determine both power-on and power-off neutral points. After selecting the flight configuration, c.g. position, and power condition, the aircraft was trimmed up hands off at the test airspeed and altitude. Once the power and trim settings were established, neither were changed during the test at that c.g. position. Next, the airspeed was varied a small amount and the aircraft stabilized at the new speed. When steady state conditions had been achieved, the elevator and stick force requirements for the new trim condition were recorded. This process was then repeated over the entire speed range for the configuration being tested. For each c.g. position and flight configuration, data was taken at eight or more steady state airspeeds.

NEUTRAL POINT: Data reduction.

The following analysis was used for each configuration and c.g. position tested. The initial step required correcting and/or putting the recorded data in the proper form by referring to the appropriate calibration curves. The c.g. for each test condition was corrected for varying fuel weight. The fuel weight for each test condition was based upon the average fuel on board during that test run. The fuel quantity on board was computed from recorded fuel flow readings and was compared with fuel added following each day's testing. These total fuel quantities were always within 1-2 gallons.

Elevator angle and stick force were initially plotted against calibrated airspeed, as in Figs. 17, 19, 22, 25, 29, 31, 34, and 37. These plots were against airspeed, rather than lift coefficient, so that a smooth curve could be constructed through more evenly spaced data points. Then more accurate curves of elevator angle and stick force divided by dynamic pressure versus lift coefficient, Figs. 18, 20, 23, 26, 30, 32, 35, and 38, were plotted. Next, slopes of the previous curves were taken at various values of lift coefficient. The values of these slopes, $d\delta_e / dC_L$ and $dF_s / q / dC_L$, were plotted versus percent M.A.C. for individual lift coefficient, Figs. 21, 24, 27, 33, 36, and 39. The stick fixed and stick free neutral points are, by definition, the c.g. locations where $d\delta_e / dC_L$ and $dF_s / q / dC_L$, respectively, go to zero. Therefore, the neutral points for various lift coefficients can be found directly from the above figures. The summaries of the neutral points for the cruise configuration and the approach configuration are found in Figs. 28 and 40.

MANEUVER POINTS

The maneuvering stability is the tendency of an aircraft to return to one "g" flight from a curved flight path where the normal acceleration is greater than one "g". The maneuvering stability of an aircraft is usually expressed in terms of the stick fixed and stick free maneuver points. These maneuver points were obtained by analysis of curves of elevator angle and stick force versus normal acceleration. The stick fixed maneuver point was determined from elevator angle versus normal acceleration data by finding when $d\delta_e / dC_{N_A}$ was equal to zero. The stick free maneuver point was found from stick force versus normal acceleration data when $dF_s / q / dC_{N_A}$ was zero.

There are three flight test methods which can be used to obtain the necessary elevator angle and stick force versus normal acceleration data. These are the "steady pull up," "wind up turn," and the "steady turn." These

methods are described in detail in Ref. 6. For this investigation, the "steady turn" method was selected. This method is a constant acceleration, constant airspeed turn. Since this method is a constant or steady state maneuver, the instrumentation requirements are simpler than in the other two methods. Other advantages of the "steady turn" method over the "steady pull up" technique are less loss of altitude and less flight time required to obtain the data. Also, more accurate stick forces are obtained from steady turn than from the "wind up turn" method.

The maneuver points were only determined for the cruise configuration since maneuvering stability in the landing approach condition is usually of no interest.

MANEUVER POINTS, Flight test.

The maneuver points were determined for the same cruise configuration as used in the neutral point study. The aircraft c.g. position, trim speed, power setting, and altitude were all selected as previously done in the neutral point investigation. Next, the aircraft was trimmed up hands off and no further trim changes were made throughout that test. There can sometimes be differences in the data obtained from right or left hand turns due to gyroscopic effects. However, a preliminary test showed this difference to be small for the "Heli-Porter" and right hand turns were used. After the aircraft was placed in a right hand turn and steady state conditions established, the values of elevator angle, stick force, and normal acceleration were recorded. This data was collected at the trim airspeed. Great care was taken to maintain the same trim airspeed to reduce experimental error.

MANEUVER POINT, Data reduction.

The recorded data was corrected and put in the proper form by referring to the calibration curves, as done in the neutral point studies. The four test c.g. positions were computed in the same manner as in the neutral point study.

The values of elevator angle and stick force versus normal acceleration were then plotted in Figs. 41 and 43. These curves were smoothed and used to draw curves of δ_e and F_s/q versus normal lift coefficients, $C_{N_A} = n\,C_L$, for each c.g. position tested, Figs. 42 and 44. The slopes of these curves were taken and plotted against percent M.A.C. in Fig. 45. The maneuver points were found by inspection of Fig. 45. A summary of the maneuver points, so determined, is presented in Fig. 46.

The stick force per "g" gradients were determined by taking the slopes of the stick force versus normal acceleration curves of Fig. 43. These gradients were evaluated only for the c.g. positions tested and are listed in Table IV.

LATERAL CONTROL

The rolling performance or lateral control of an aircraft is usually specified by its roll rate, p, or its helix angle, $pb/2V$, in radians. The parameter $pb/2V$ must be interpreted carefully for an airplane such as the "Heli-Porter" since b is large while V is small. Along with determining the helix angle, an attempt was made to record lateral forces at different aileron angles. However, due to a malfunction in the camera, no aileron data was collected when the forces were recorded.

The data for the evaluation of the helix angle was taken at three different cruise speeds plus the landing approach configuration. The three cruise speeds tested were 90 mph, 107 mph, and 116 mph; while, the landing approach configuration was flown at 65 mph. The power setting for each trim speed was that necessary for hands off level flight at the test altitude.

LATERAL CONTROL, Flight test.

To determine the amount of aileron available at any speed, two preliminary tests were performed. First, on the ground, the maximum aileron

obtainable for full deflection of the stick was determined. Secondly, the maximum aileron available for the four test speeds were determined to check for any cable or control system losses.

After completing the above tests the roll rate data at each of the trim speeds for varying amounts of aileron was collected. The roll rate was based on the time to roll from 45^{o} right wing down to 45^{o} left wing down. During each roll maneuver an attempt was made to keep the rudder zeroed so that all roll rates would be due to aileron only.

LATERAL CONTROL, Data reduction.

As in the longitudinal case, the recorded data was corrected by use of the appropriate calibration curves. The roll rate, p, was then calculated and plotted versus total aileron deflection in Fig. 47. Entering these curves with the total aileron available at that test speed, the maximum roll rate was determined. Knowing the test speed, maximum roll rate, and wing span, a value of $pb/2V$ for each test speed was calculated. The final results of the lateral investigation are shown as maximum roll rate, $pb/2V$, and total aileron available versus airspeed in Fig. 48.

THEORETICAL ANALYSIS

An analytical investigation of the static longitudinal stability, maneuverability, and lateral controllability of the "Heli-Porter" was performed using the theories and procedures of Ref. 7. The following theoretical values for a 25% M.A.C. c.g. flaps up cruise configuration were determined: the power-on and power-off stick fixed and stick free neutral points; the power-on stick fixed and stick free maneuver points; and the helix angle, $pb/2V$, for power-on level flight conditions. These values were compared to the corresponding results obtained from the flight tests.

The stick fixed neutral point can be expressed as

$$N_o = x_{c.g.} - \left.\frac{dC_m}{dC_L}\right|_{A/C} \tag{1}$$

where $dC_m/dC_L\big|_{A/C}$, the static margin, is found by differentiating the moment equation below by lift coefficient.

$$C_{m_{c.g.}} = C_N \frac{x_a}{c_w} + C_c \frac{z_a}{c_w} + C_{m_{a.c.}} + C_{m_{fuse}} + C_{N_t} \frac{S_t}{S_w} \frac{\ell_t}{c_w} \eta_t + C_{m_{power}} \tag{2}$$

If the above derivative is taken, the static margin for power-on controls fixed can be determined from the following relationship:

$$\left.\frac{dC_m}{dC_L}\right|_{\substack{\text{fixed}\\ \text{power}\\ \text{on}}} = \frac{x_a}{c} + C_{L_w}\left[\frac{2}{\pi e\, AR} - \frac{.035}{a_{w_o}}\right]\frac{z_a}{c_w} + \frac{dC_{m_{a.c.}}}{dC_L}$$

$$+ \frac{K_f W_f^2 L_f}{S_w c_w a_w} - \frac{a_t}{a_w}\bar{V}\left[1 - \frac{d\epsilon}{d\alpha} - \frac{d\epsilon_p}{d\alpha}\right]\eta_t - C_{L_t}\bar{V}\frac{d\eta_t}{dC_L}$$

$$+ \frac{dT_c}{dC_L}\frac{2 D_p^2 h}{S_w c_w} N + \frac{dC_{N_p}}{dC_L}\frac{\ell_p S_p}{S_w c_w} N \tag{3}$$

The power-off stick fixed static margin was found from the following:

$$\left.\frac{dC_m}{dC_L}\right|_{\substack{\text{fixed}\\ \text{power}\\ \text{off}}} = \frac{x_a}{c_w} + C_{L_w}\left[\frac{2}{\pi e\, AR} - \frac{.035}{a_{w_o}}\right]\frac{z_a}{c_w} + \frac{dC_{m_{a.c.}}}{dC_L} + \frac{K_f W_f^2 L_f}{S_w c_w a_w}$$

$$- \frac{a_t}{a_w} V\left[1 - \frac{d\epsilon}{d\alpha}\right]\eta_t + \frac{a_t}{a_w}\frac{\bar{V}\eta_t}{.07}\left(\frac{dC_N}{d\alpha}\right)_{PT_c=0}\left(\frac{d\beta}{d\alpha}\right)$$

$$+ \left(\frac{dC_N}{d\alpha}\right)_{PT_c=0}\frac{d\beta}{d\alpha}\frac{\ell_p S_p}{S_w a_w c_w} \tag{4}$$

A more complete derivation of the above equation can be found in Ref. 7. Once the static margins are determined, the corresponding neutral points are easily found from equation (1).

When the elevator is freed, the fixed stick neutral point is modified by an amount $dC_m / dC_L \Big|_{\text{elevator}}^{\text{free}}$. This term is usually destabilizing and was found from the following equation:

$$\left.\frac{dC_m}{dC_L}\right|_{\text{elevator}}^{\text{free}} = \frac{C_{h_\alpha}\, a_t\, \bar{V}\, \eta_t}{C_{h_\delta}\, a_w} \left[1 - \frac{d\epsilon}{d\alpha}\right] \tag{5}$$

and is greatly affected by the elevator hinge moment parameters, C_{h_α} and C_{h_δ}. The two dimensional hinge moment parameters were found from Ref. 8 and corrected for three dimensional flow effects. Having determined C_{h_α} and C_{h_δ}, the stick free neutral points were found from the following equation:

$$N_o' = N_o - \left.\frac{dC_m}{dC_L}\right|_{\text{elevator}}^{\text{free}} \tag{6}$$

In maneuvering flight the pitching moment is due to both the basic static stability and the curvature of the aircraft's flight path. Therefore, the stick fixed and stick free maneuver points for the power-on cruise configuration are given by:

$$N_m = N_o + \left.\frac{dC_m}{dC_L}\right|_{\text{maneuver}}^{\text{fixed}} \tag{7}$$

$$N_m' = N_o' + \left.\frac{dC_m}{dC_L}\right|_{\text{maneuver}}^{\text{free}} \tag{8}$$

where

$$\left.\frac{dC_m}{dC_L}\right|_{\substack{\text{fixed}\\ \text{maneuver}}} = \frac{-63\, g\, \ell_t\, \rho\, C_{m_\delta}}{2\, \tau_e\, (\frac{w}{S_w})} \left[1 + \frac{1}{n^2}\right] \tag{9}$$

$$\left.\frac{dC_m}{dC_L}\right|_{\substack{\text{free}\\ \text{maneuver}}} = \frac{57.3\, \ell_t\, \rho\, C_{m_\delta}}{2\, (\frac{w}{S_w})\, C_{h_\delta}} \left[C_{h_\alpha} - \frac{1.1\, C_{h_\delta}}{\tau_e}\right] \left[1 + \frac{1}{n^2}\right] \tag{10}$$

The above quantities are the effects of flight path curvature for a steady constant "g" turn.

The lateral control performance parameter $pb/2V$ was found from the equation:

$$\frac{pb}{2V} = \left[\frac{C_{\ell_\delta}}{\tau_a}\right] \frac{\tau_a\, \delta_a{}^{o}\, K}{114.6\, C_{\ell_p}} \tag{11}$$

All calculations and assumptions made in determining the neutral points, maneuver points, and helix angle can be found in Appendix A. The results of this analytical study are presented in Table III. They were based on the following flight conditions:

V = 105 mph = 154 ft/sec

Altitude = 8000 ft

Weight = 3593 lbs

c.g. at 25.2% M.A.C.

Power Condition = 60% Rated Power

n = 1.5 "g"

DISCUSSION OF RESULTS

The results compiled during the flight tests are found in Figs. 28, 40, 46, and 48. For ease of reference, copies of these figures are included in this section of the report. The variations of neutral point with C_L for the various flight configurations tested are shown in Figs. 28 and 40, while similar curves for the maneuver points are shown in Fig. 46. The lateral characteristics of the "Heli-Porter" are shown in Fig. 48.

Table III contains a comparison of the flight test and analytical results for the flight conditions outlined in the theoretical section of this report.

TABLE III

SUMMARY OF FLIGHT TEST AND ANALYTICAL RESULTS

Parameter		Theoretical Results	Flight Test Results
N_o	power-on	.4649	.4790
	power-off	.4963	.4960
N_o'	power-on	.3657	.4060
	power-off	.4119	.4150
N_m	power-on	.6952	.7000
N_m'	power-on	.6814	.5450
$\frac{pb}{2V}$	power-on	.1188	.1201

FIG. 28

NEUTRAL POINT SUMMARY
CRUISE CONFIGURATION

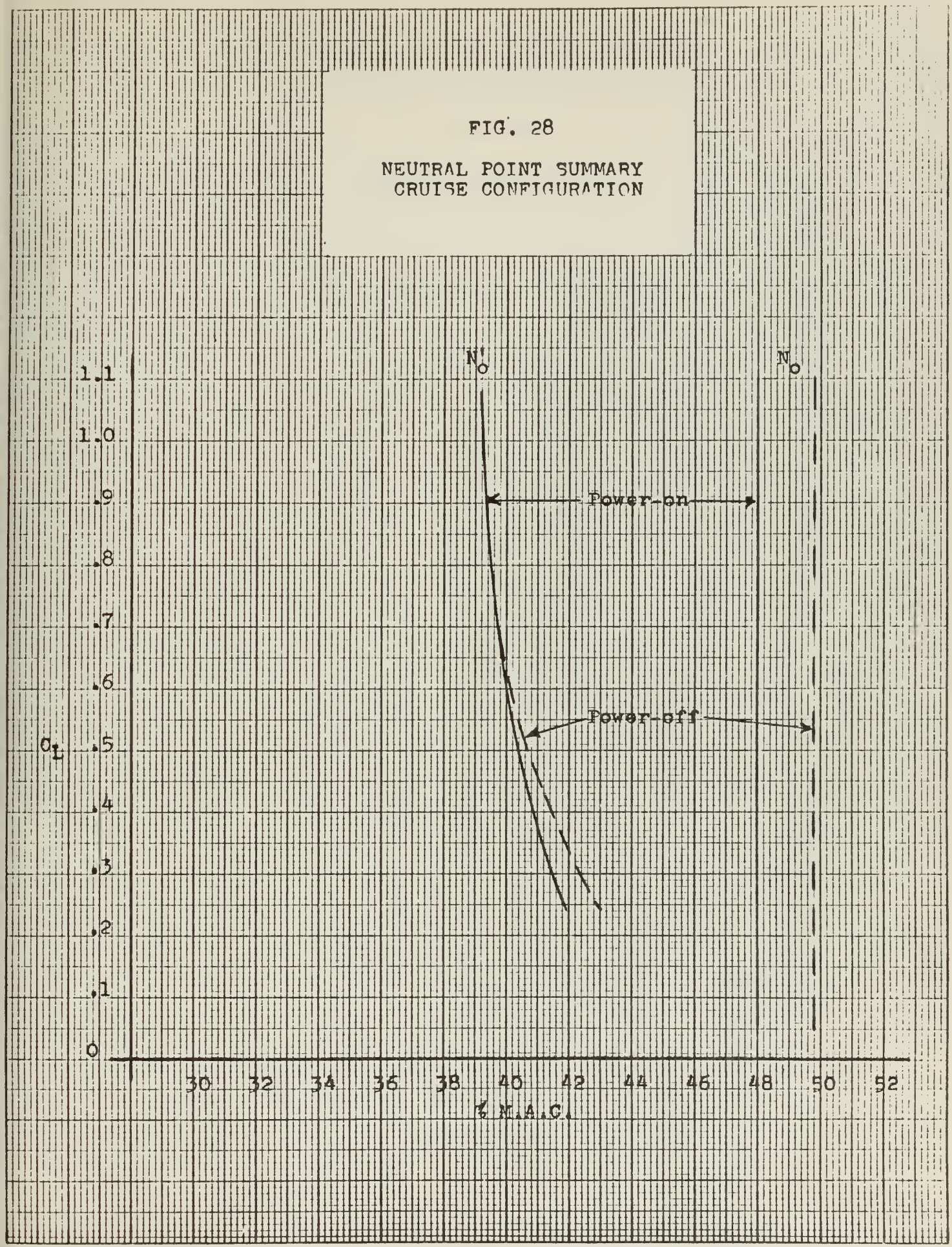

FIG. 40

NEUTRAL POINT SUMMARY
APPROACH CONFIGURATION

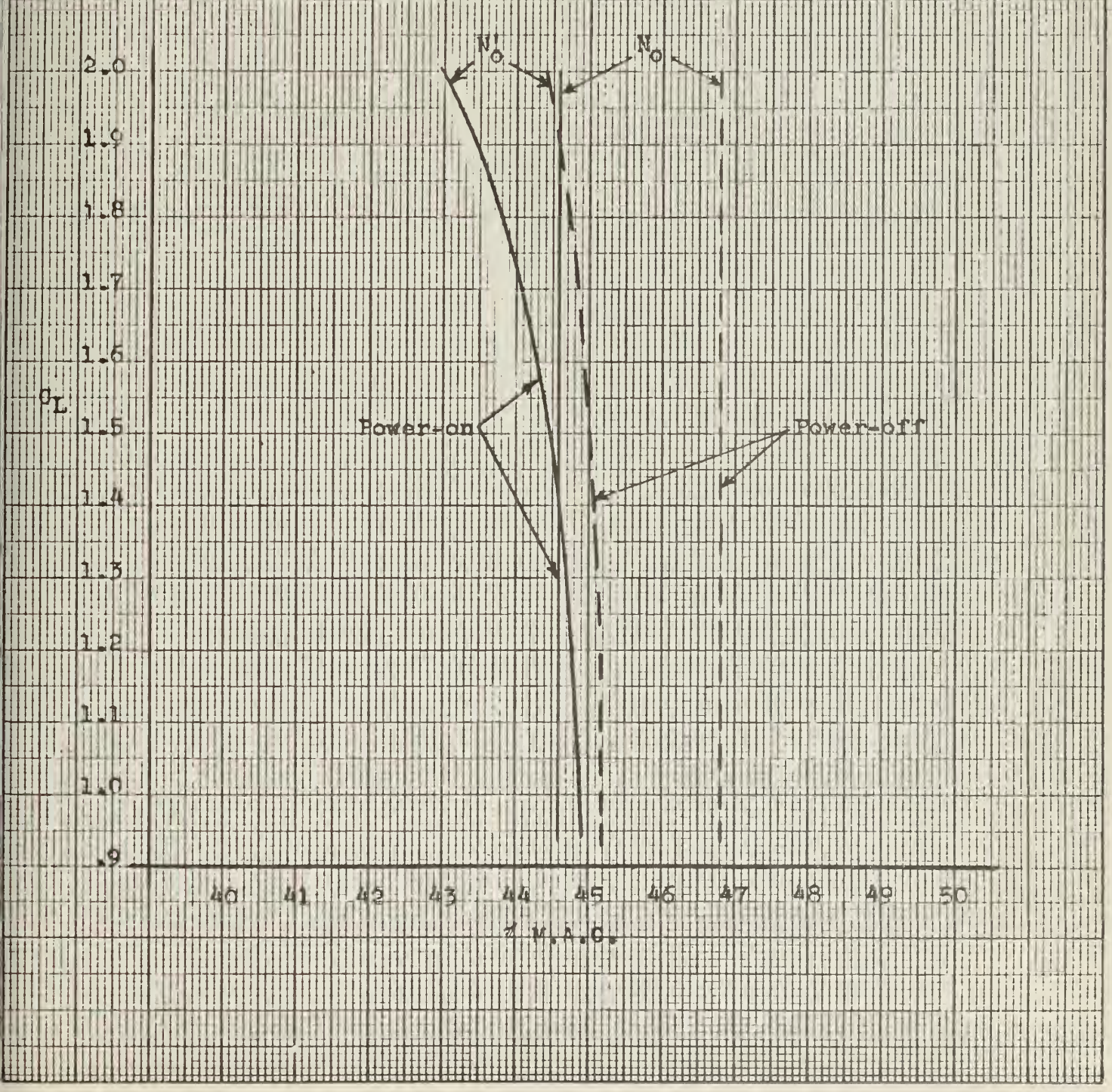

FIG. 46

MANEUVER POINT SUMMARY
CRUISE CONFIGURATION

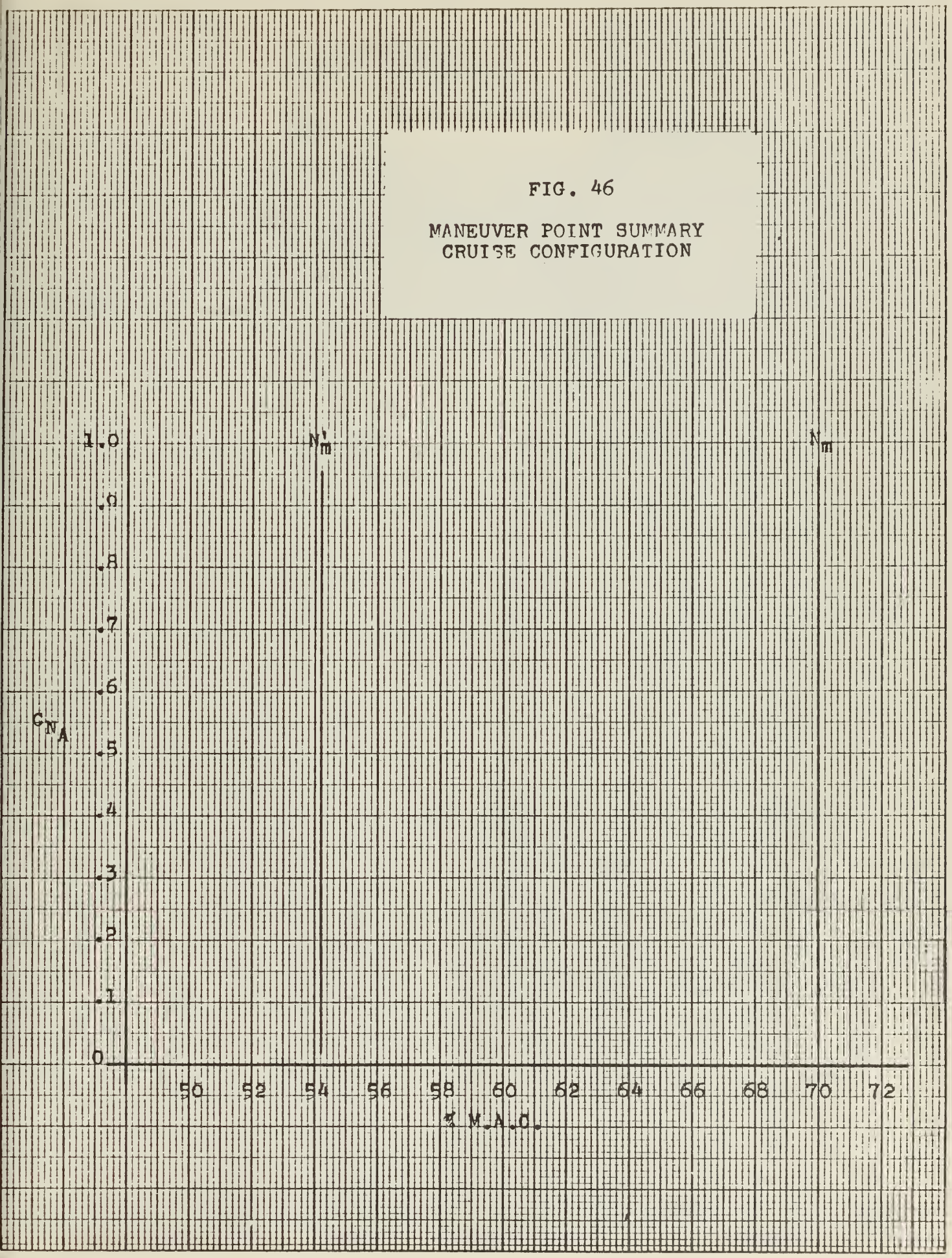

FIG. 48

SUMMARY OF
LATERAL PERFORMANCE

p, $\frac{pb}{2V}$, and δ_a vs. AIRSPEED

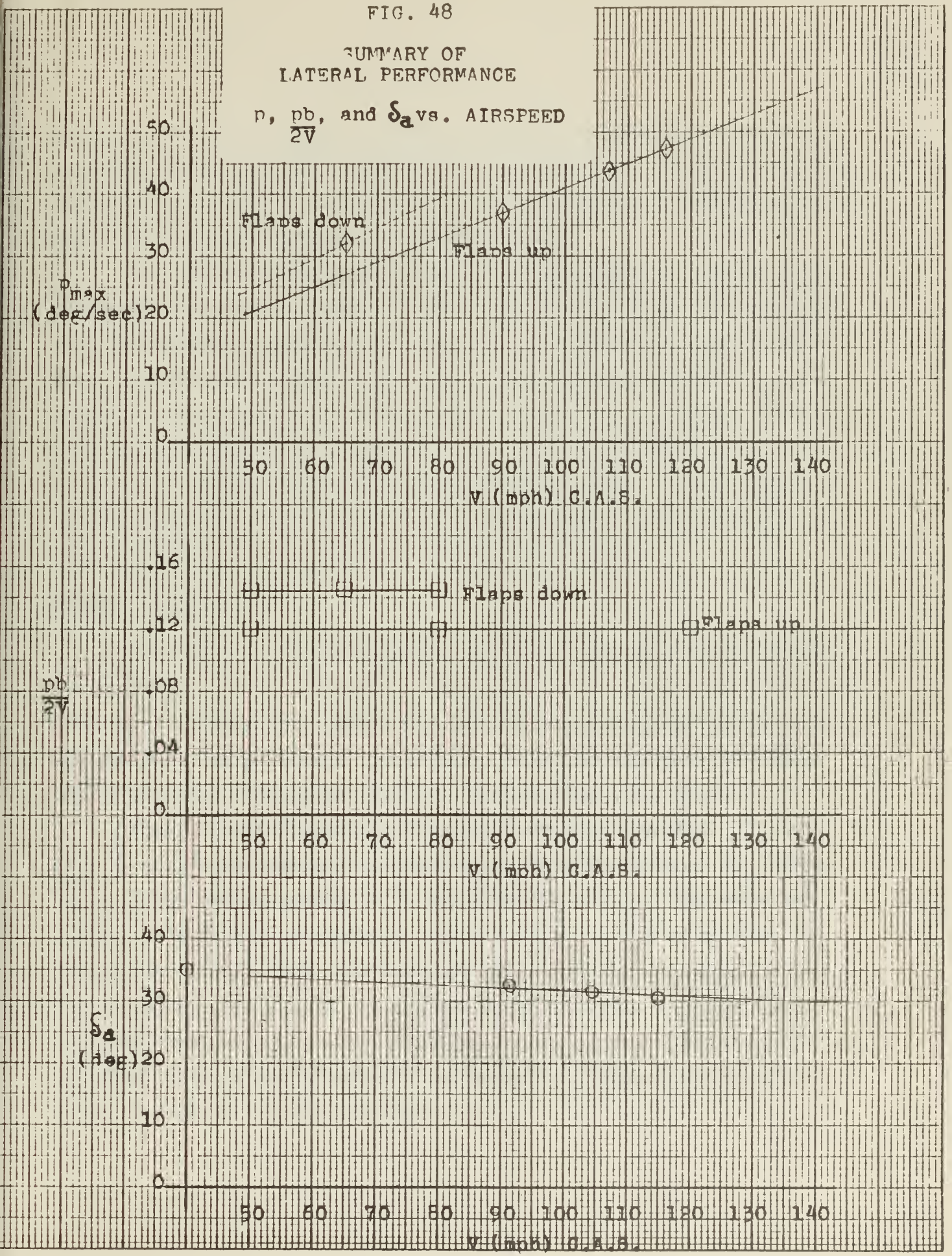

As can be seen from Table III, favorable agreement between the analytical and flight test results were obtained for all parameters, except the stick free maneuver point, N_m'. As expected, the effects of power and freeing of the elevator resulted in a decrease in static stability.

The differences between the analytical and flight test results can be attributed to errors in estimation of tail efficiency, η_t, and determination of hinge moment parameters C_{h_α} and C_{h_δ}. For all calculations in this study, conservative values of η_t, C_{h_α}, and C_{h_δ} were chosen. If more accurate values of these parameters are desired, they can be determined empirically or from wind tunnel tests. It can be concluded from the above comparison that the analytical approach outlined in Ref. 7 gives a good first approximation to the static longitudinal stability, maneuvering stability, and lateral controllability of a STOL type aircraft.

NEUTRAL POINT

The static longitudinal stability characteristics of the "Heli-Porter" are presented in Figs. 28 and 40. These figures are plots of stick fixed and stick free neutral points versus C_L for the power-on and power-off cruise and approach configurations. Both figures show the typical destabilizing effects of power, freeing the elevator, and lowering of the flaps.

Figs. 28 and 40 show that the stick fixed neutral points, N_o, for both the cruise and approach configurations are independent of C_L; while the stick free neutral points, N_o', are functions of C_L. The stick free stability in each test configuration seems to improve with decreasing C_L (increasing speed). This is in disagreement with Ref. 9 which states that a high wing aircraft usually has more stability at higher C_L (low speed). This deviation from theory was probably caused by errors in the initial fairing of the stick force versus velocity curves. These curves were faired through the mid-speed range.

Figs. 28 and 40 show that the effects of power are more pronounced in the approach configuration than in the cruise configuration. Lowering of the flaps is seen to have resulted in a decrease in the stick fixed stability, N_o, and a slight increase in stick free stability, N_o', of the aircraft. These variations in stability are probably a result of an increase in downwash and upwash on the wing. The effect of increased downwash is to reduce the stabilizing influence of the horizontal tail, while increased upwash increases the destabilizing contribution of the propeller and fuselage.

MANEUVER POINT

The maneuvering stability characteristics of the "Heli-Porter" are shown in Fig. 46 plotted as N_m and N_m' versus C_{N_A} for the power-on cruise configuration. It is observed from Fig. 46 that the "Heli-Porter" has normal maneuver point characteristics. The result of maneuvering flight is shown as an increase in the overall longitudinal stability of the aircraft. Once again, freeing the elevator caused a decrease in maneuvering stability.

The increase in the static stability over the maneuvering stability for the stick fixed case is seen to be from $N_o = .49$ to $N_m = .70$. This large increase is considered to be reasonable since the maneuvering stability of an aircraft is inversely proportional to wing loading (see Appendix A) which is very small for the "Heli-Porter," W / S = 11-12 lbs. It is noted that the destabilizing tendency of freeing the elevator is more pronounced in maneuvering flight. This large reduction in maneuvering stability is probably due to insufficient stick force per "g" data. Unfortunately, during this phase only a short range of normal accelerations, 1.0 to 1.5 "g", were tested making it difficult to accurately predict the stick force per "g" gradients and location of the stick free maneuver point. This also accounts for the large discrepancy found between the flight test and analytical values of N_m'.

The stick force per "g" gradients for the "Heli-Porter" are considerably higher than those specified as a minimum for light aircraft, (20.0 lbs/g) from Ref. 10. The following stick force per "g" gradients for the "Heli-Porter" were determined:

TABLE IV

STICK FORCE PER "g" GRADIENTS

c.g. (% M.A.C.)	$\frac{F_s}{n}$ ($\frac{\text{Lbs}}{\text{"g"}}$)
16.47%	64.6
18.44%	30.6
24.94%	30.4
30.34%	29.8

The 16.47% c.g. position stick force per "g" is considerably higher than the others and is probably in error. However, the remaining gradients are extremely high and fall into the large cargo or bomber category of aircraft (i.e., 30 lbs. per "g") where a control wheel instead of a stick is used to achieve these high forces. The magnitude of these forces for the "Heli-Porter" would be extremely fatiguing to a pilot during prolonged maneuvering flight.

LATERAL CONTROL

The lateral controllability characteristics of the "Heli-Porter" are presented in Fig. 48 plotted as δ_a, p, and pb/2V versus calibrated airspeed. It is seen that the "Heli-Porter" possesses normal aircraft rolling

characteristics, Ref. 7. Its helix angle, $pb/2V$, and aileron deflection, δ_a, are relatively independent of velocity; while its roll rate, p, increases linearly with velocity.

Fig. 48 shows that maximum δ_a available is fairly constant through the speed range tested and is nearly equal to the aircraft's total available aileron at zero velocity. This indicates that the aircraft has little mechanical losses (control wire stretch, etc.) in its aileron control system.

As noted in Fig. 48, the "Heli-Porter" has rolling characteristics, $pb/2V = .12$, comparable to those of a high performance aircraft. But, again, the lateral stick force necessary to obtain this performance was high. Due to a malfunction of the camera on the photo-panel during this test phase, it was impossible to obtain aileron angle data to correlate with recorded force data. However, the maximum lateral stick force data, which increased with speed, ranged from 21-27 lbs.

Fig. 48 also indicates that the "Heli-Porter" may have better rolling performance in the approach configuration than in the cruise configuration, ($pb/2V = .14$ vs. $pb/2V = .12$). This, however, may not be the case since the aircraft was tested only at one airspeed in the approach configuration.

Ref. 1 indicated that the aircraft had negative stick free dihedral effect when the aircraft was placed in a bank of more than 5 degrees. For this reason, a qualitative study of the stick free dihedral effect was performed. The results of these tests indicated a lack of dihedral effect.

CONCLUSIONS

As a result of this investigation, the following conclusions were reached:

1. The "Heli-Porter" has adequate stick fixed and stick free static longitudinal stability in the approach and the cruise configuration both for power-on and power-off conditions.
2. The aircraft has an extremely high level of maneuvering stability.
3. The stick force per "g" and control forces in general are considered excessive if prolonged periods of maneuvering flight are anticipated.
4. The roll performance of the "Heli-Porter" is comparable to that of a high performance aircraft; but the stick forces required to achieve this performance are excessive.
5. The analytical study as outlined in Ref. 7 provides a good first approximation for the longitudinal static and maneuvering stability and the lateral controllability of a STOL aircraft.
6. The stick fixed neutral points and both the stick fixed and stick free maneuver points are independent of C_L, while the stick free neutral points are not.
7. The destabilizing effects of power are more pronounced in the approach configuration than in the cruise configuration.
8. Lowering of the flaps resulted in a decrease in stick fixed longitudinal stability and a slight increase in stick free stability.
9. The c.g. range given by the manufacturer is well forward of any neutral points or maneuver points determined in this report.

RECOMMENDATIONS

It is recommended that:

1. A more complete test of stick force per "g" be conducted on the "Heli-Porter."
2. Further tests be performed to determine the magnitude of the lateral control forces.
3. The control force levels be reduced.
4. A lateral study be performed to investigate further the lack of stick free dihedral effect.

REFERENCES

1. Takeoff and Landing Evaluation of the Pilatus Turbo Porter Model PC-6/A Airplane, Report of USA TECOM Project No. 4-3-1048-01, September 1963.

2. Lenox, G. W., Lt., USN and Lindell, C. A., Capt., USMC; "A Flight Test Determination of the Static Longitudinal Stability of the Cessna 310d Airplane," Princeton University Aeronautical Engineering Report No. 547, May 1961.

3. Airplane Weight and Balance. Swiss Federal Air Office Approved Model PC-6/350-H1-"Porter," "Pilatus" Aircraft Ltd., February 1963.

4. Dwinnell, T. H.; Principles of Aerodynamics, 1949, 1st Ed., McGraw Hill Book Co., New York.

5. Matson, R. S. and Spillers, W. H., Jr.; "An Analysis of Various Methods of Flight Testing for Neutral Points," Princeton University Aeronautical Engineering Report No. 275, 1955.

6. Advisory Group for Aeronautical Research and Development Flight Test Manual, Volume II, Stability and Control, Edited by Perkins, C.D.

7. Perkins, C. D. and Hage, R. E.; Airplane Performance, Stability, and Control, 1949, John Wiley and Sons, Inc., New York.

8. Sears, R. I.; Wind Tunnel Data on the Aerodynamic Characteristics of Airplane Control Surfaces, N.A.C.A. WR L-663, 1943.

9. Seckel, E.; Stability and Control of Airplanes and Helicopters, 1964, Academic Press Inc., New York.

10. Flying Qualities of Piloted Airplanes. MIL-F-8785 (AS6), Department of the Air Force and Bureau of Aeronautics.

11. Aerodynamics of Porter Aircraft, "Pilatus" Aircraft Ltd., Report No. RPC6-14, 7/29/65, Fairchild Hiller Aircraft Corporation.

12. Ribner, H. S.; "Notes on the Propeller and Slipstream in Relation to Stability," N.A.C.A. WR L-25, 1944.

TABLE I

Pilatus "HELI-PORTER" Model PC-6/350

Aircraft Specifications

I.1 GENERAL

Wing span	49 ft. 8 in.
including Nav. lights	49 ft. 10-1/2 in.
Overall length	33 ft. 5-1/2 in.
Overall height	10 ft. 6 in.
Wheel track	9 ft. 10 in.
Wing area	306.7 sq. ft.
Wing loading	14.2 lb./sq. ft.
Fuselage max width	2.56 ft.
Fuselage max height	5.25 ft.

I.2 WEIGHTS

Weight empty (weight and balance)	2771 lbs.
Useful load	1549
Max. take-off weight	4320 lbs.

I.3 POWER UNIT

Engine:

Model	LYCOMING IGO-540-A1A
Type	Six Cylinder, Horizontally Opposed, Air Cooled, Dual Spark Ignition, Geared Drive, Fuel Injection with Internal Piston Cooling and Dry Sump
Take-off Horsepower	350 HP at 3400 RPM
Rated Horsepower	325 HP at 3000 RPM

TABLE I (continued)

Propeller:

Model	HARTZELL HC-B3Z-2B
	Blades No. 9349
Type	Three blades, constant speed, metal propeller, feathering
Diameter	93 in.

I.4 WING ASSEMBLY

Wing:

Profile	NACA 64-514 constant over whole span
Plan	rectangular
Span	49 ft. 8 in.
Area	306.7 sq. ft.
Chord	6 ft 2-3/4 in.
Aspect Ratio	7.96
Angle of Incidence	2^{o}
Dihedral Angle	1^{o}
Taper Ratio	1.0

Landing Flaps:

Design	Camber changing flap with slats, two parts each side
Area total	40.2 sq. ft.
Travel	0 to 38^{o}

Aileron:

Design	Same as landing flaps without slats
Area total	41.2 sq. ft.
Travel	20^{o} upwards, 13.5^{o} downwards
Horn balance	

TABLE I (continued)

I.5 TAIL GROUP

Vertical tail surfaces:

Fin:

Area	28.6 sq. ft.

Rudder:

Area	10.3 sq. ft.
Travel	30^{o} each side
Trim tab travel	6^{o} each side

Horizontal tail surface:

Profile	NACA 0015 with slightly modified nose
Total area	65.343 sq. ft.
Chord	4.052 ft.
Span	6.733 ft.
AR_t	4.285

Stabilizer:

Area	43.3 sq. ft.
Span	15 ft. 9 in.
Travel	$+2^{o}$ -10^{o}
Chord	2.57 ft.

Elevator:

Area	22.7 sq. ft.
Chord	1.47 ft.
Travel	25^{o} down - 30^{o} up
Trim tabs	36^{o} upwards

TABLE II

Pilatus "HELI-PORTER" Model PC-6/350

Aircraft Limitations

II.1 SPEEDS

		mph
min.	Flaps down	52
	Flaps up	60
max.	Flaps down	84
	Flaps up	174
	Maneuvering	122

II.2 CENTER-OF-GRAVITY

The permissible c.g. range is between 11.0 and 33.0% of M.A.C. (Mean Aerodynamic Chord = 75 inch).

The c.g. datum is the leading edge of the wing. Leveling mean is the cabin floor.

1. Forward Limit = 15.25 in. aft of the wing leading edge reference line.
2. Aft Limit = 24.75 in. aft of the wing leading edge reference line.

II.3 LOAD FACTORS

The maximum permissible load factors are: +3.8 and -1.5.

FIG. 1

PHOTOGRAPH OF TEST AIRCRAFT

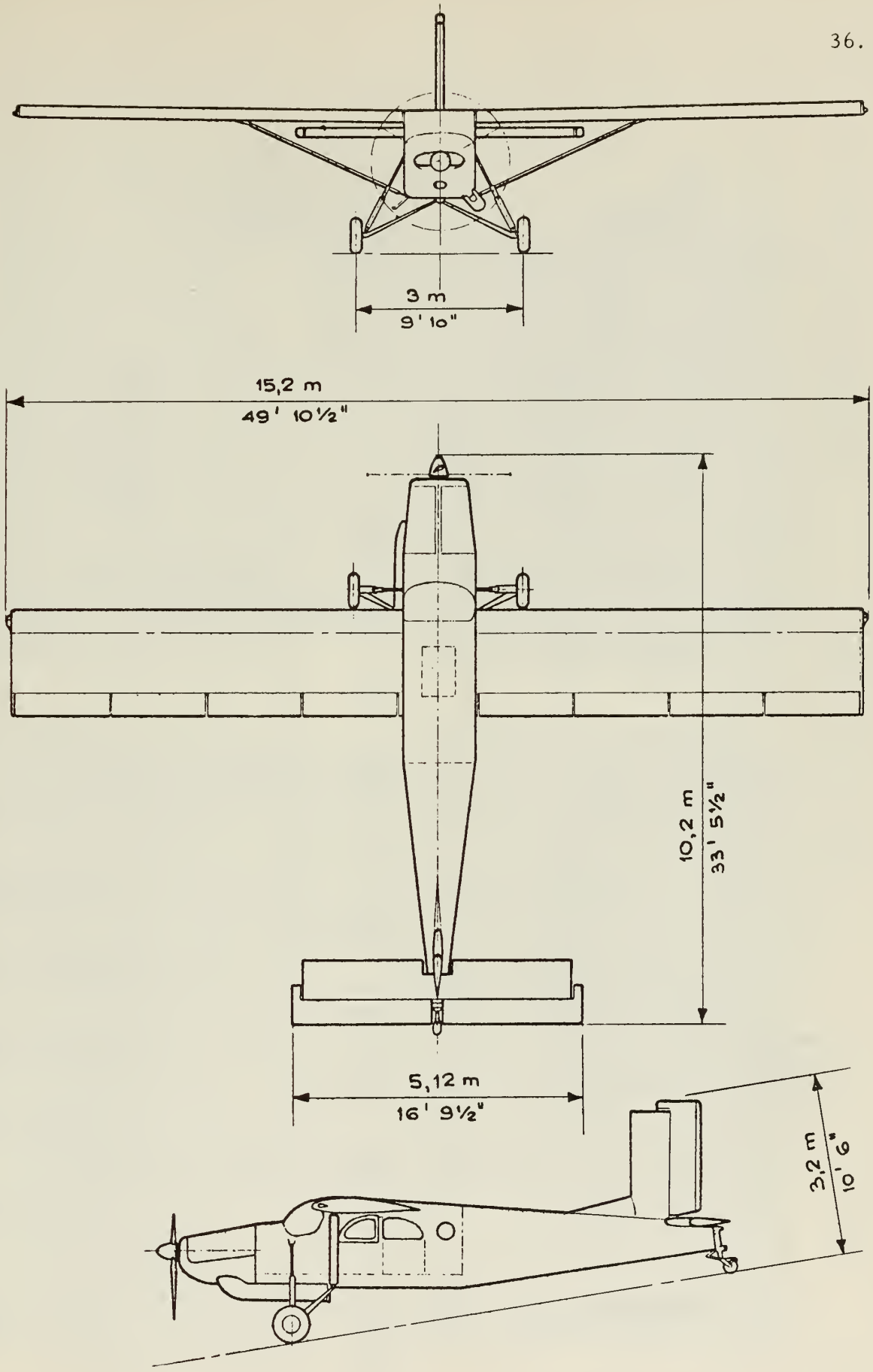

FIG. 2
THREE-VIEW DRAWING
OF TEST AIRCRAFT

FIG. 3
WING & FUSELAGE STATION DIAGRAM OF TEST AIRCRAFT

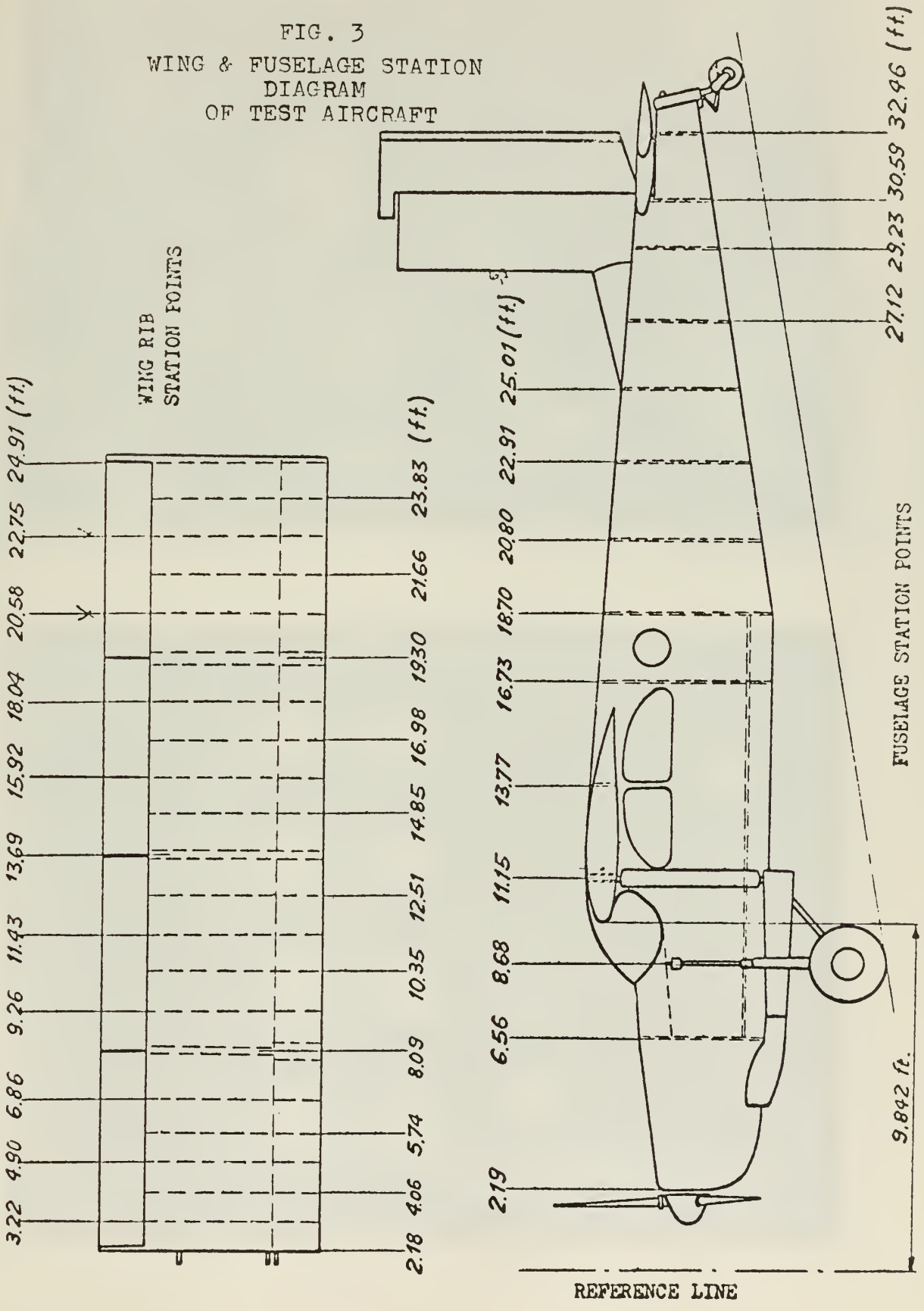

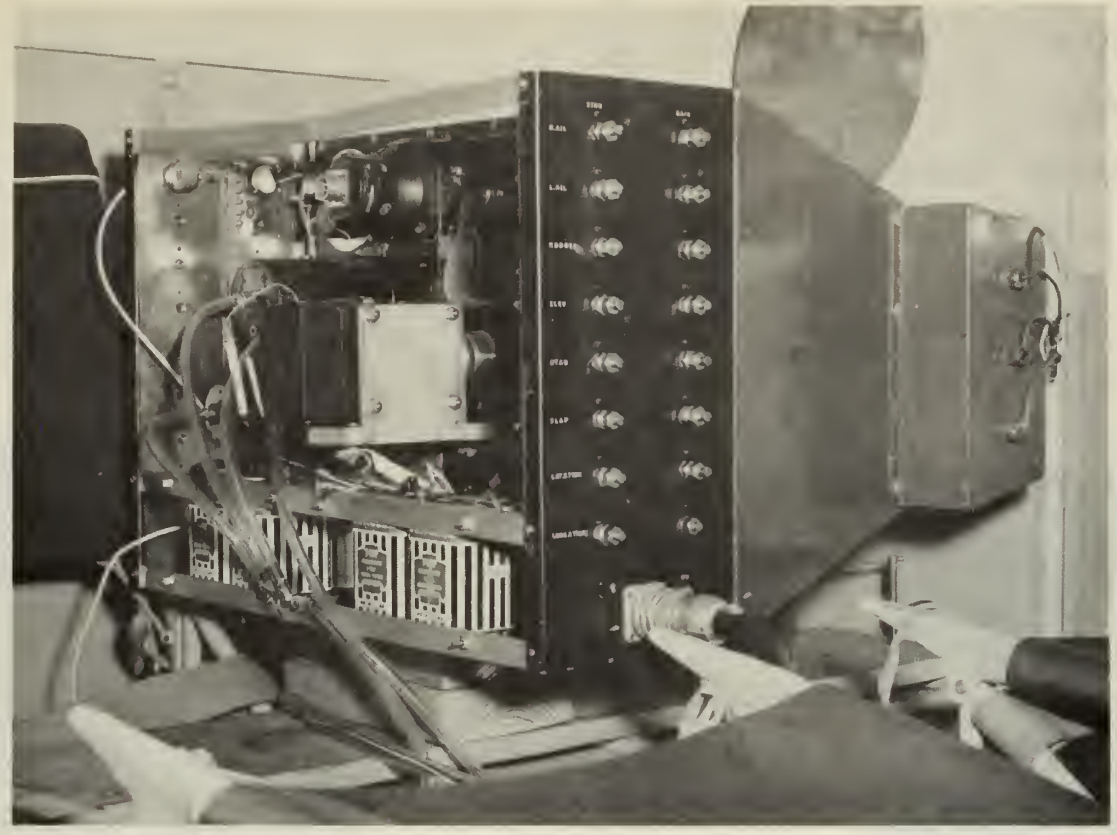

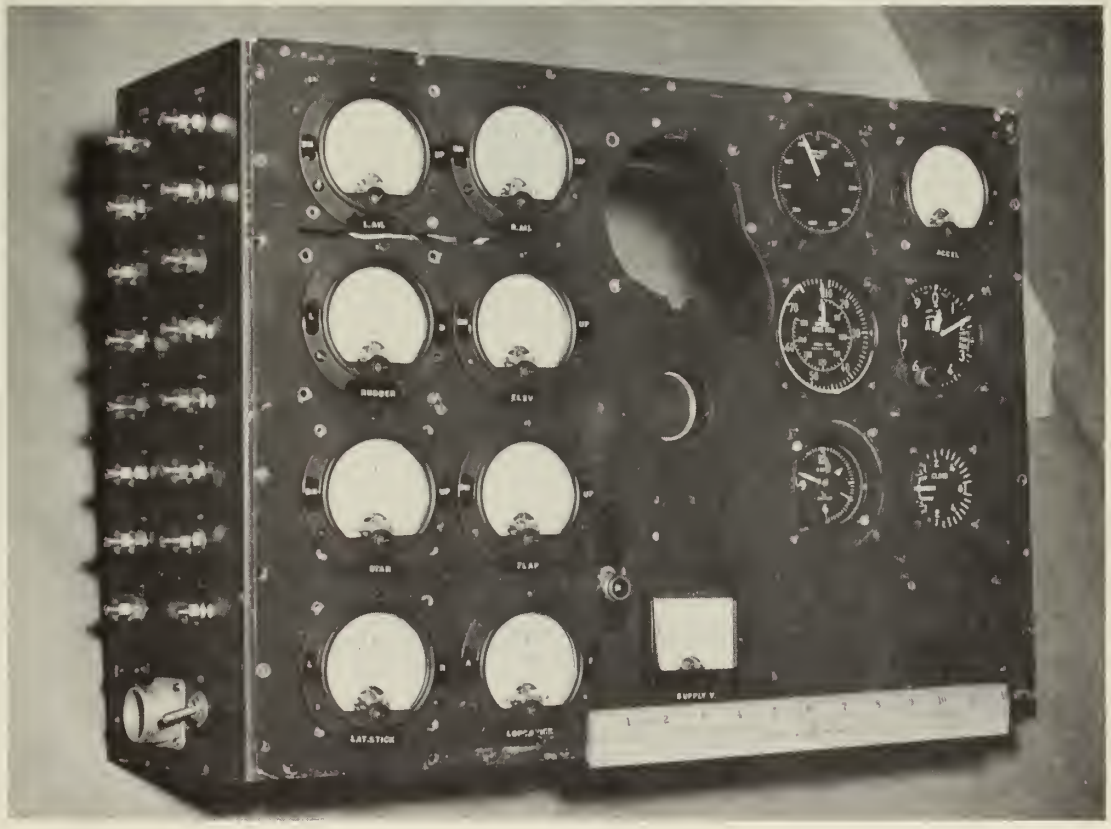

FIG. 4
PHOTOGRAPH OF PHOTO-PANEL

FIG. 5

LOCATION AND INSTALLATION
OF
POTENTIOMETERS
ON
CONTROL SURFACES

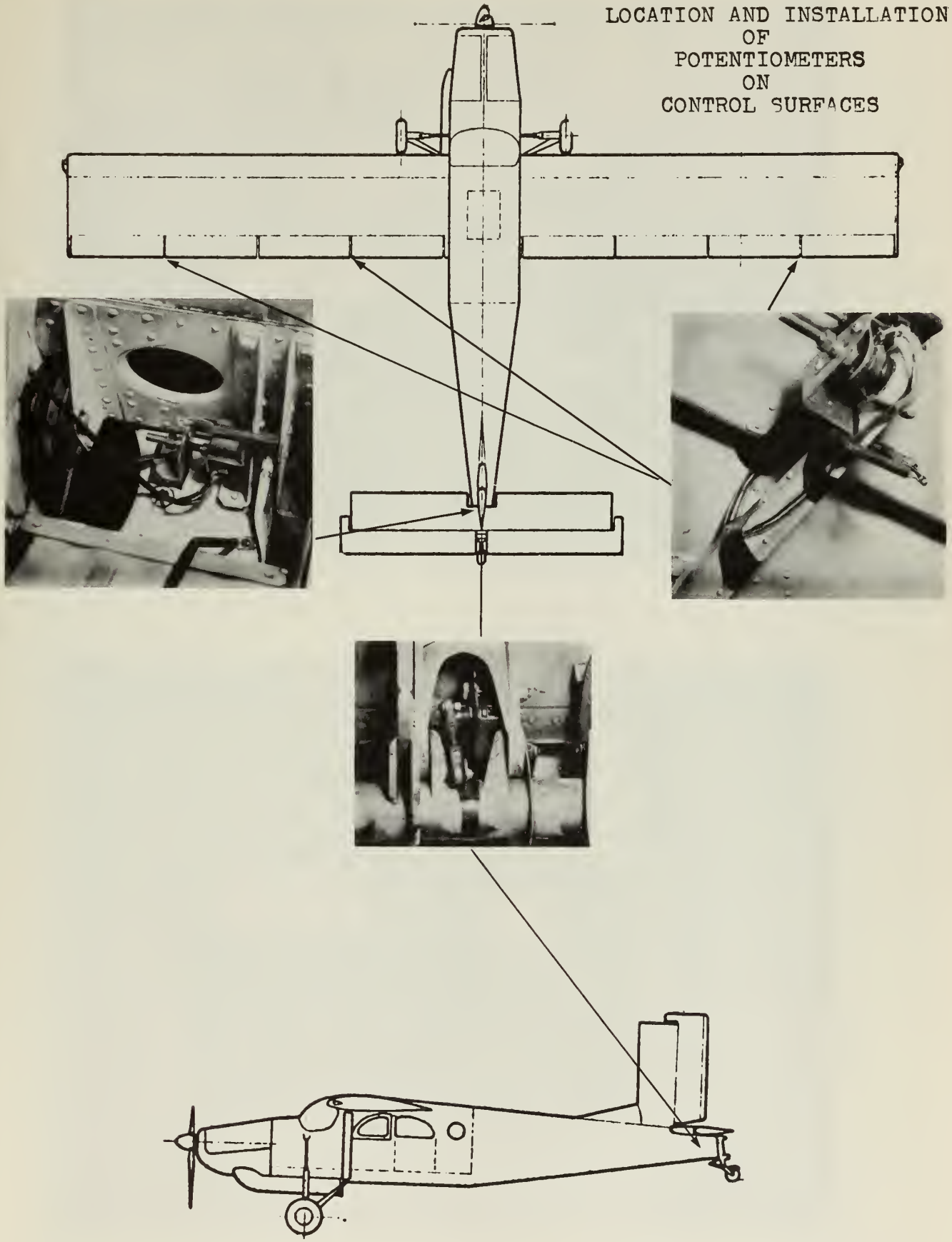

FORCE STICK INSTALLATION

FORCE STICK INSTRUMENTATION

FIG. 6
PHOTOGRAPHS OF FORCE STICK

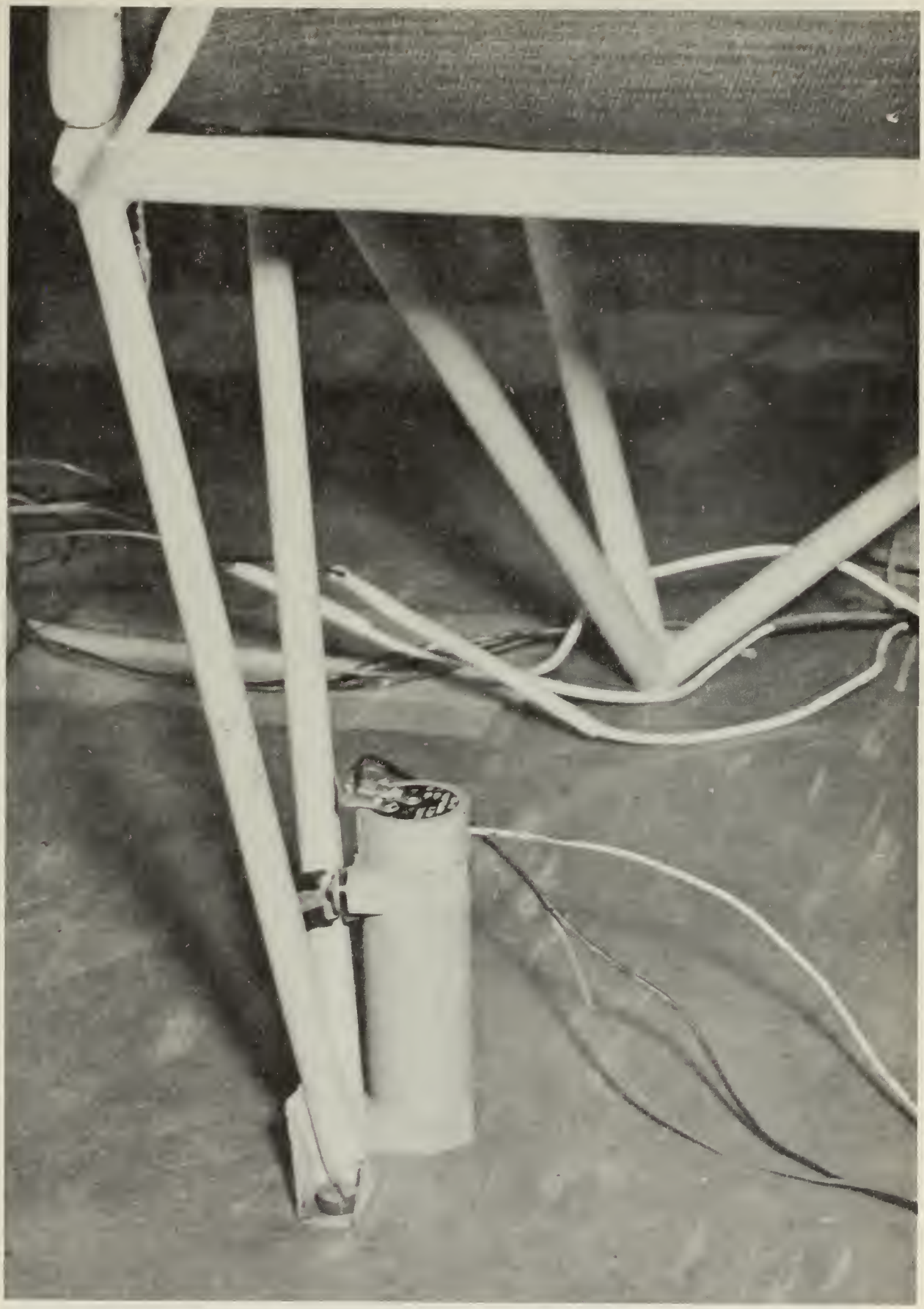

FIG. 7
ACCELEROMETER INSTALLATION

FIG. 8
TEST BOOM ON AIRCRAFT

FIG. 9

ELEVATOR ANGLE CALIBRATION

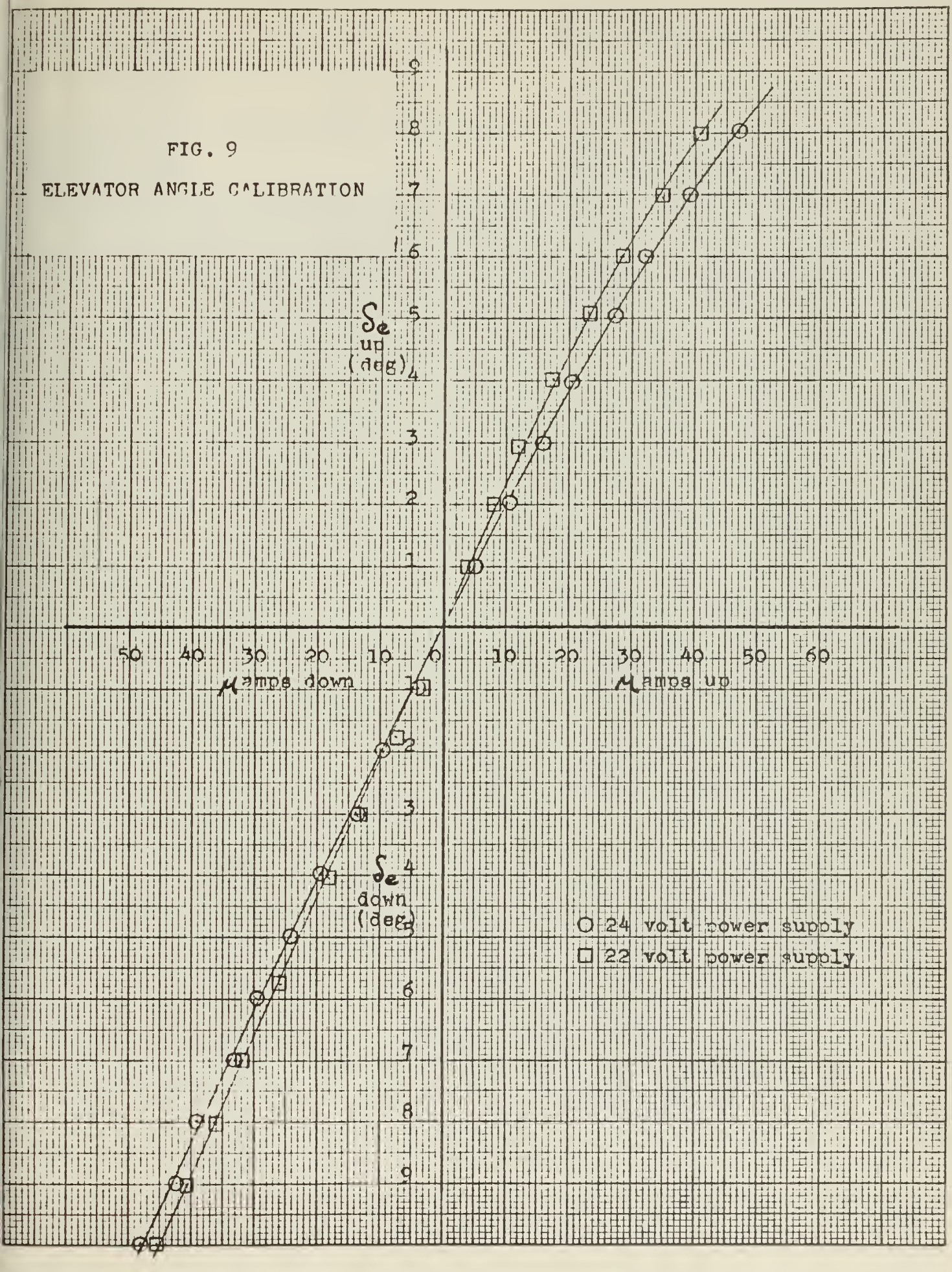

FIG. 10

AILERON ANGLE CALIBRATION

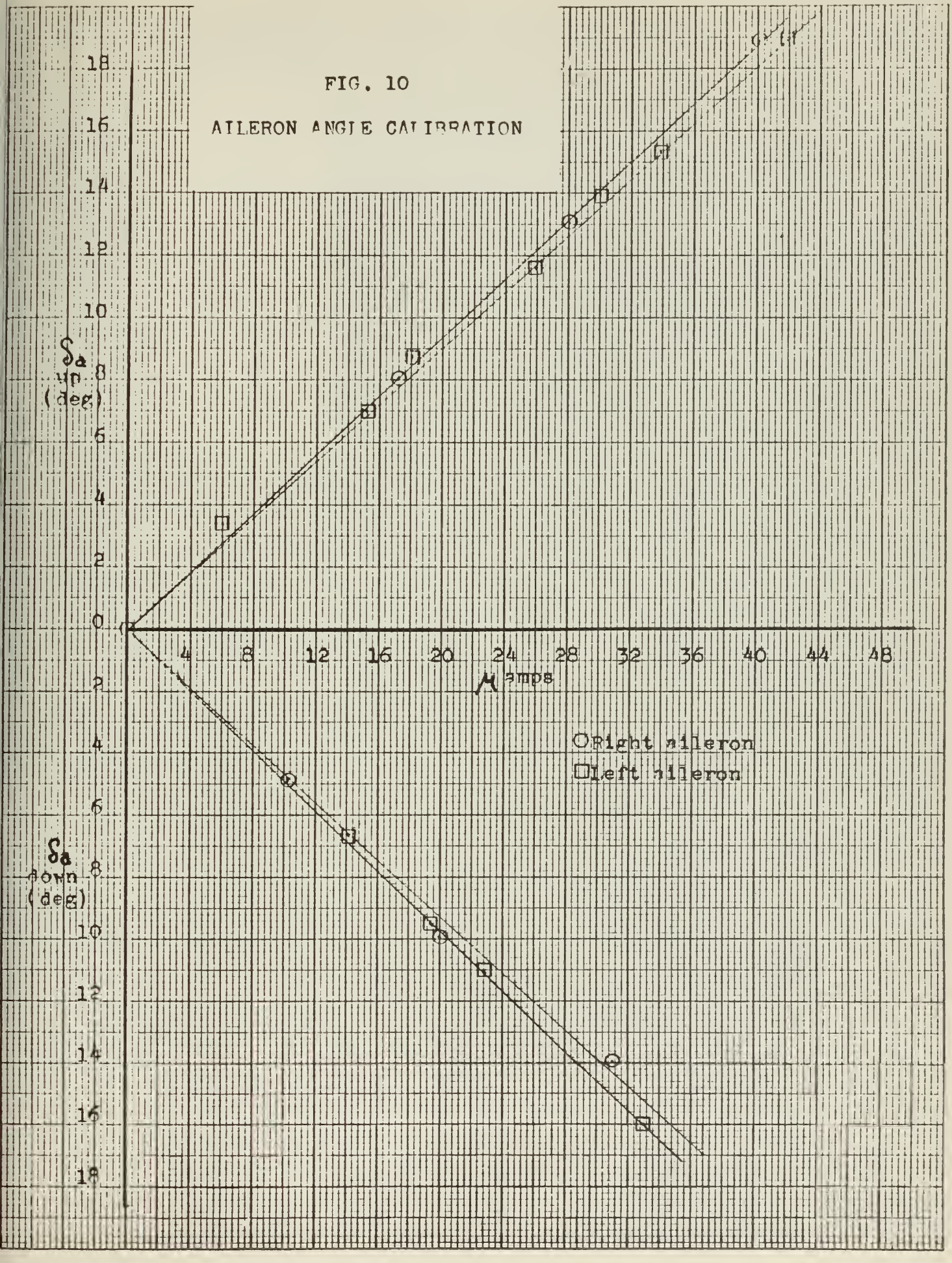

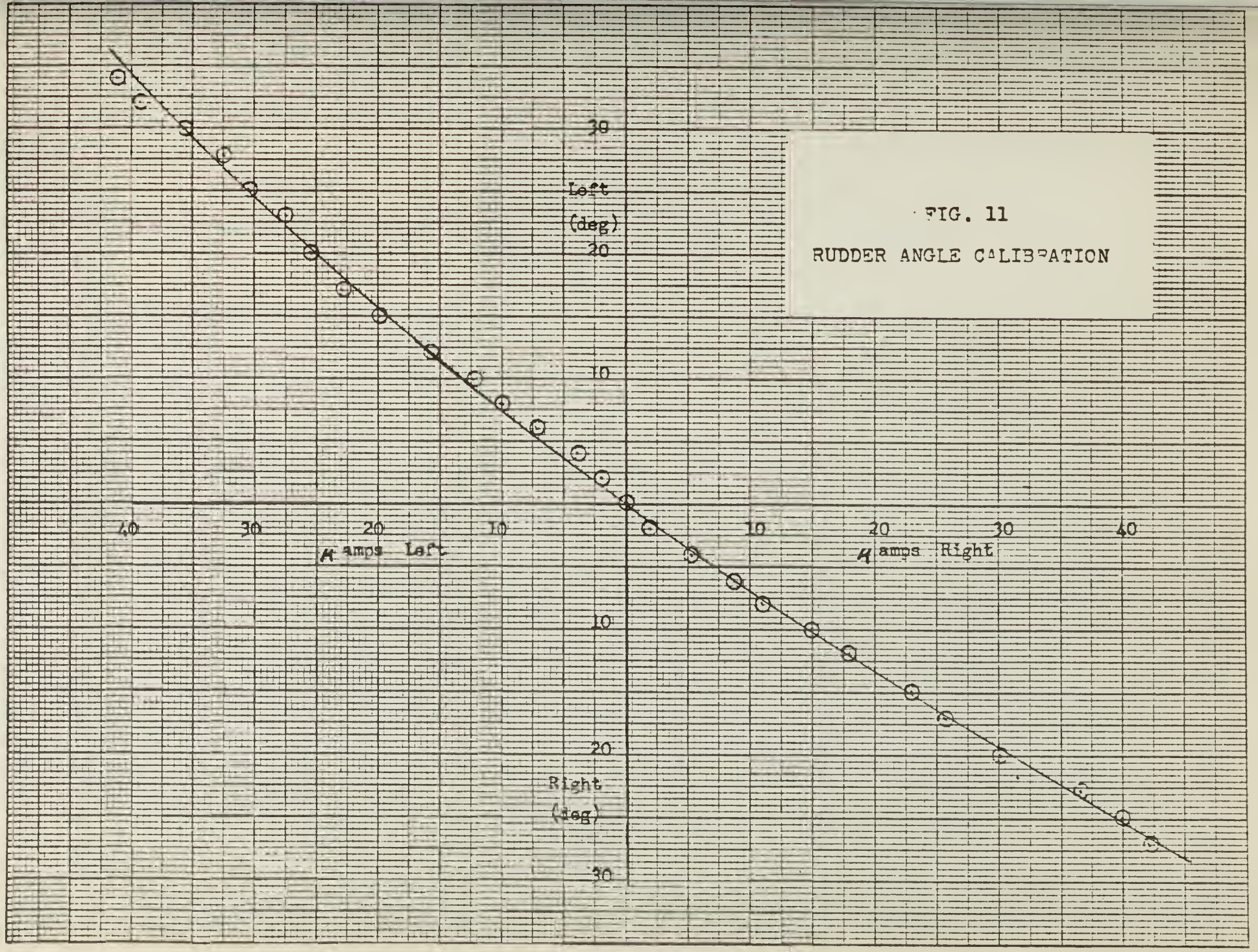

FIG. 11

RUDDER ANGLE CALIBRATION

FIG. 12

STABILIZER ANGLE CALIBRATION

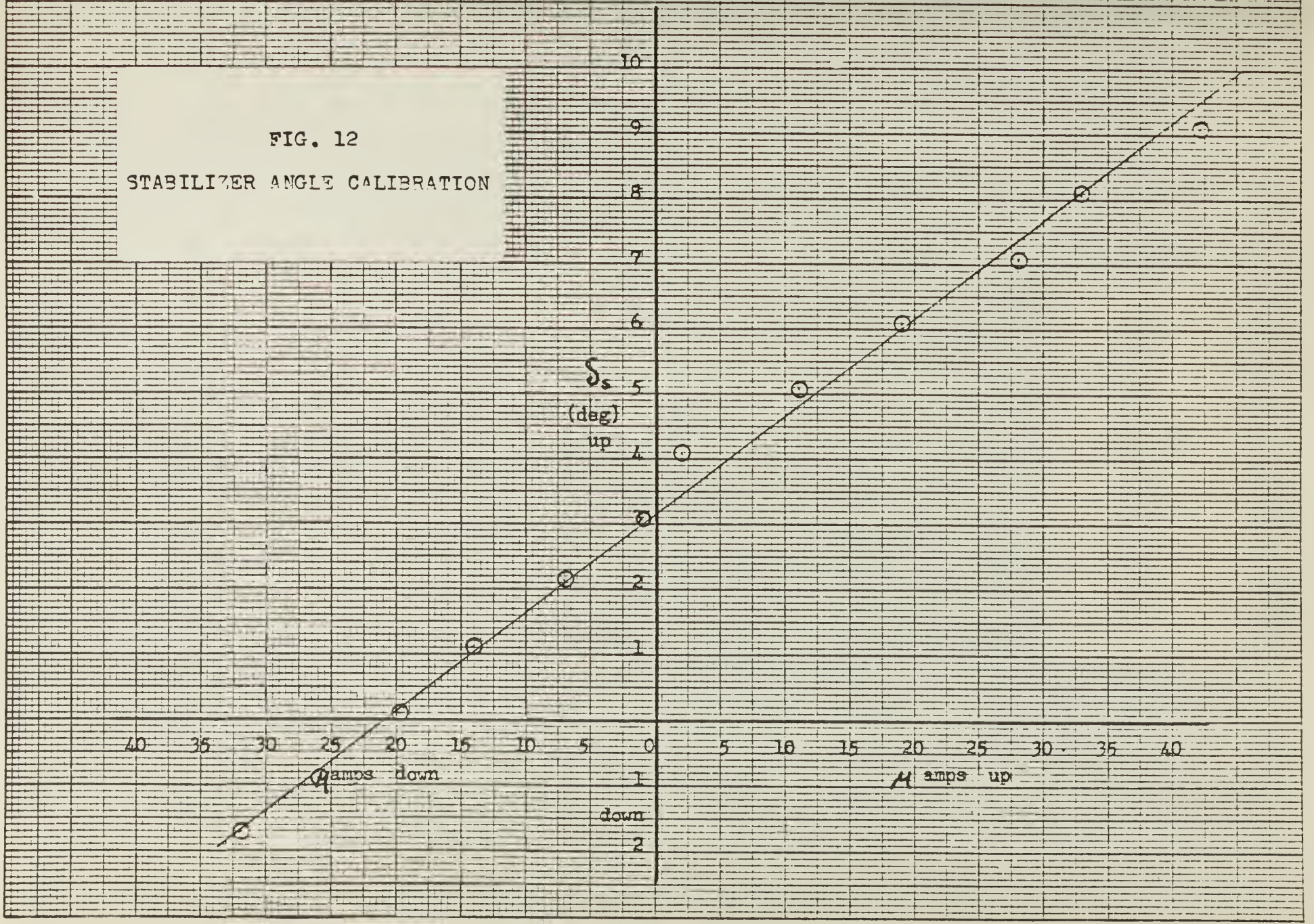

FIG. 13

FLAP ANGLE CALIBRATION

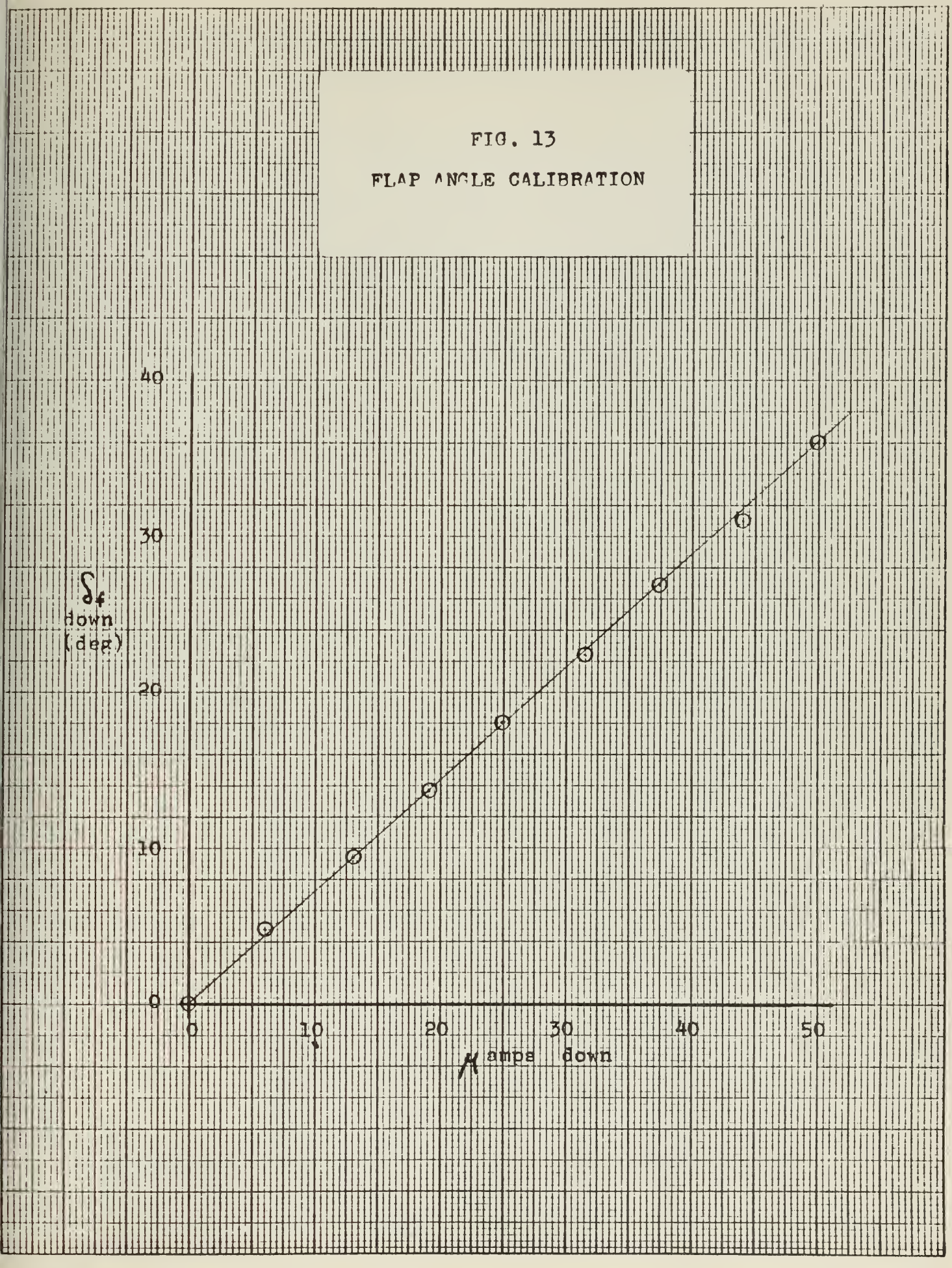

FIG. 14

FORCE STICK CALIBRATION

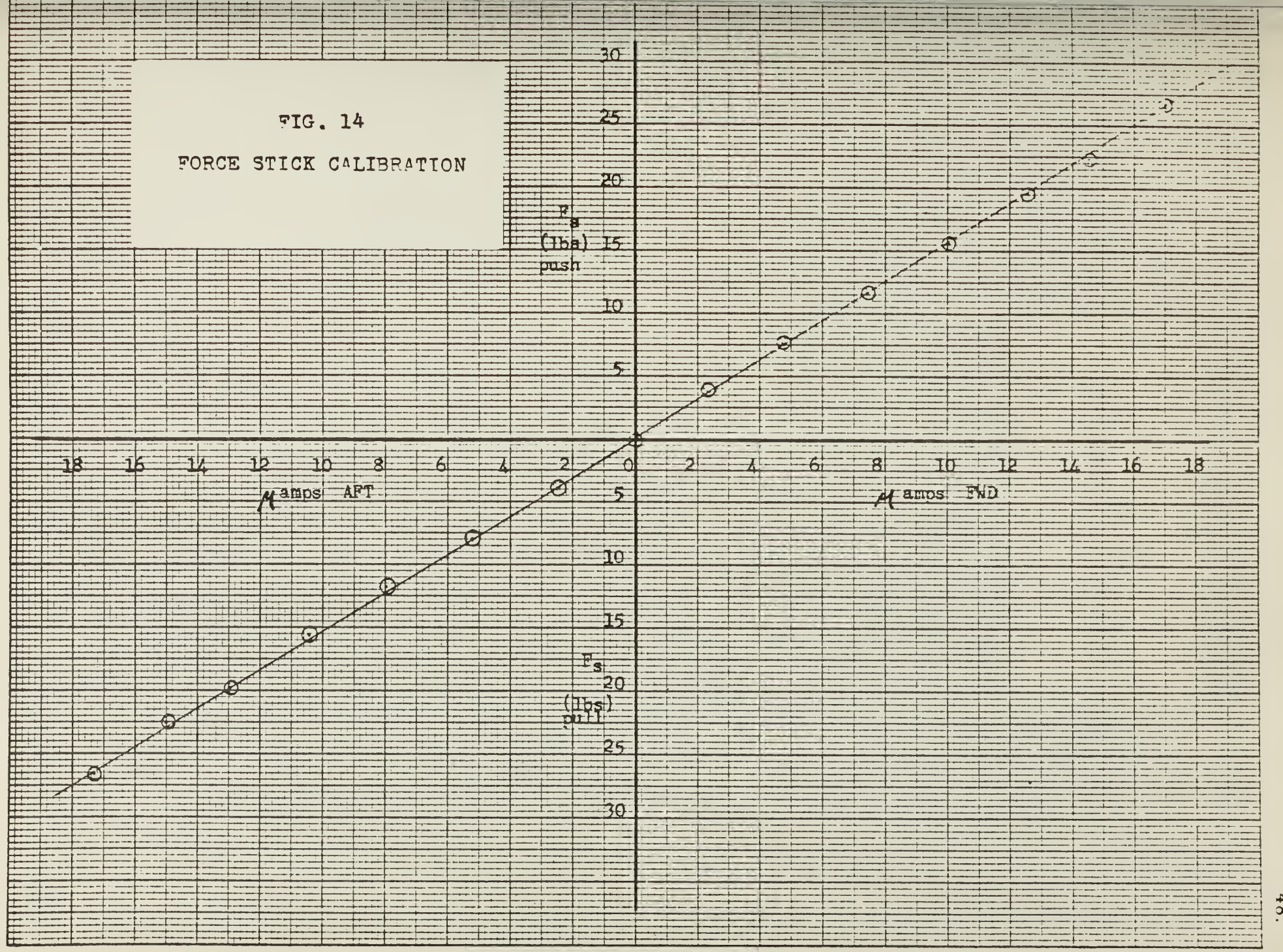

FIG. 15

ACCELEROMETER CALIBRATION

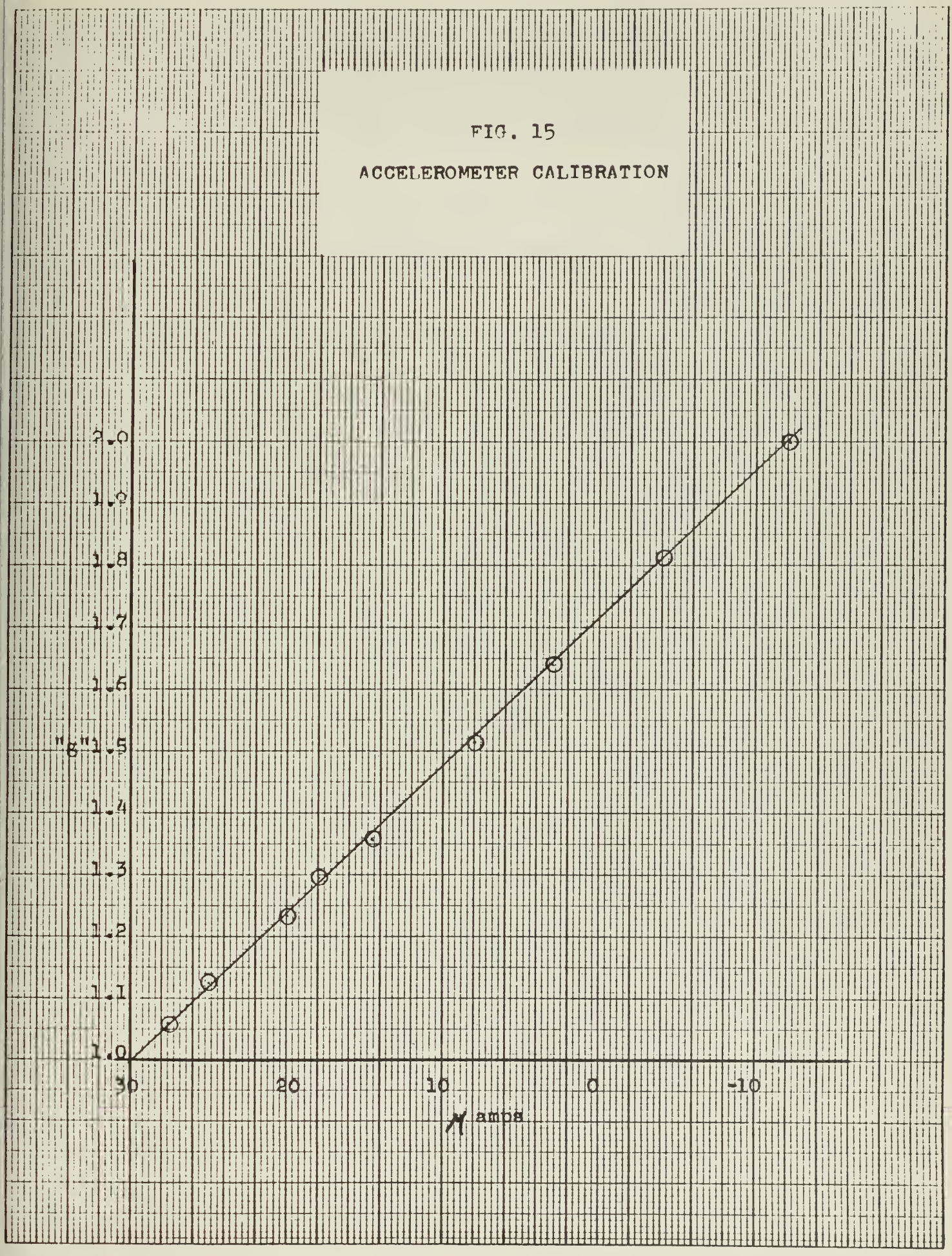

FIG. 16

AIRSPEED CALIBRATION

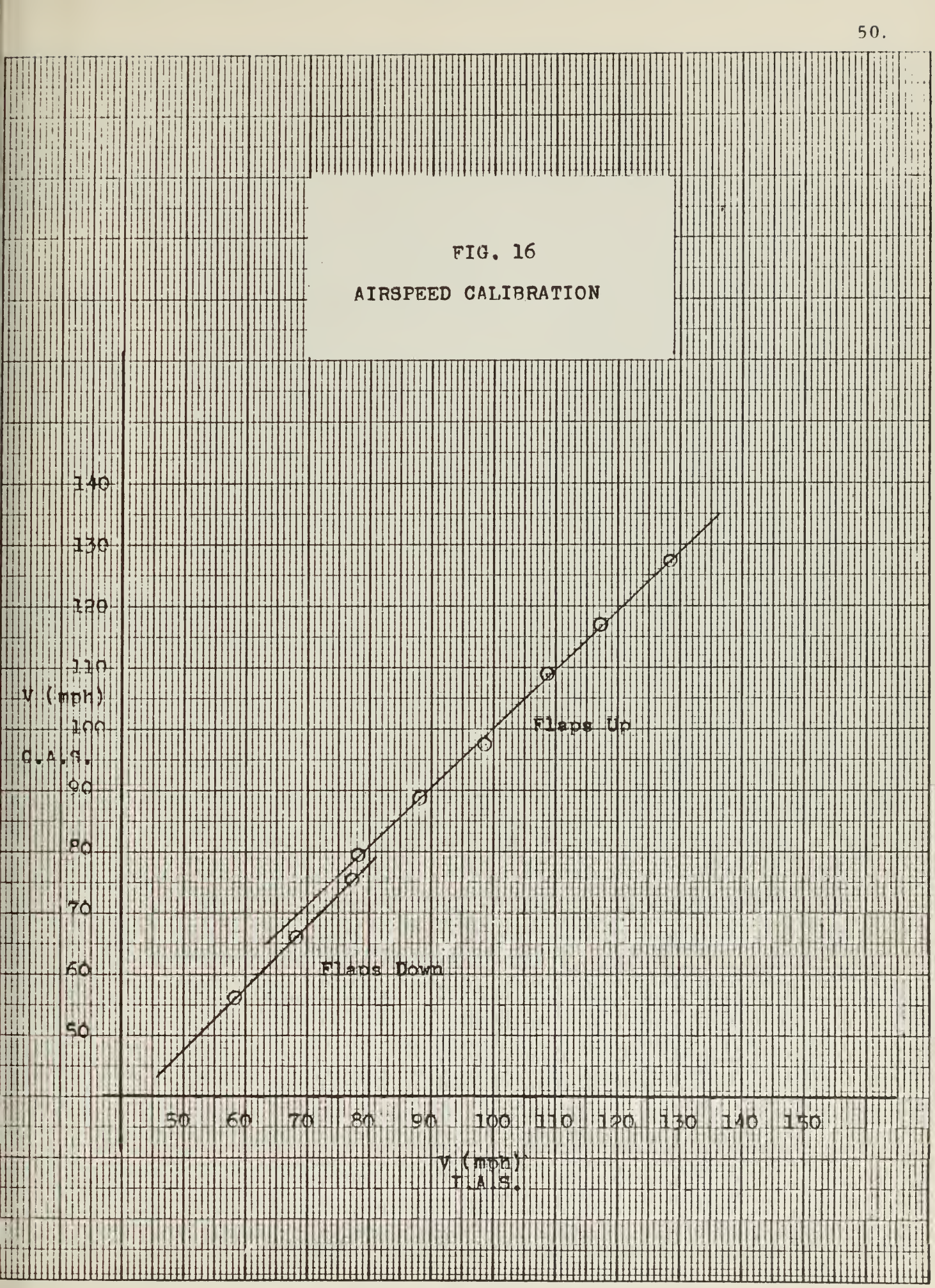

FIG. 17

FLIGHT TEST DATA
CRUISE CONFIGURATION
POWER-ON

ELEVATOR ANGLE vs. AIRSPEED

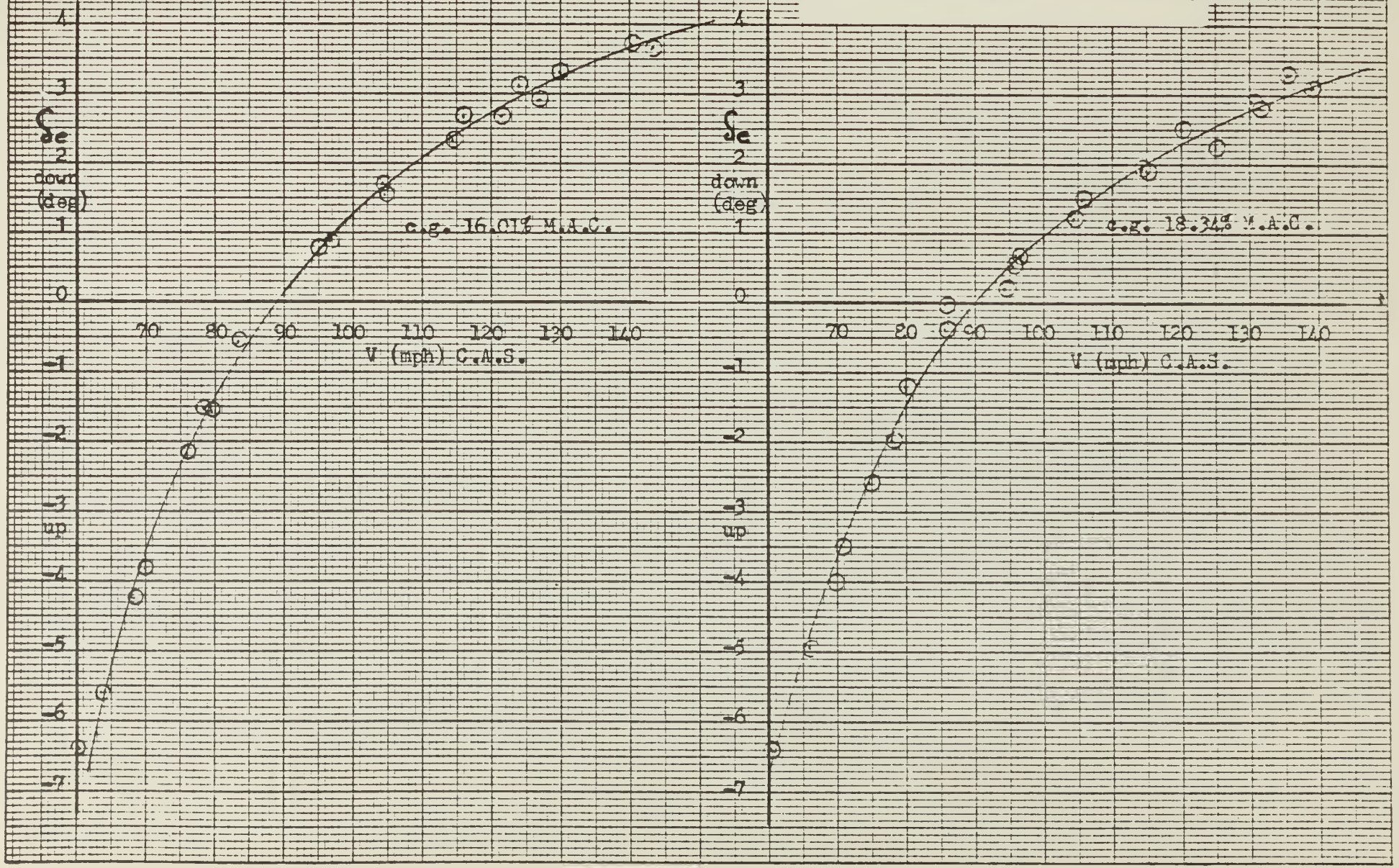

FIG. 17

FLIGHT TEST DATA
CRUISE CONFIGURATION
POWER-ON

ELEVATOR ANGLE vs. AIRSPEED

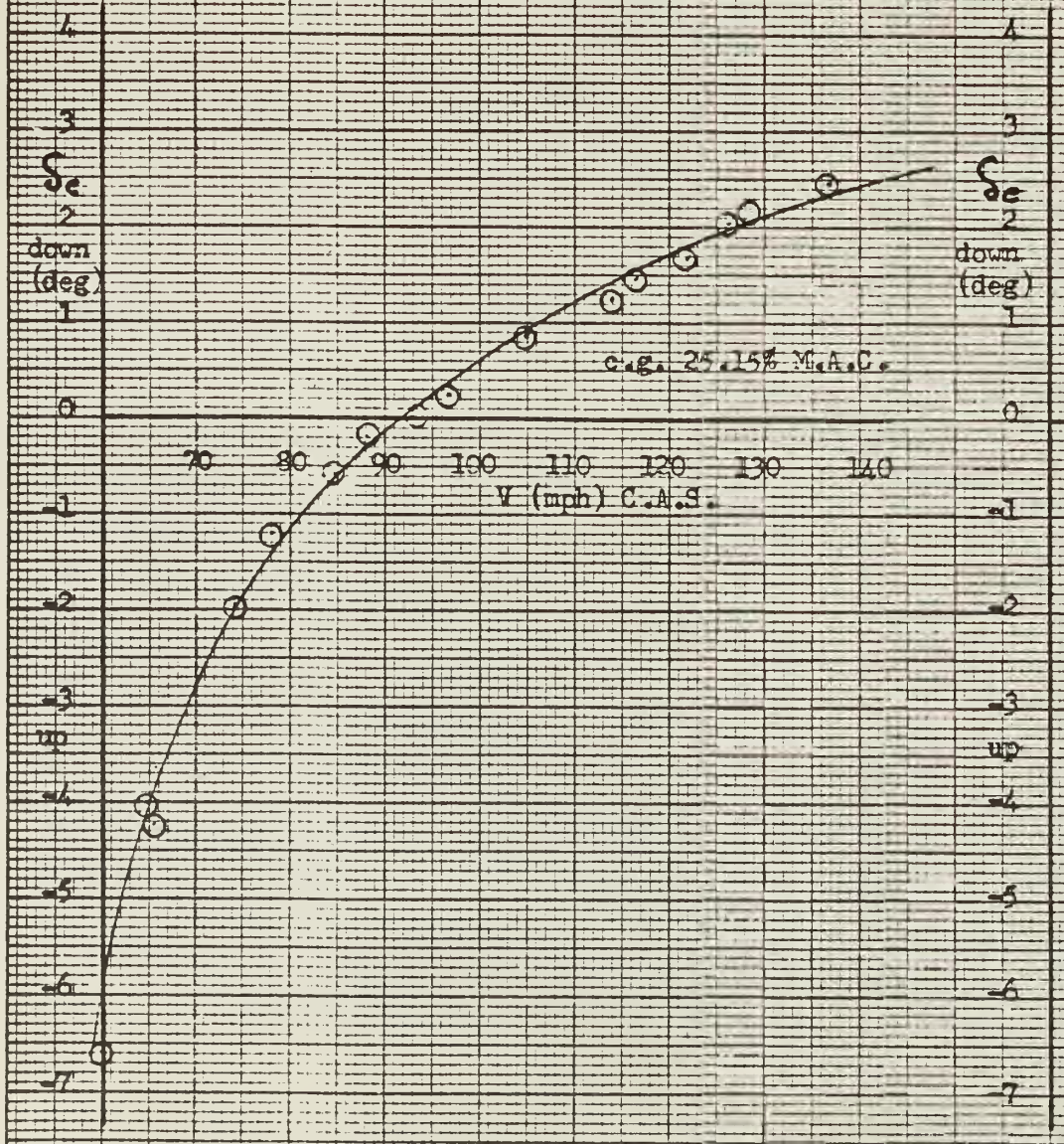

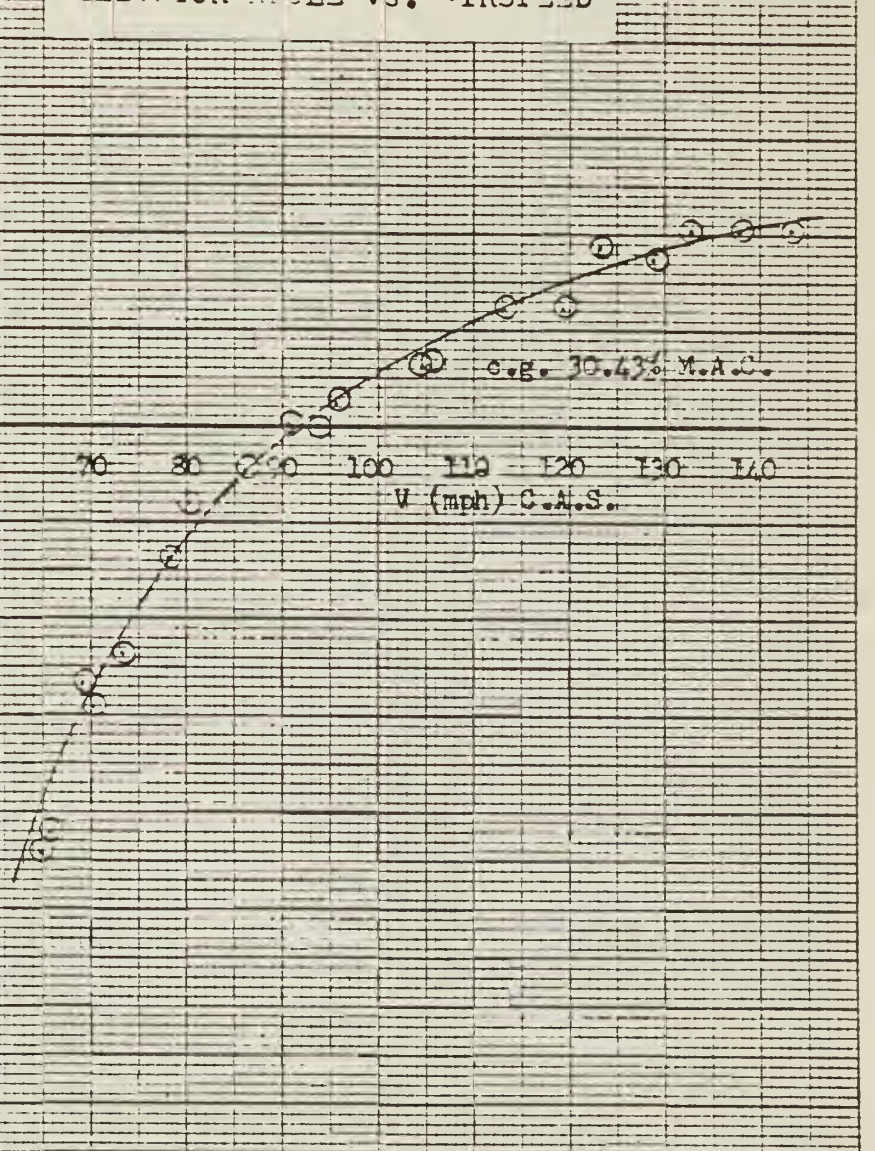

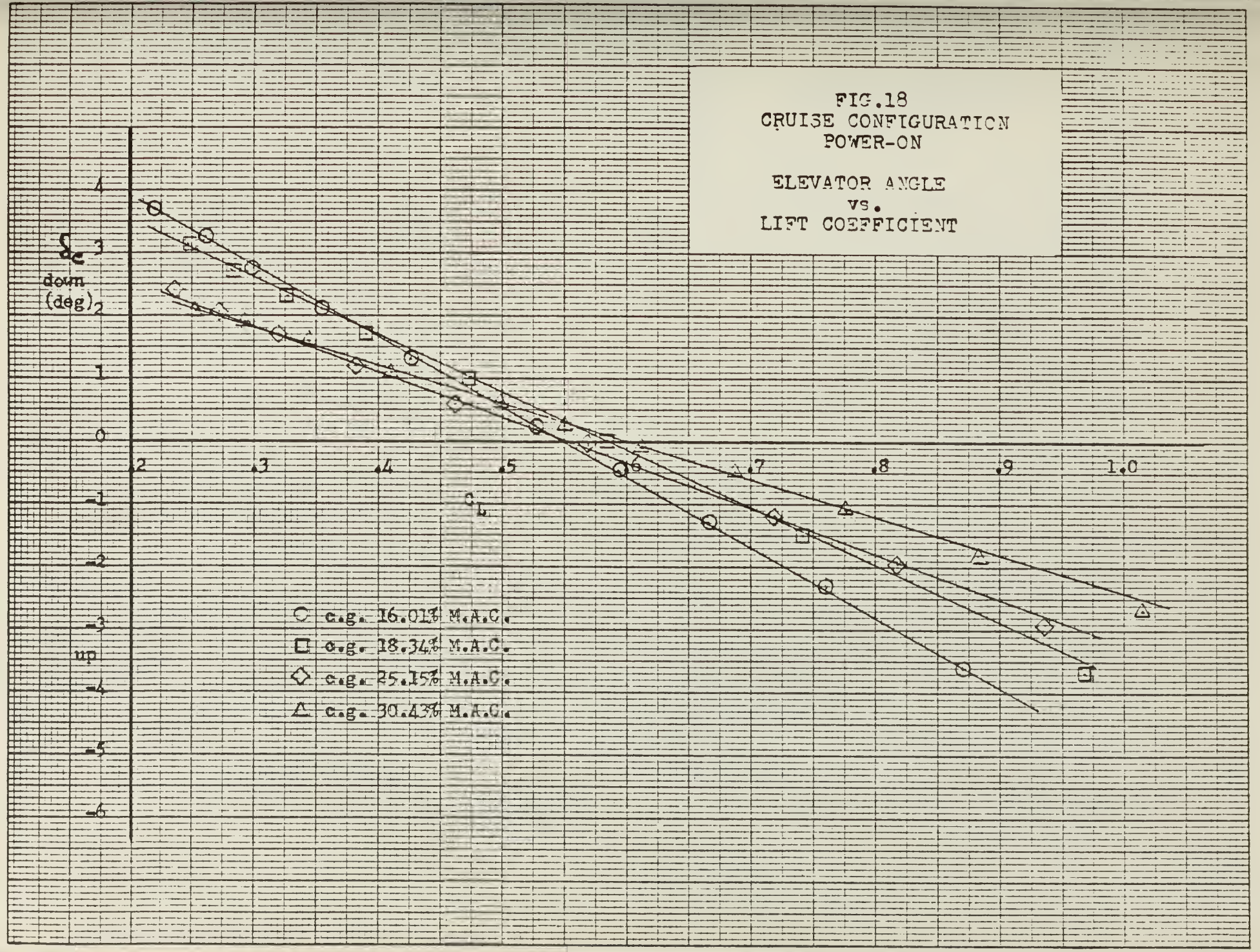
FIG.18
CRUISE CONFIGURATION
POWER-ON
ELEVATOR ANGLE
vs.
LIFT COEFFICIENT
δ_e down (deg)
4
3
2
1
0
-1
-2
-3
-4
-5
-6
up
.2
.3
.4
.5
.6
.7
.8
.9
1.0
C_L
c.g. 16.01% M.A.C.
c.g. 18.34% M.A.C.
c.g. 25.15% M.A.C.
c.g. 30.43% M.A.C.

FIG. 19

FLIGHT TEST DATA
CRUISE CONFIGURATION
POWER-OFF

ELEVATOR ANGLE vs. AIRSPEED

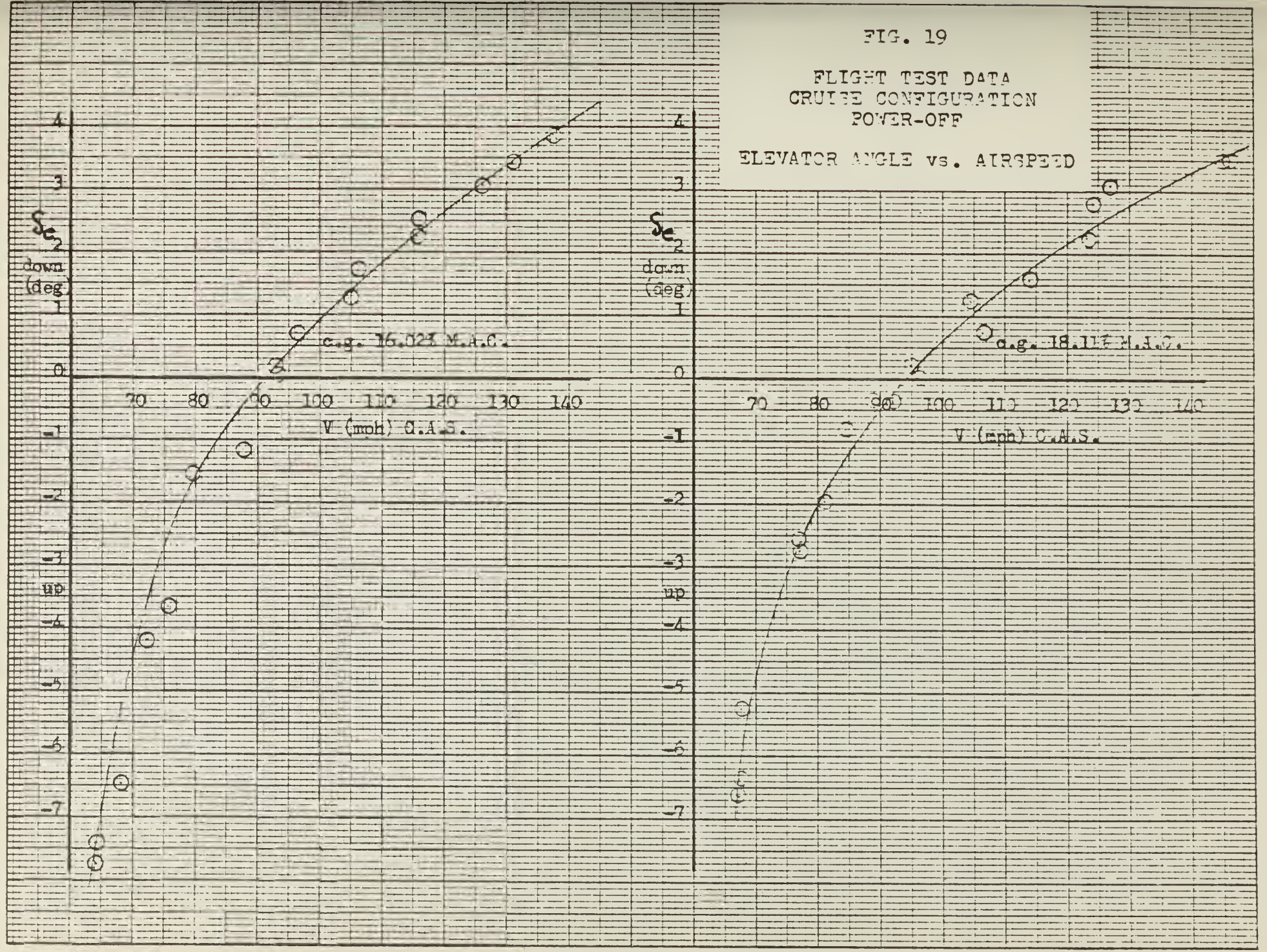

FIG. 19

FLIGHT TEST DATA
CRUISE CONFIGURATION
POWER-OFF

ELEVATOR ANGLE vs. AIRSPEED

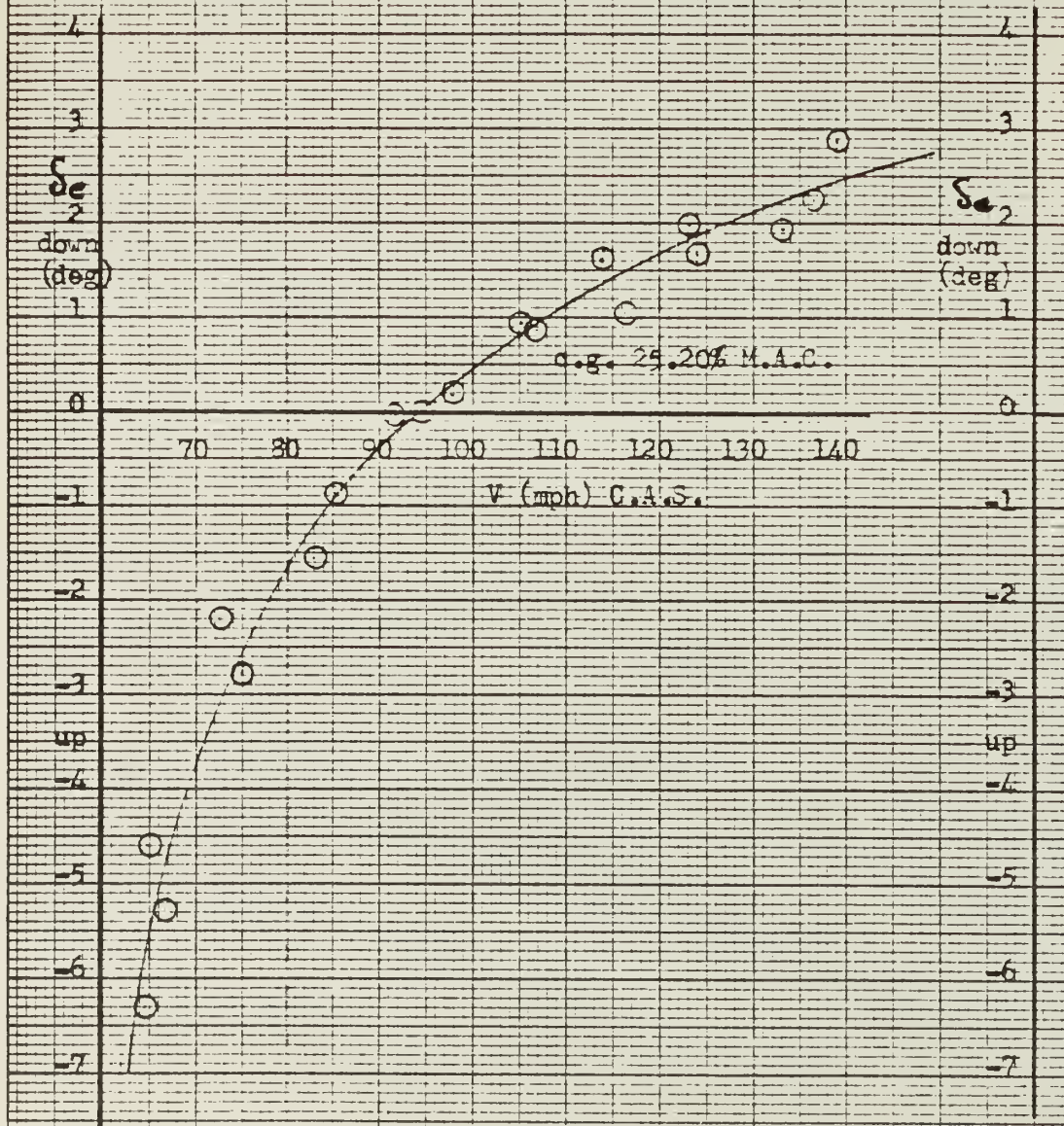

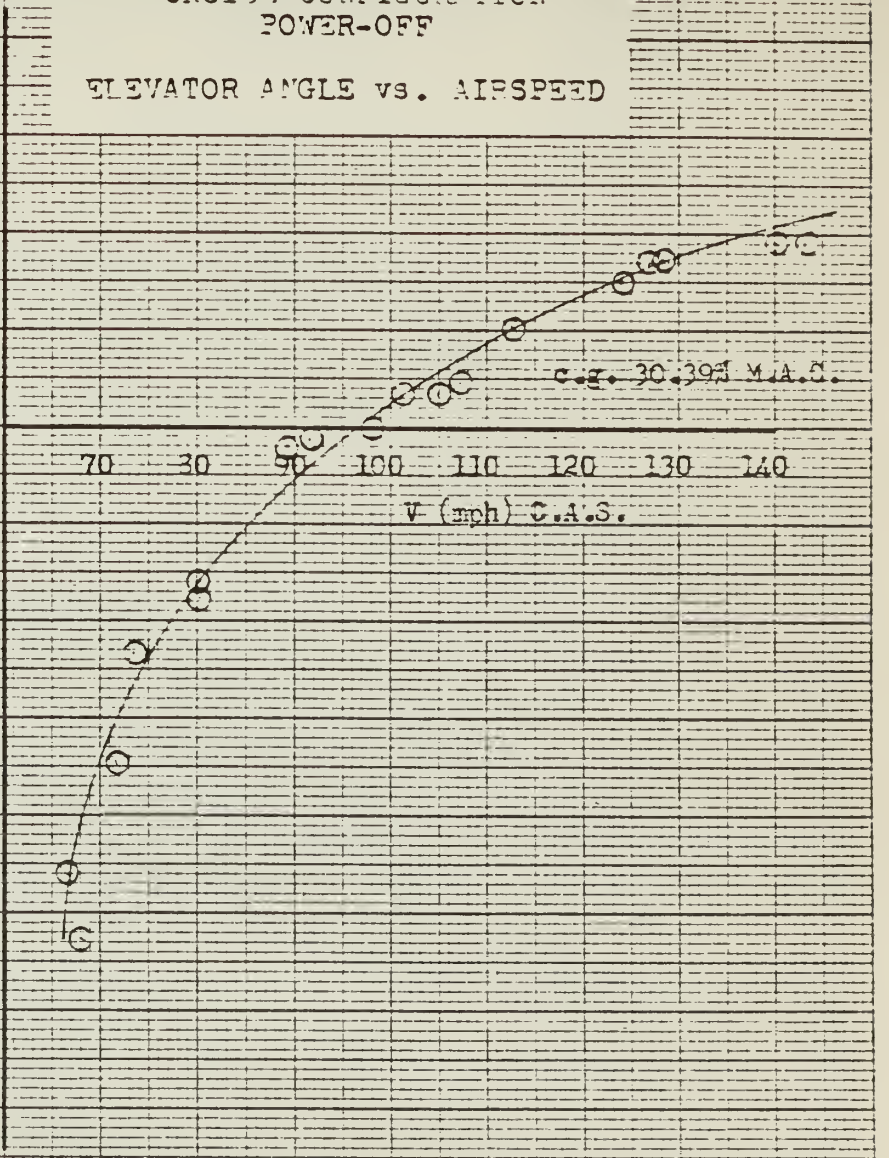

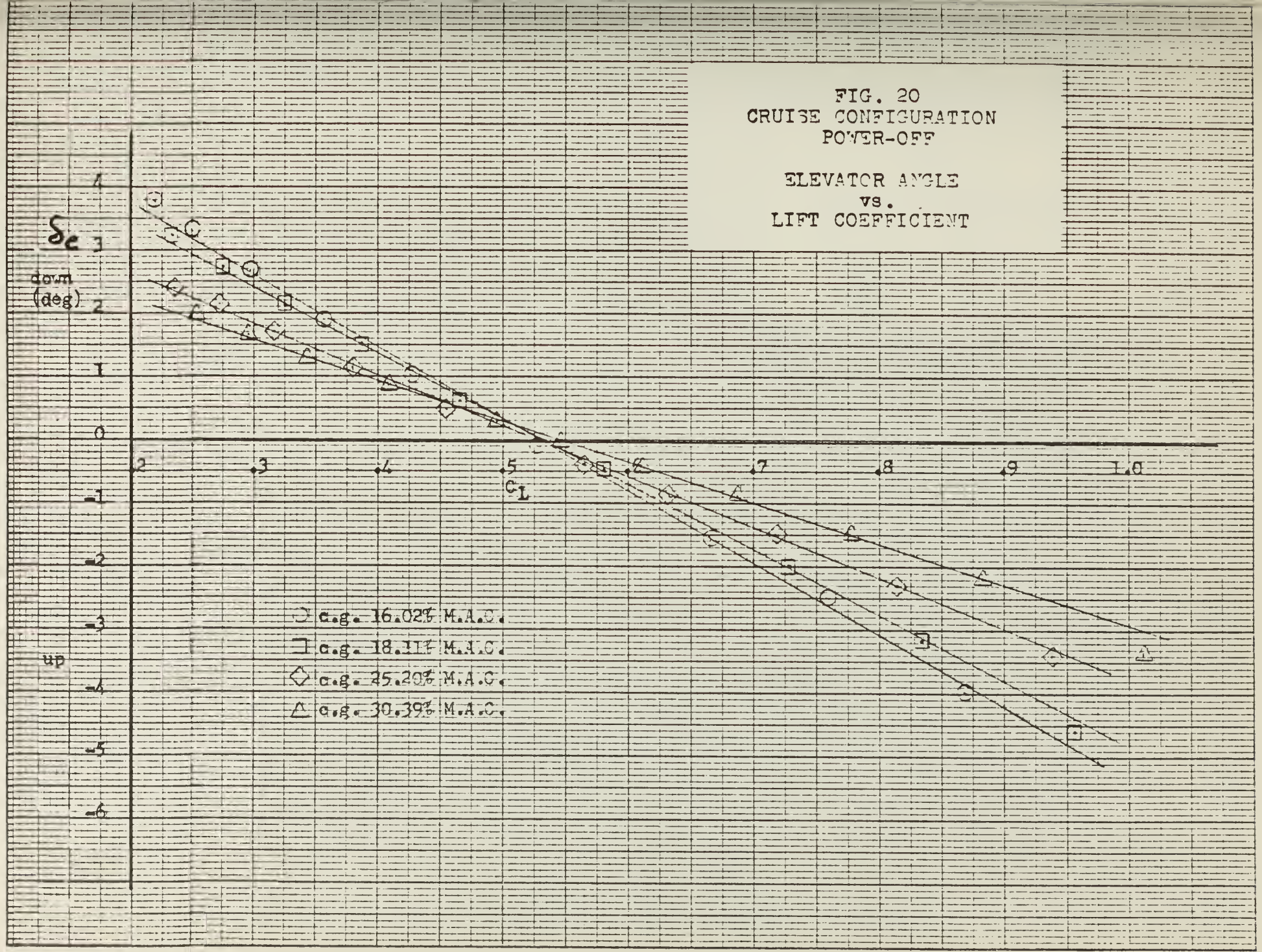
FIG. 20
CRUISE CONFIGURATION
POWER-OFF
ELEVATOR ANGLE
vs.
LIFT COEFFICIENT
δ_e
down
(deg)
up
4
3
2
1
0
-1
-2
-3
-4
-5
-6
.2
.3
.4
.5
.6
.7
.8
.9
1.0
C_L
c.g. 16.02% M.A.C.
c.g. 18.11% M.A.C.
c.g. 25.20% M.A.C.
c.g. 30.39% M.A.C.

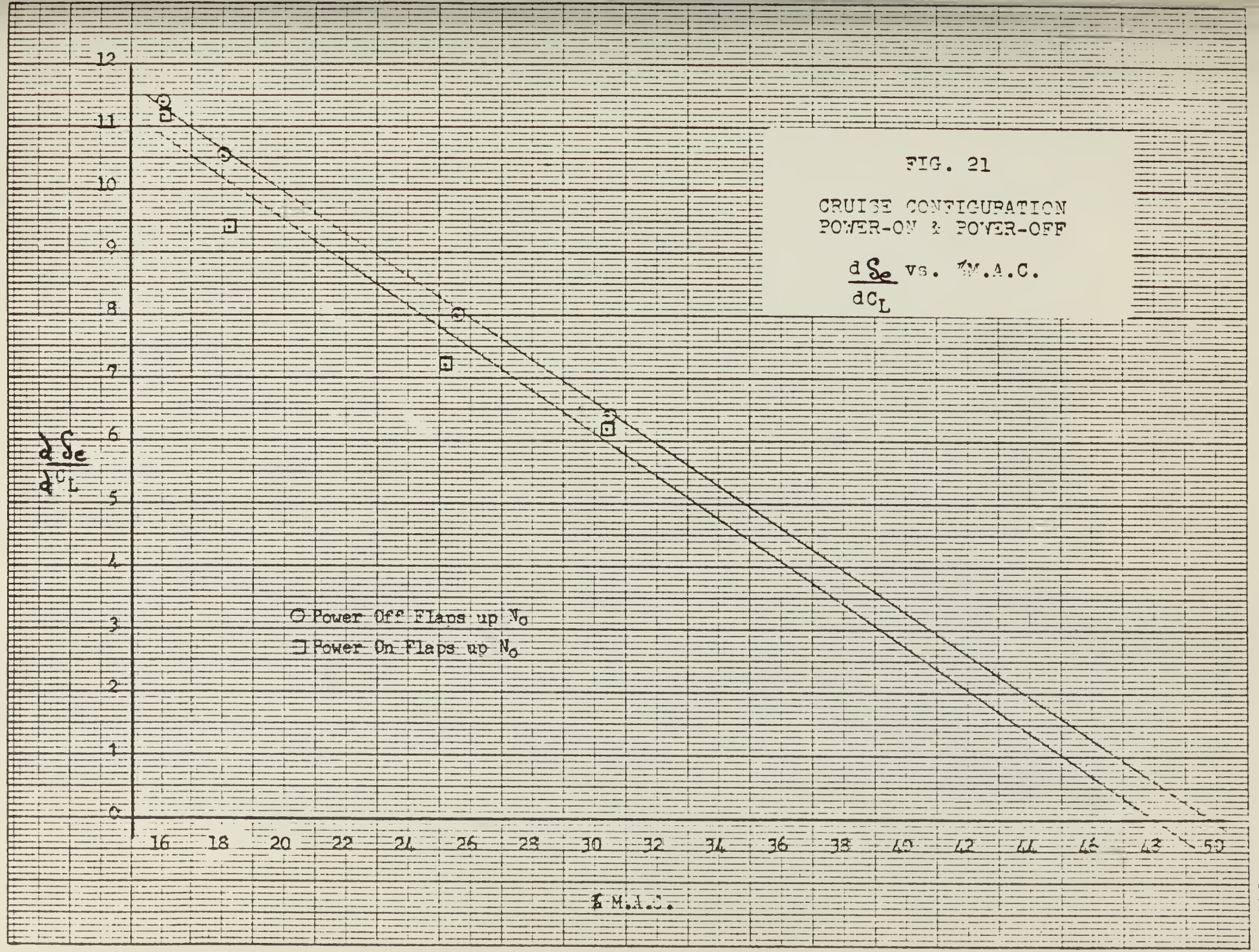
FIG. 21
CRUISE CONFIGURATION
POWER-ON & POWER-OFF
$\frac{d\varepsilon}{dC_L}$ vs. %M.A.C.
$\frac{d\varepsilon}{dC_L}$
0
1
2
3
4
5
6
7
8
9
10
11
12
16
18
20
22
24
26
28
30
32
34
36
38
40
42
44
46
48
50
% M.A.C.
O Power Off Flaps up N_o
□ Power On Flaps up N_o

FIG. 22

FLIGHT TEST DATA
CRUISE CONFIGURATION
POWER-ON

STICK FORCE vs. AIRSPEED

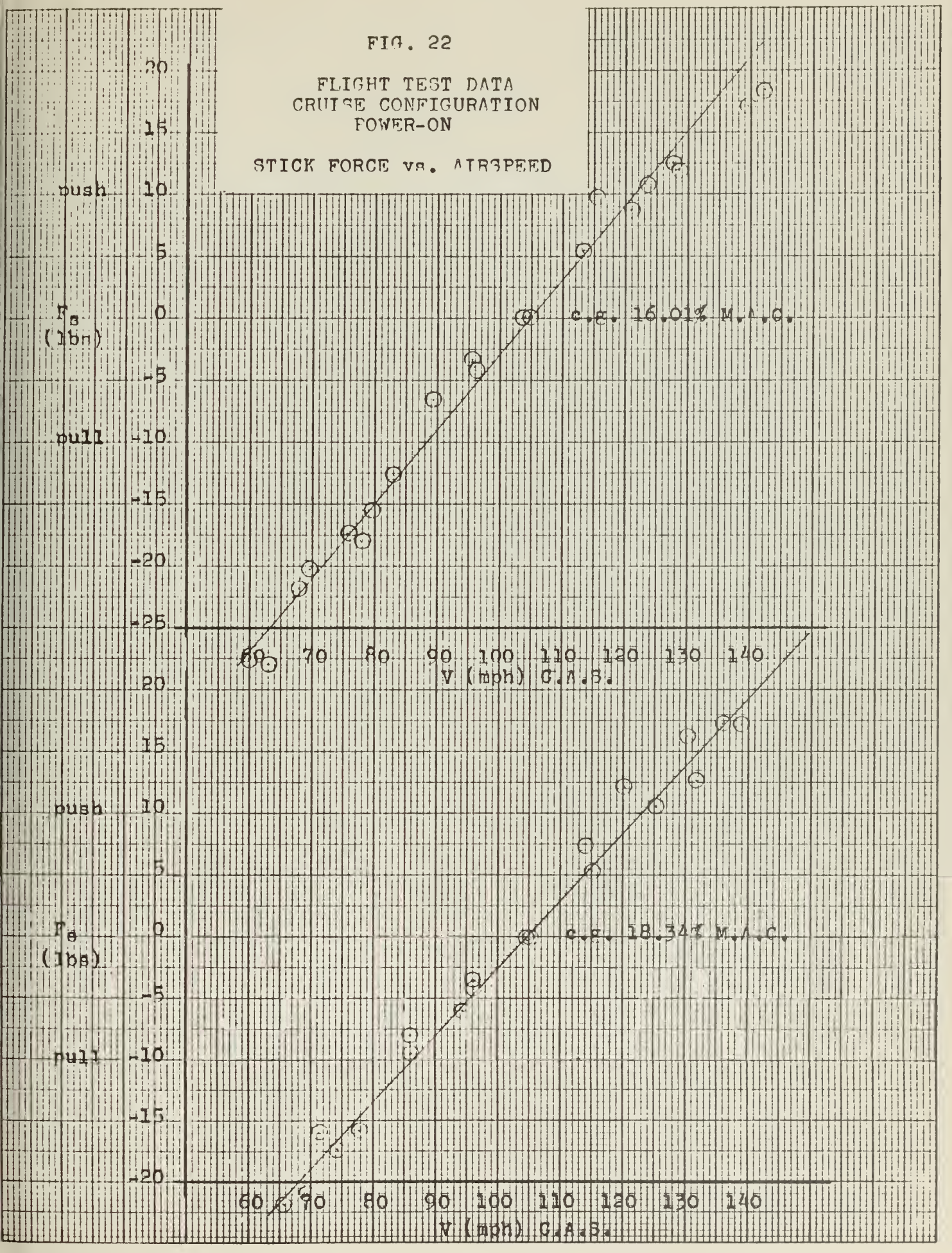

FIG. 22

FLIGHT TEST DATA
CRUISE CONFIGURATION
POWER-ON

STICK FORCE vs. AIRSPEED

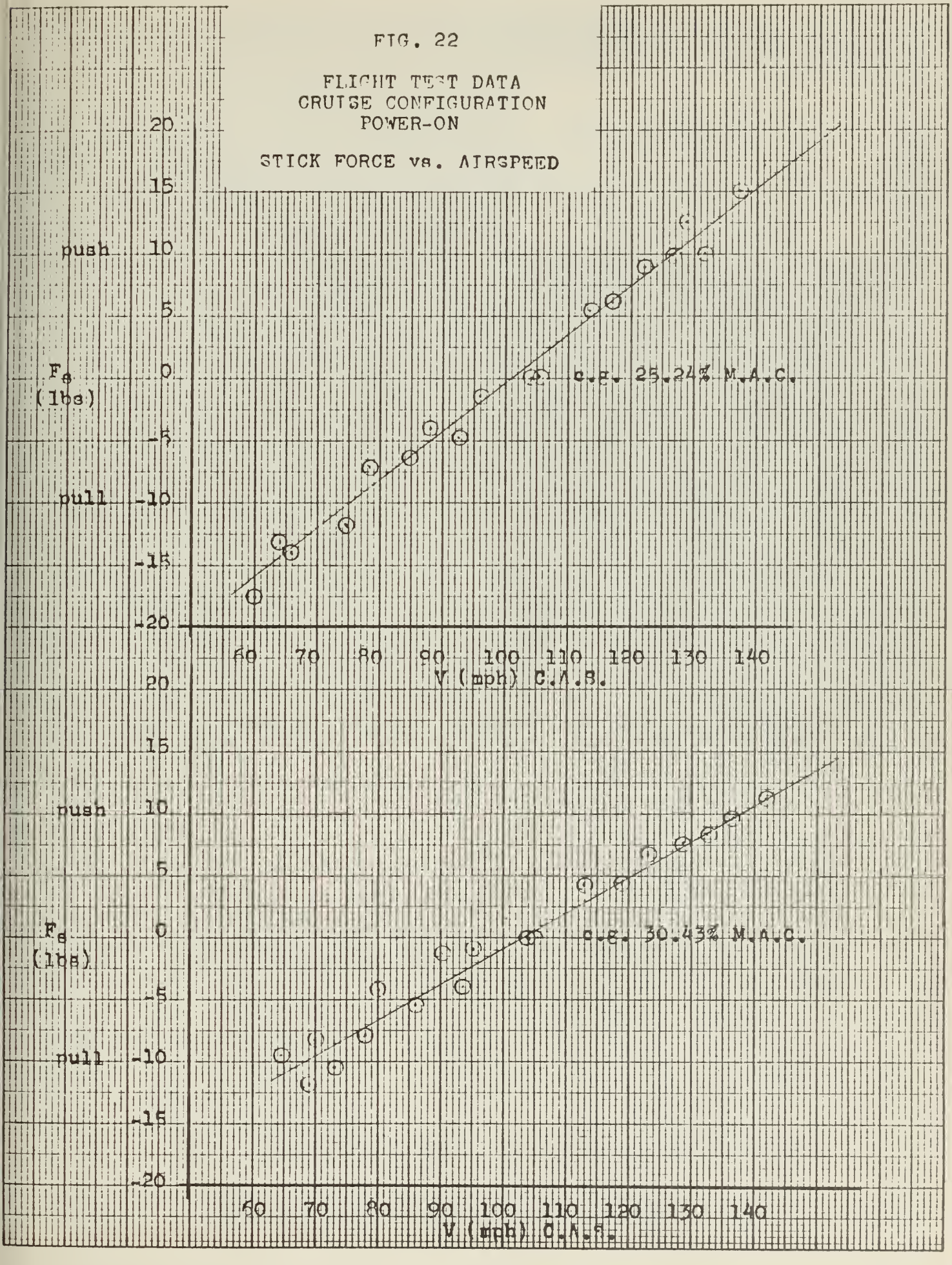

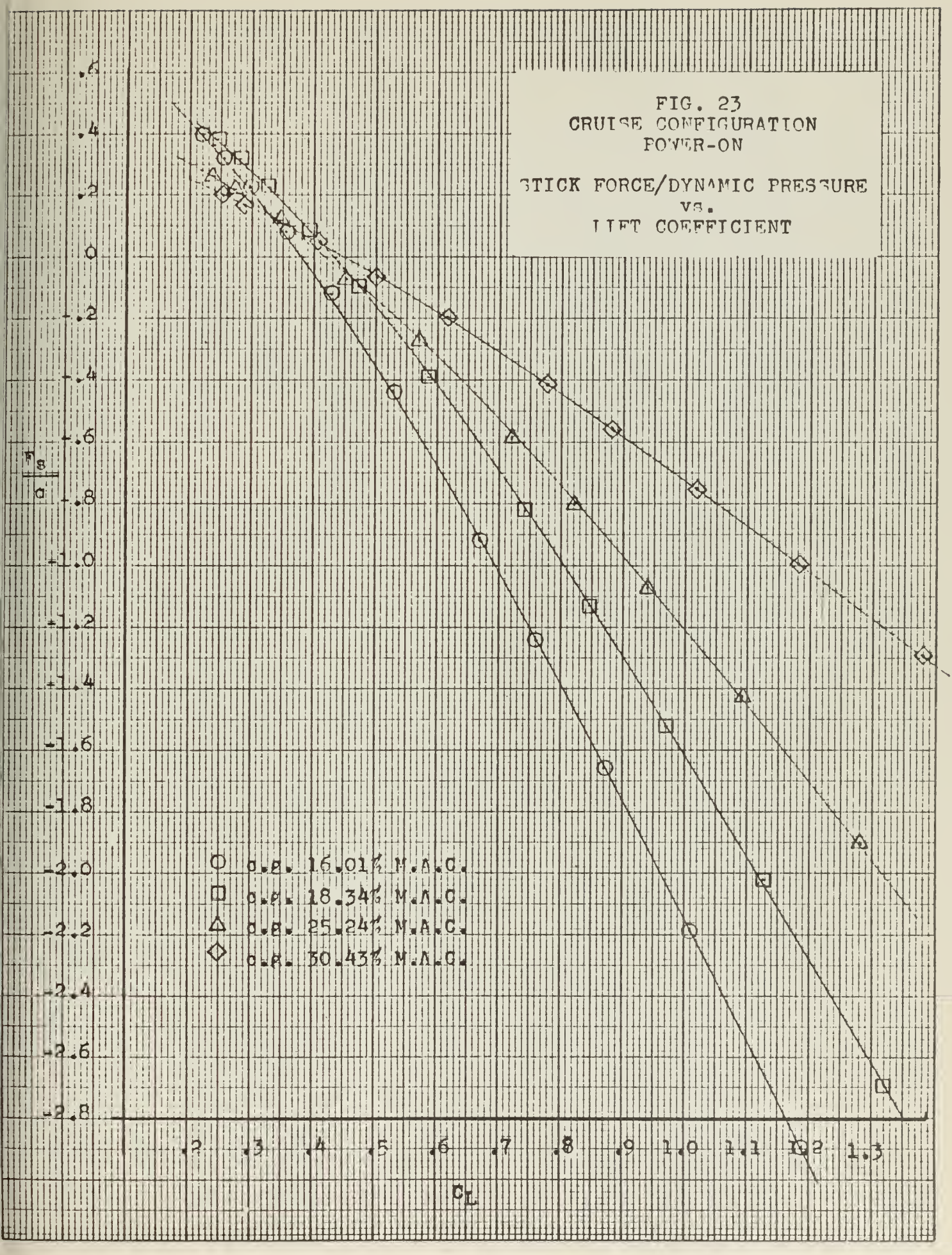
FIG. 23
CRUISE CONFIGURATION
POWER-ON
STICK FORCE/DYNAMIC PRESSURE
VS.
LIFT COEFFICIENT
.6
.4
.2
0
-.2
-.4
-.6
-.8
-1.0
-1.2
-1.4
-1.6
-1.8
-2.0
-2.2
-2.4
-2.6
-2.8
Fs/q
.2
.3
.4
.5
.6
.7
.8
.9
1.0
1.1
1.2
1.3
CL
○ c.g. 16.01% M.A.C.
□ c.g. 18.34% M.A.C.
△ c.g. 25.24% M.A.C.
◇ c.g. 30.43% M.A.C.

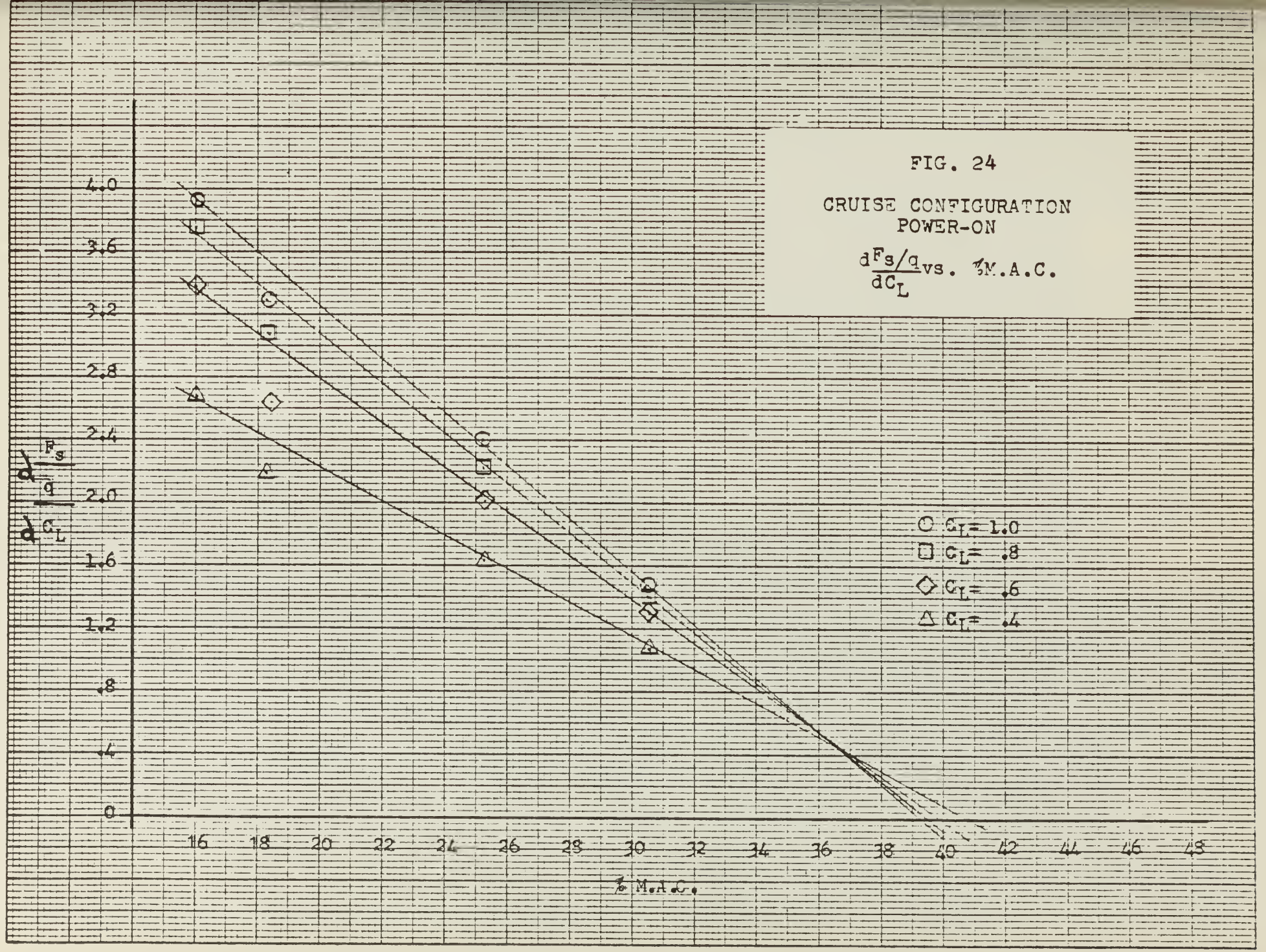
FIG. 24
CRUISE CONFIGURATION
POWER-ON
$\frac{d\frac{F_s}{q}}{dC_L}$ vs. % M.A.C.
$\frac{d\frac{F_s}{q}}{dC_L}$
4.0
3.6
3.2
2.8
2.4
2.0
1.6
1.2
.8
.4
0
16
18
20
22
24
26
28
30
32
34
36
38
40
42
44
46
48
% M.A.C.
○ C_L = 1.0
□ C_L = .8
◇ C_L = .6
△ C_L = .4

FIG. 25

FLIGHT TEST DATA
CRUISE CONFIGURATION
POWER-OFF

STICK FORCE vs. AIRSPEED

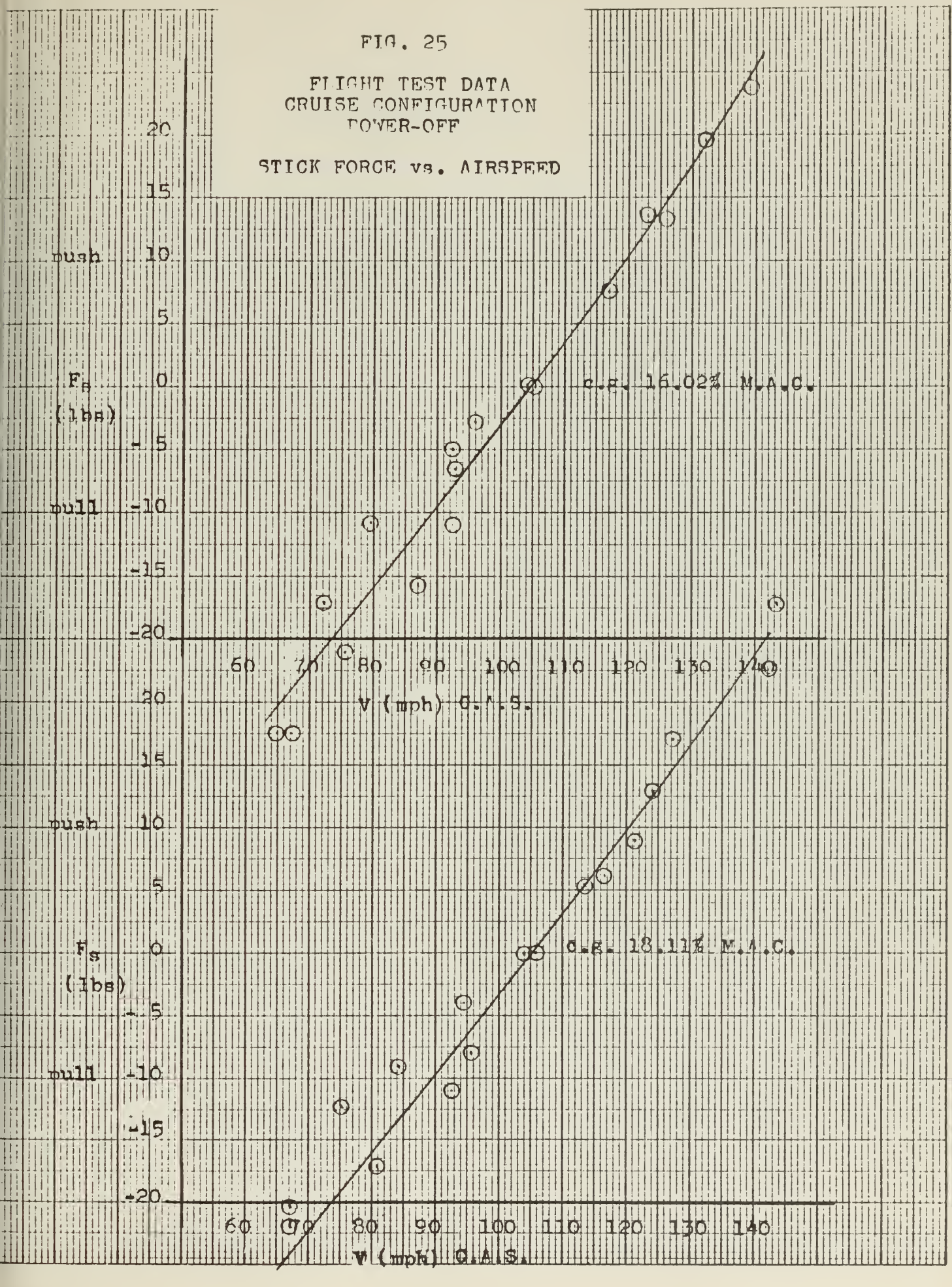

FIG. 25

FLIGHT TEST DATA
CRUISE CONFIGURATION
POWER-OFF

STICK FORCE vs. AIRSPEED

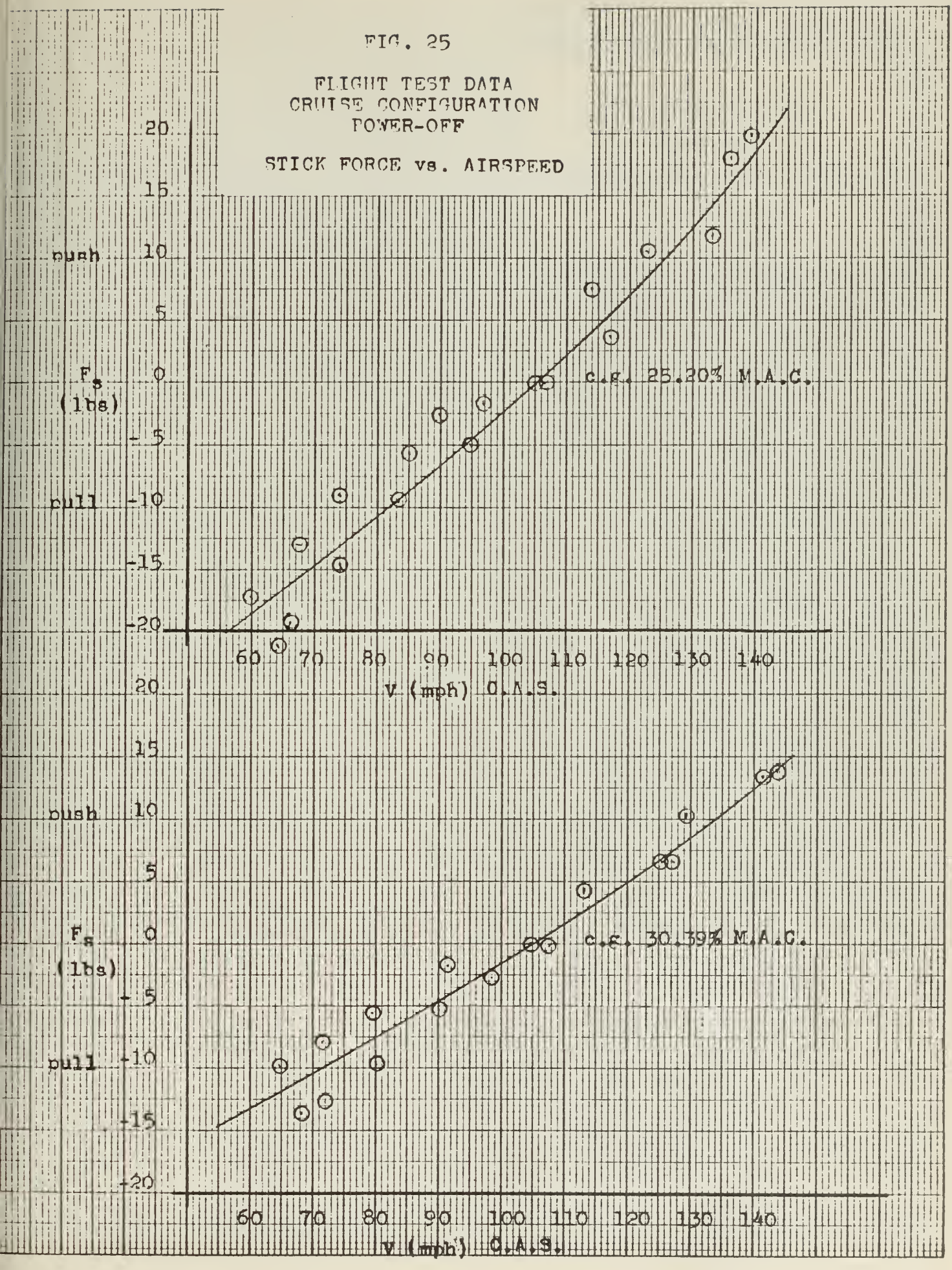

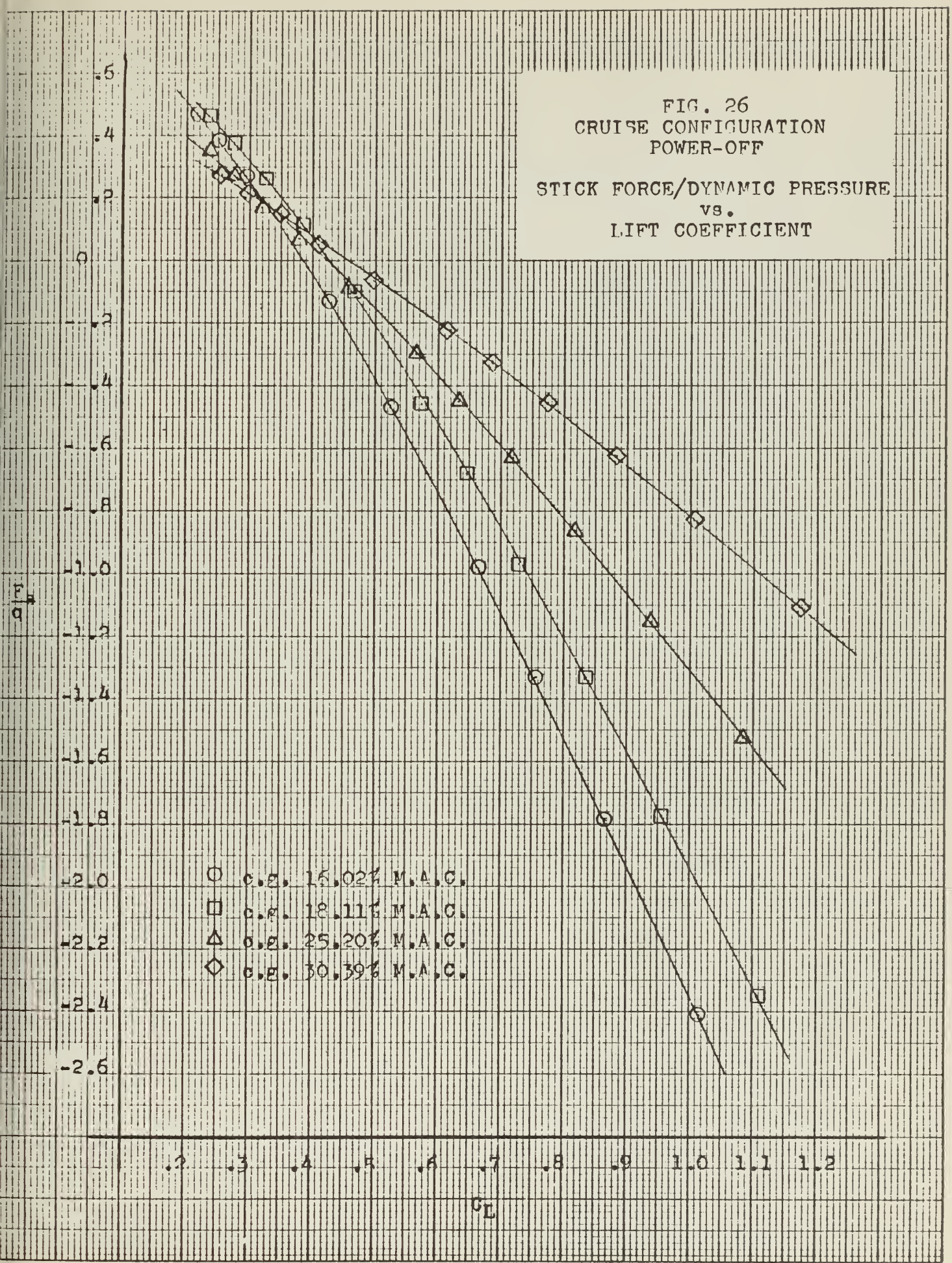
FIG. 26
CRUISE CONFIGURATION
POWER-OFF
STICK FORCE/DYNAMIC PRESSURE
vs.
LIFT COEFFICIENT
.6
.4
.2
0
-.2
-.4
-.6
-.8
-1.0
-1.2
-1.4
-1.6
-1.8
-2.0
-2.2
-2.4
-2.6
$\frac{F_s}{q}$
○ c.g. 16.02% M.A.C.
□ c.g. 18.11% M.A.C.
△ c.g. 25.20% M.A.C.
◇ c.g. 30.39% M.A.C.
.2
.3
.4
.5
.6
.7
.8
.9
1.0
1.1
1.2
C_L

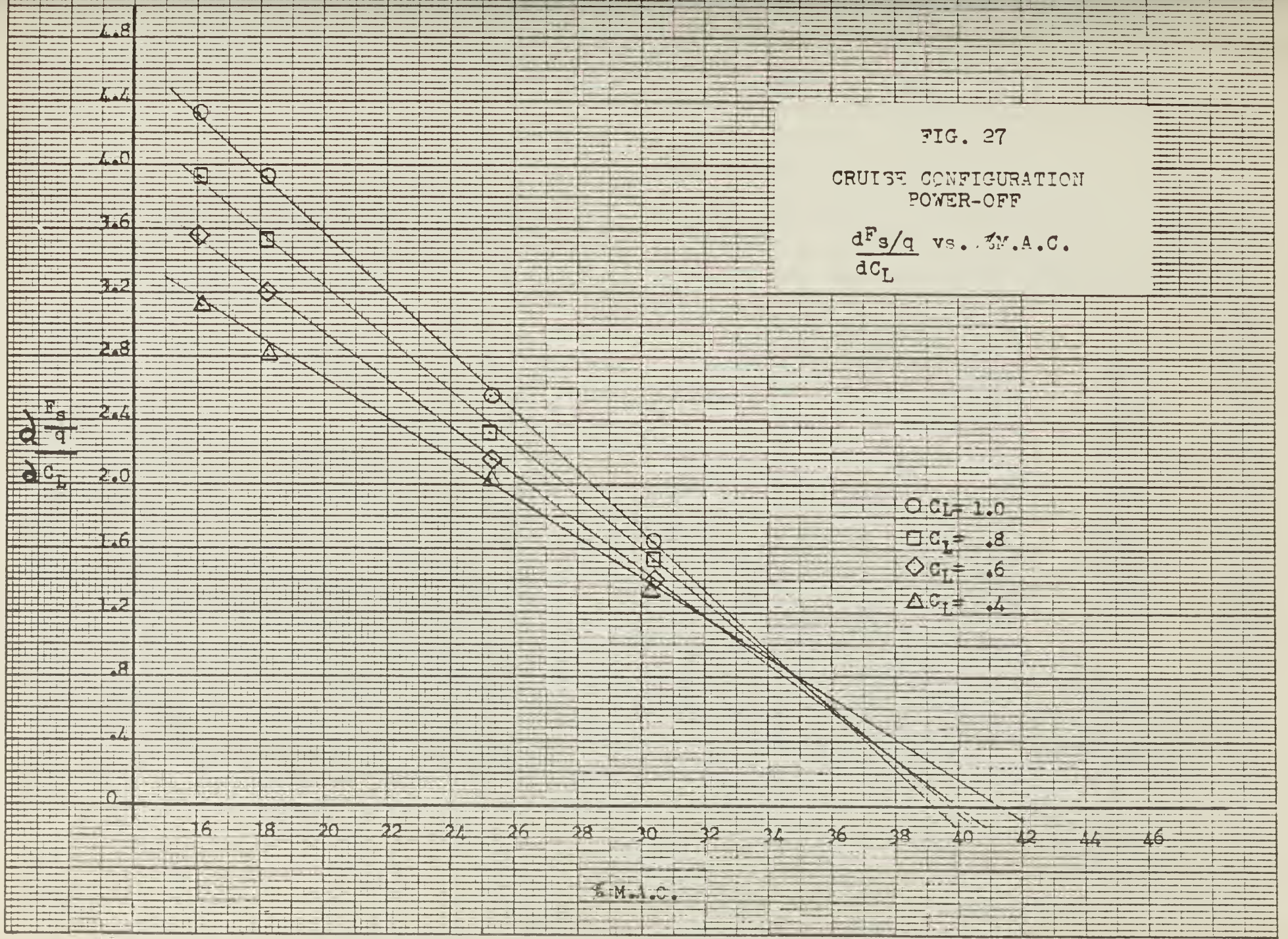
FIG. 27
CRUISE CONFIGURATION
POWER-OFF
$\frac{dF_s/q}{dC_L}$ vs. %M.A.C.
$\frac{\partial \frac{F_s}{q}}{\partial C_L}$
4.8
4.4
4.0
3.6
3.2
2.8
2.4
2.0
1.6
1.2
.8
.4
0
16
18
20
22
24
26
28
30
32
34
36
38
40
42
44
46
% M.A.C.
○ C_L = 1.0
□ C_L = .8
◇ C_L = .6
△ C_L = .4

FIG. 28

NEUTRAL POINT SUMMARY
CRUISE CONFIGURATION

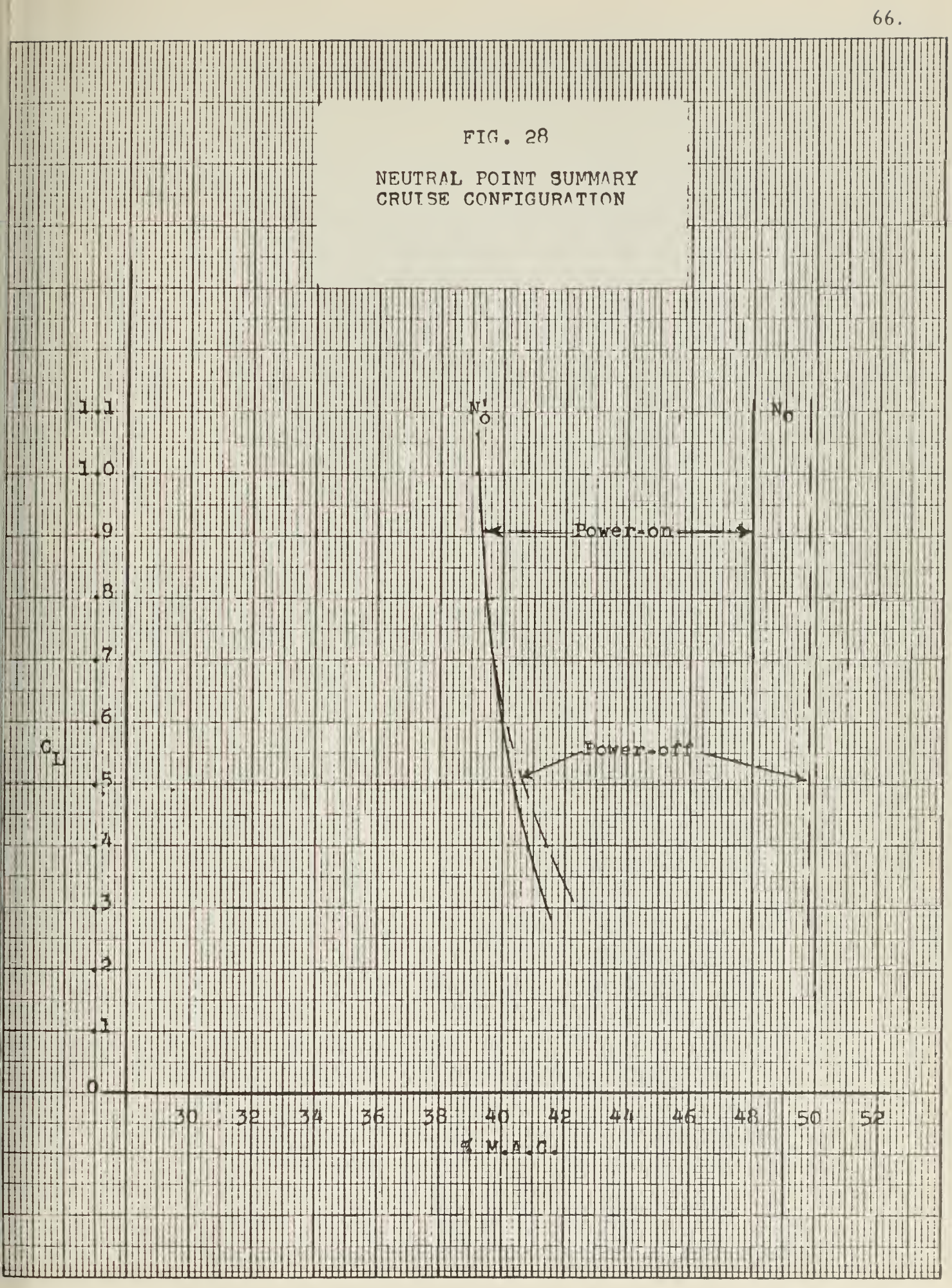

FIG. 29

FLIGHT TEST DATA
APPROACH CONFIGURATION
POWER -ON

ELEVATOR ANGLE vs. AIRSPEED

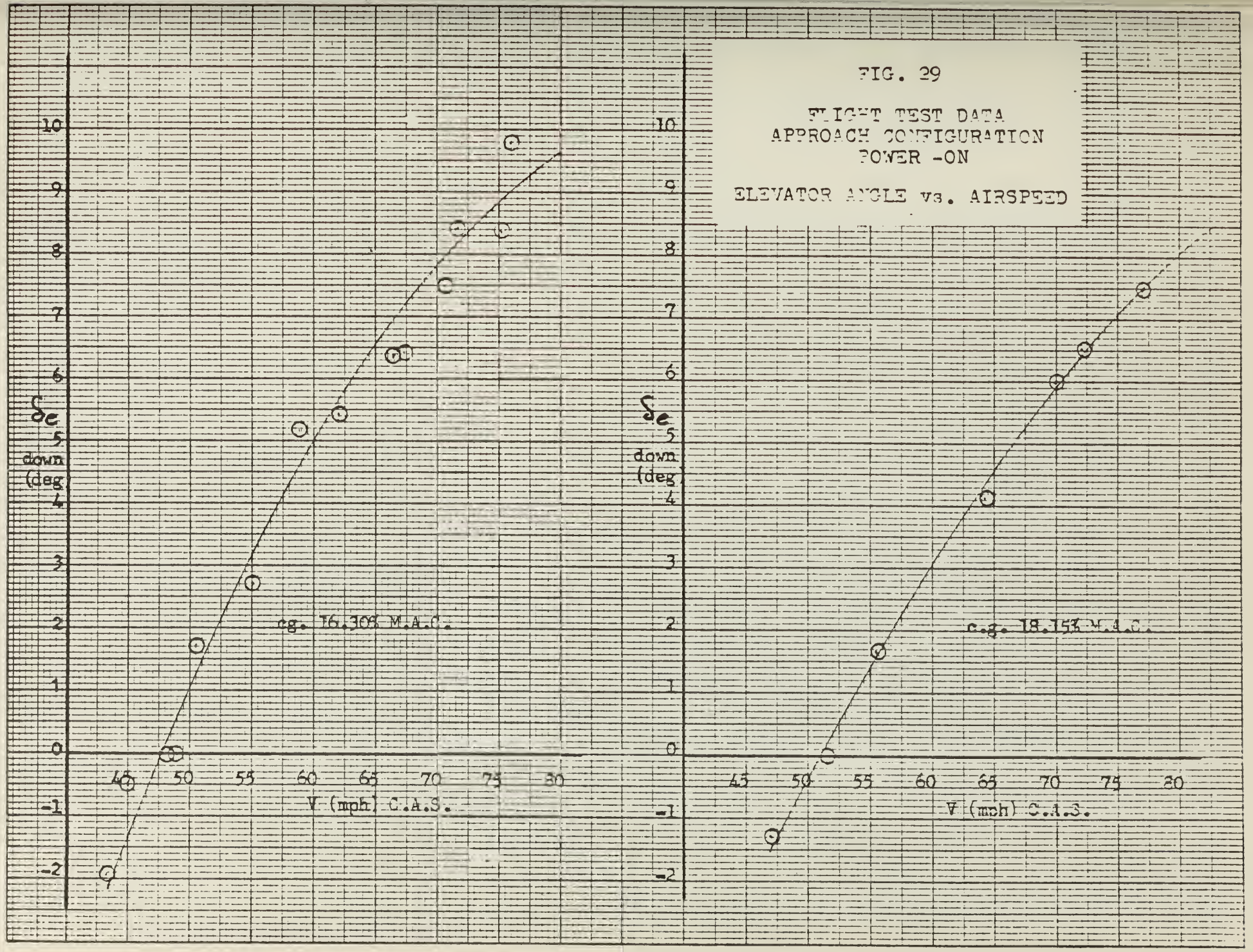

FIG. 29

FLIGHT TEST DATA
APPROACH CONFIGURATION
POWER-ON

ELEVATOR ANGLE vs. AIRSPEED

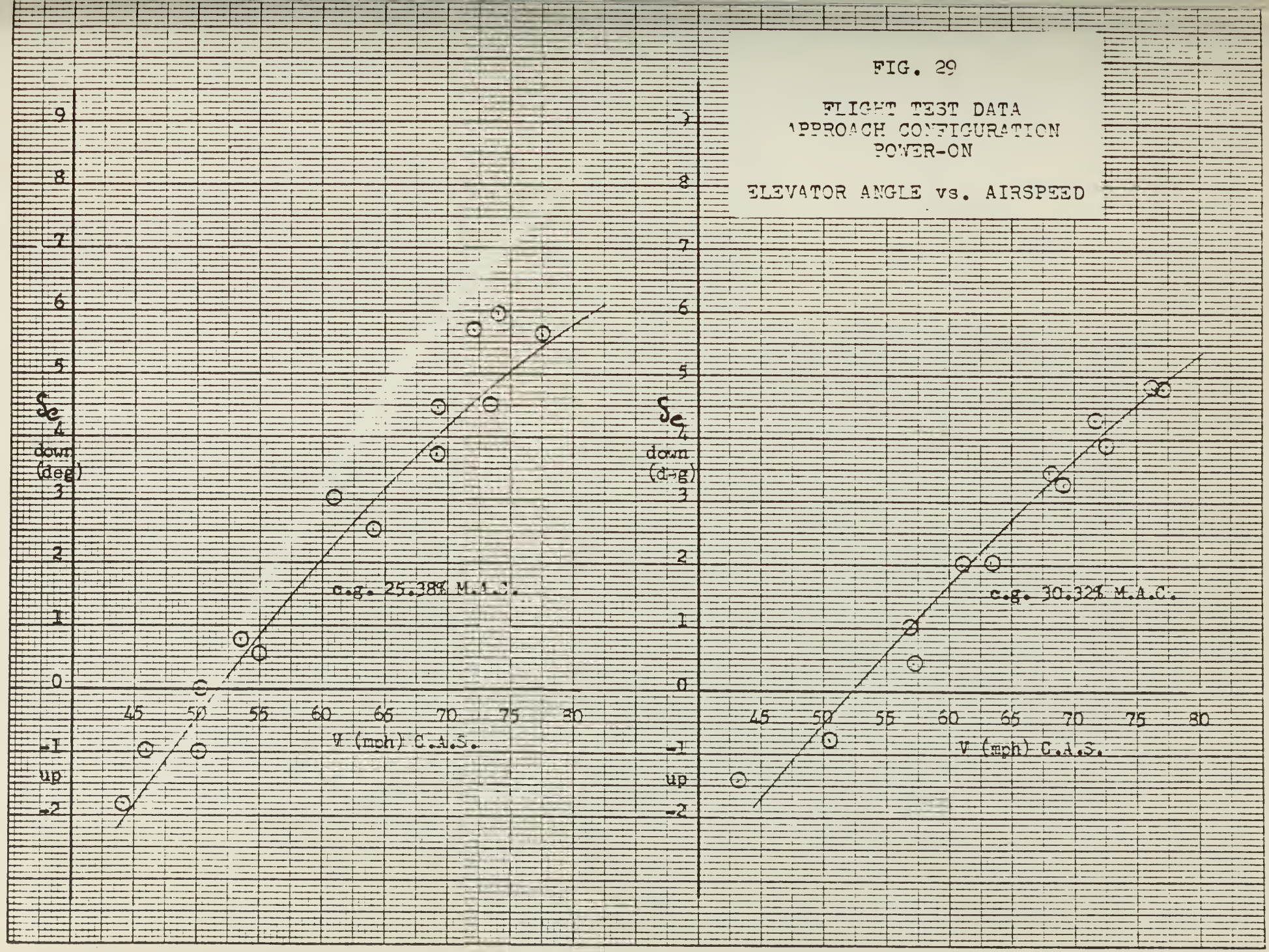

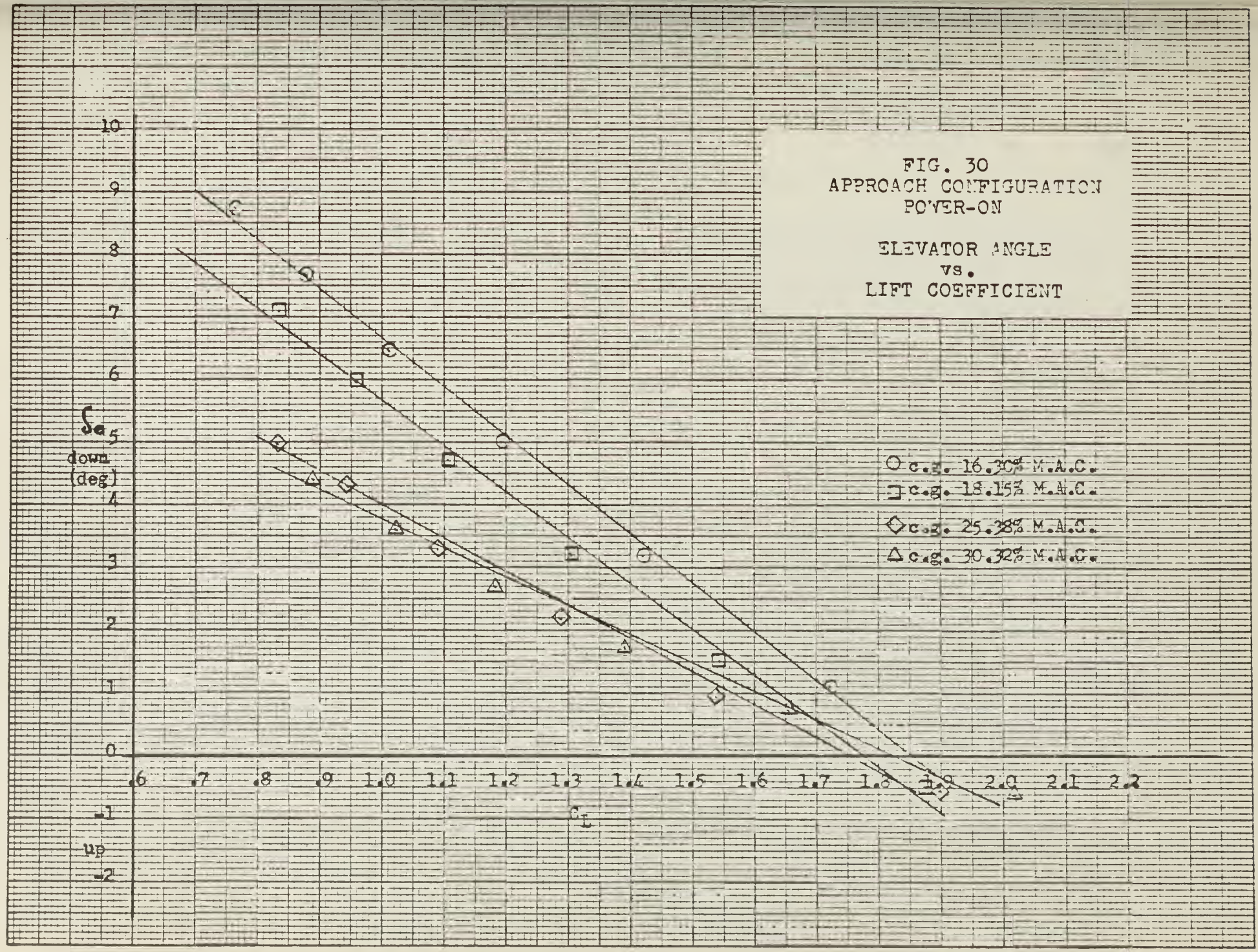
FIG. 30
APPROACH CONFIGURATION
POWER-ON
ELEVATOR ANGLE
vs.
LIFT COEFFICIENT
c.g. 16.30% M.A.C.
c.g. 18.15% M.A.C.
c.g. 25.38% M.A.C.
c.g. 30.32% M.A.C.
δe5
down
(deg)
up
CL
10
9
8
7
6
4
3
2
1
0
-1
-2
.6
.7
.8
.9
1.0
1.1
1.2
1.3
1.4
1.5
1.6
1.7
1.8
2.0
2.1
2.2

FIG. 31

FLIGHT TEST DATA
APPROACH CONFIGURATION
POWER-OFF

ELEVATOR ANGLE vs. AIRSPEED

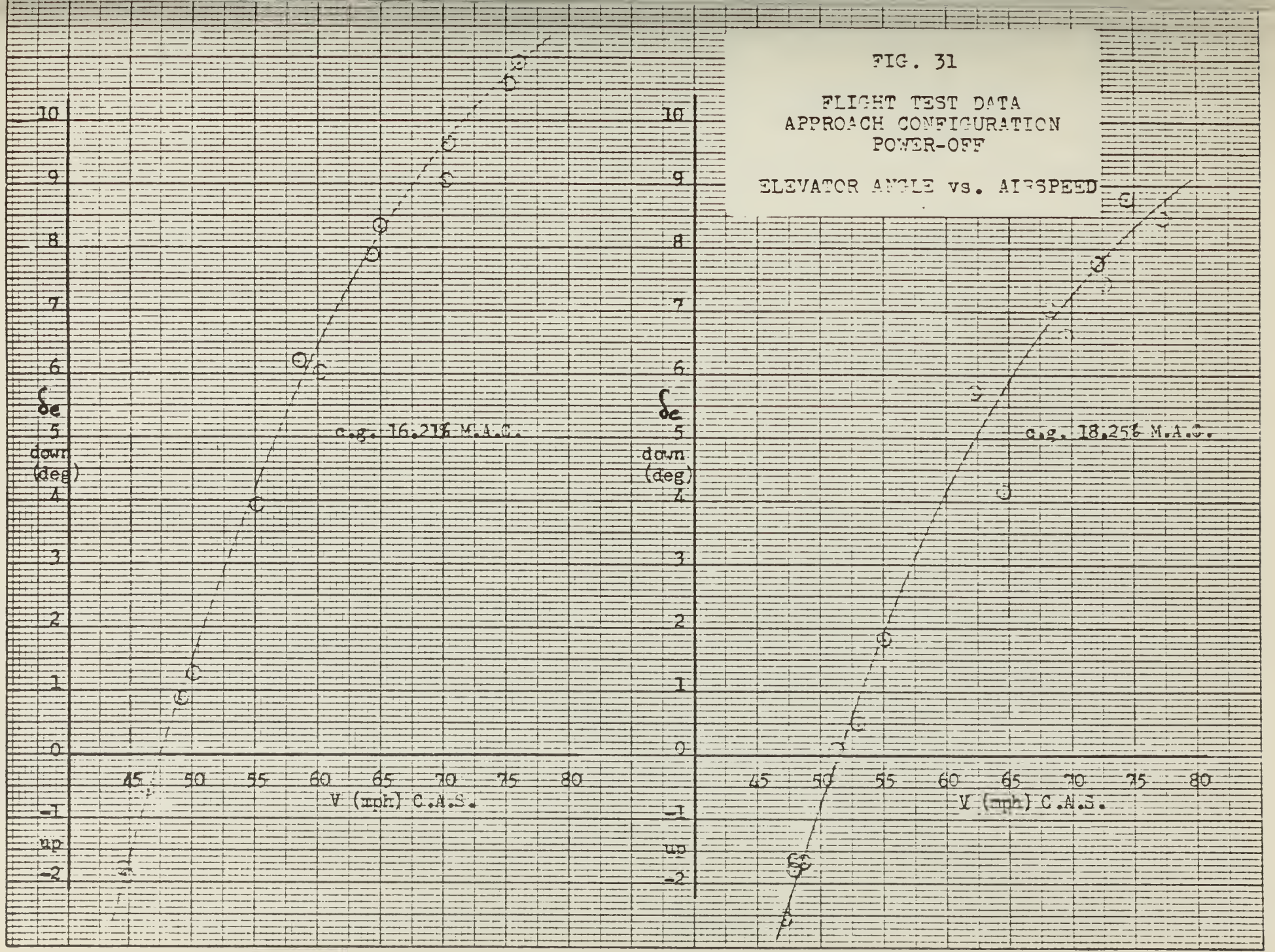

FIG. 31

FLIGHT TEST DATA
APPROACH CONFIGURATION
POWER-OFF

ELEVATOR ANGLE vs. AIRSPEED

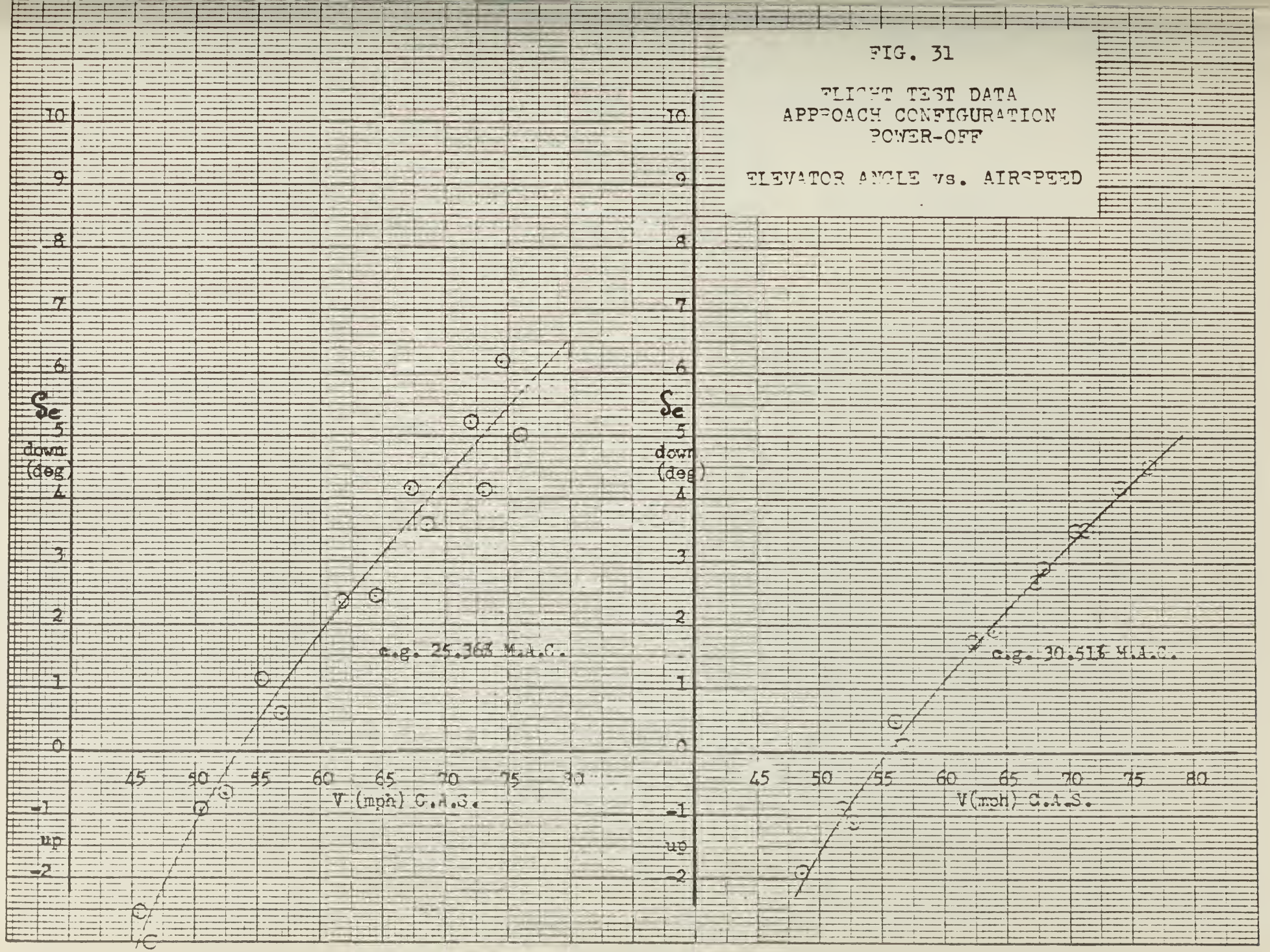

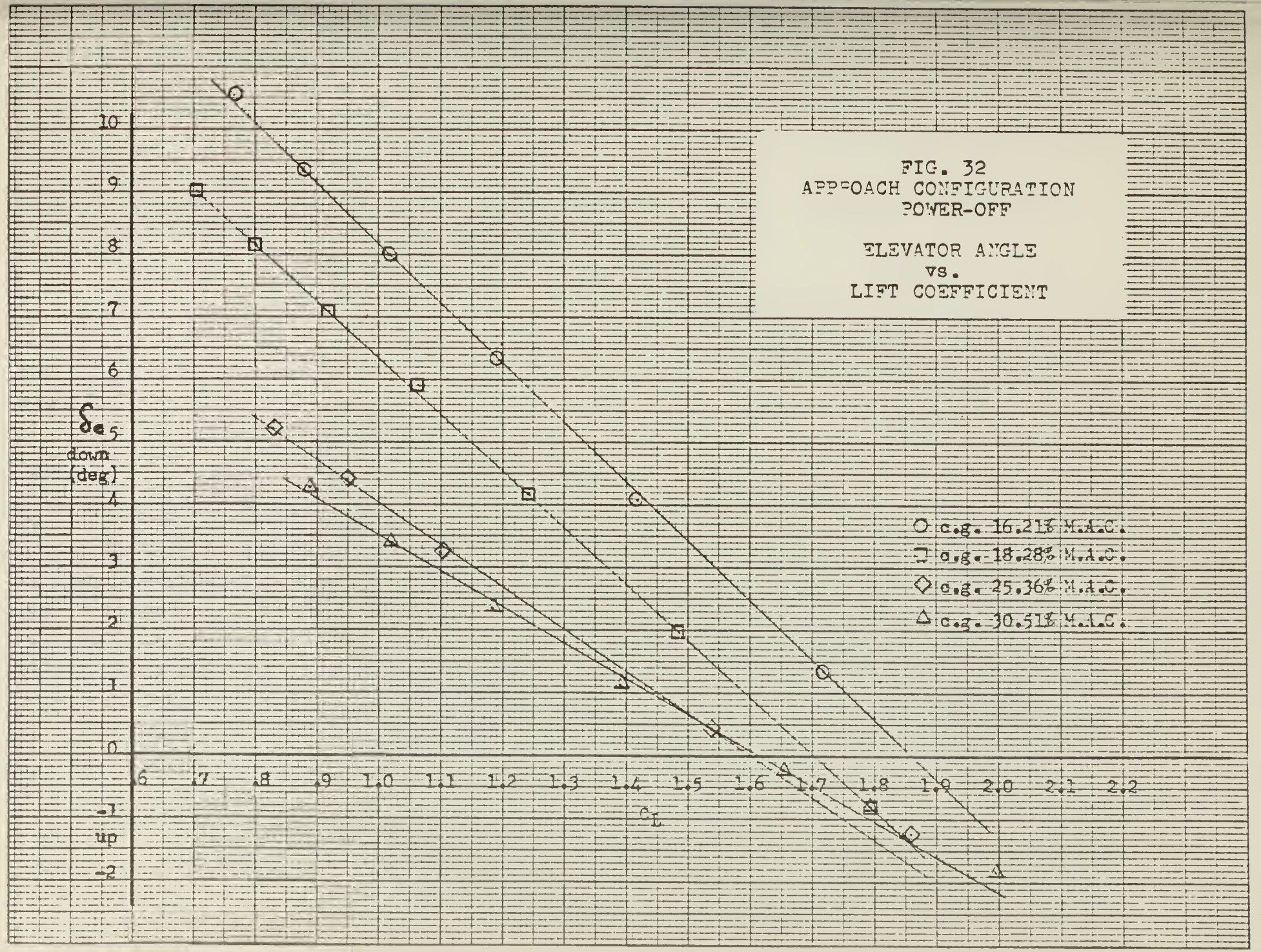
FIG. 32
APPROACH CONFIGURATION
POWER-OFF
ELEVATOR ANGLE
vs.
LIFT COEFFICIENT
δe down (deg)
up
CL
○ c.g. 16.21% M.A.C.
□ c.g. 18.28% M.A.C.
◇ c.g. 25.36% M.A.C.
△ c.g. 30.51% M.A.C.
10
9
8
7
6
5
4
3
2
1
0
-1
-2
.6
.7
.8
.9
1.0
1.1
1.2
1.3
1.4
1.5
1.6
1.7
1.8
1.9
2.0
2.1
2.2

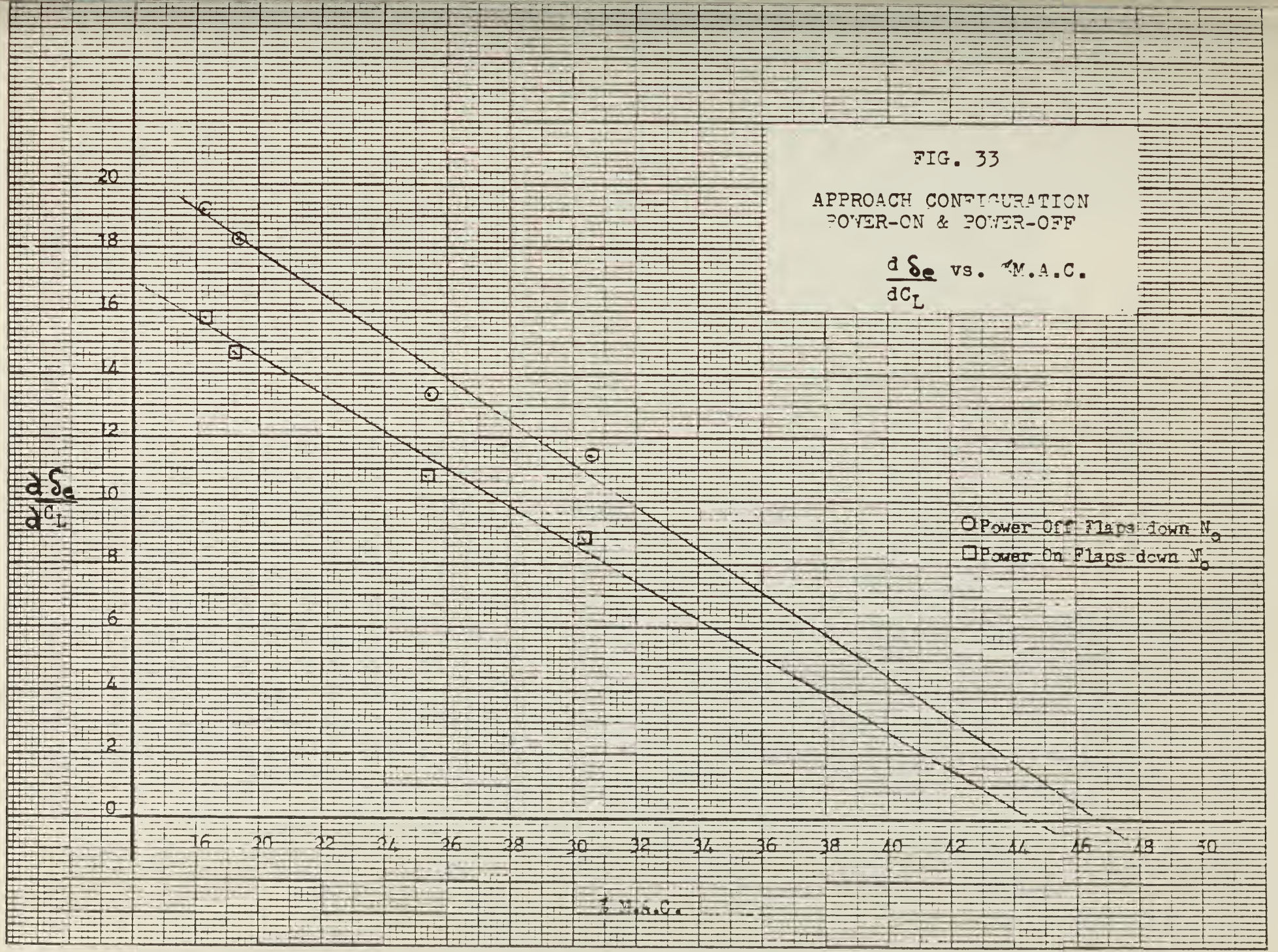
FIG. 33
APPROACH CONFIGURATION
POWER-ON & POWER-OFF
$\frac{d\delta_e}{dC_L}$ vs. C.G.
$\frac{d\delta_e}{dC_L}$
20
18
16
14
12
10
8
6
4
2
0
16
20
22
24
26
28
30
32
34
36
38
40
42
44
46
48
50
% M.A.C.
○Power Off Flaps down N_o
□Power On Flaps down N_o

FIG. 34

FLIGHT TEST DATA
APPROACH CONFIGURATION
POWER-ON

STICK FORCE vs. AIRSPEED

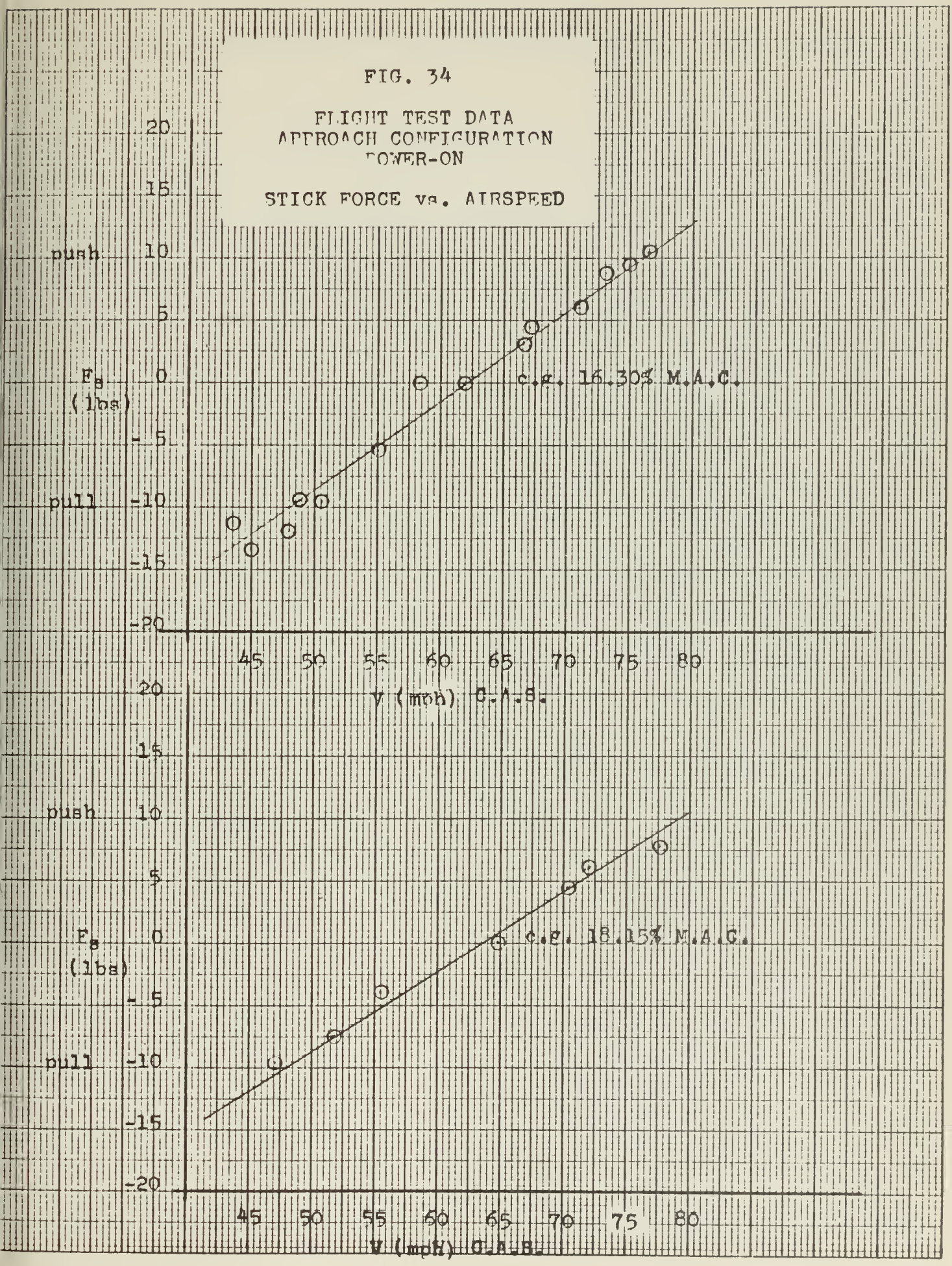

FIG. 34

FLIGHT TEST DATA
APPROACH CONFIGURATION
POWER-ON

STICK FORCE vs. AIRSPEED

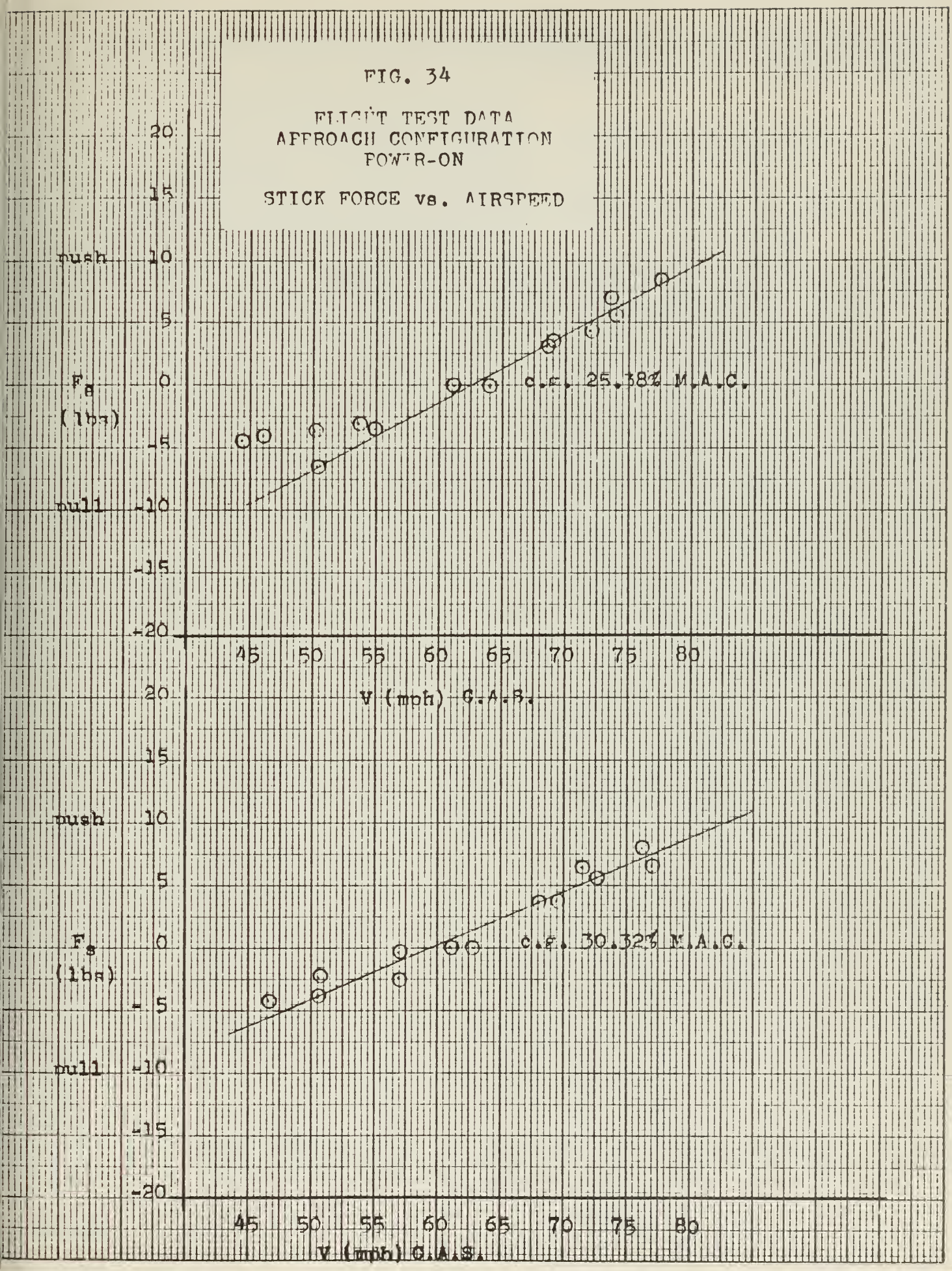

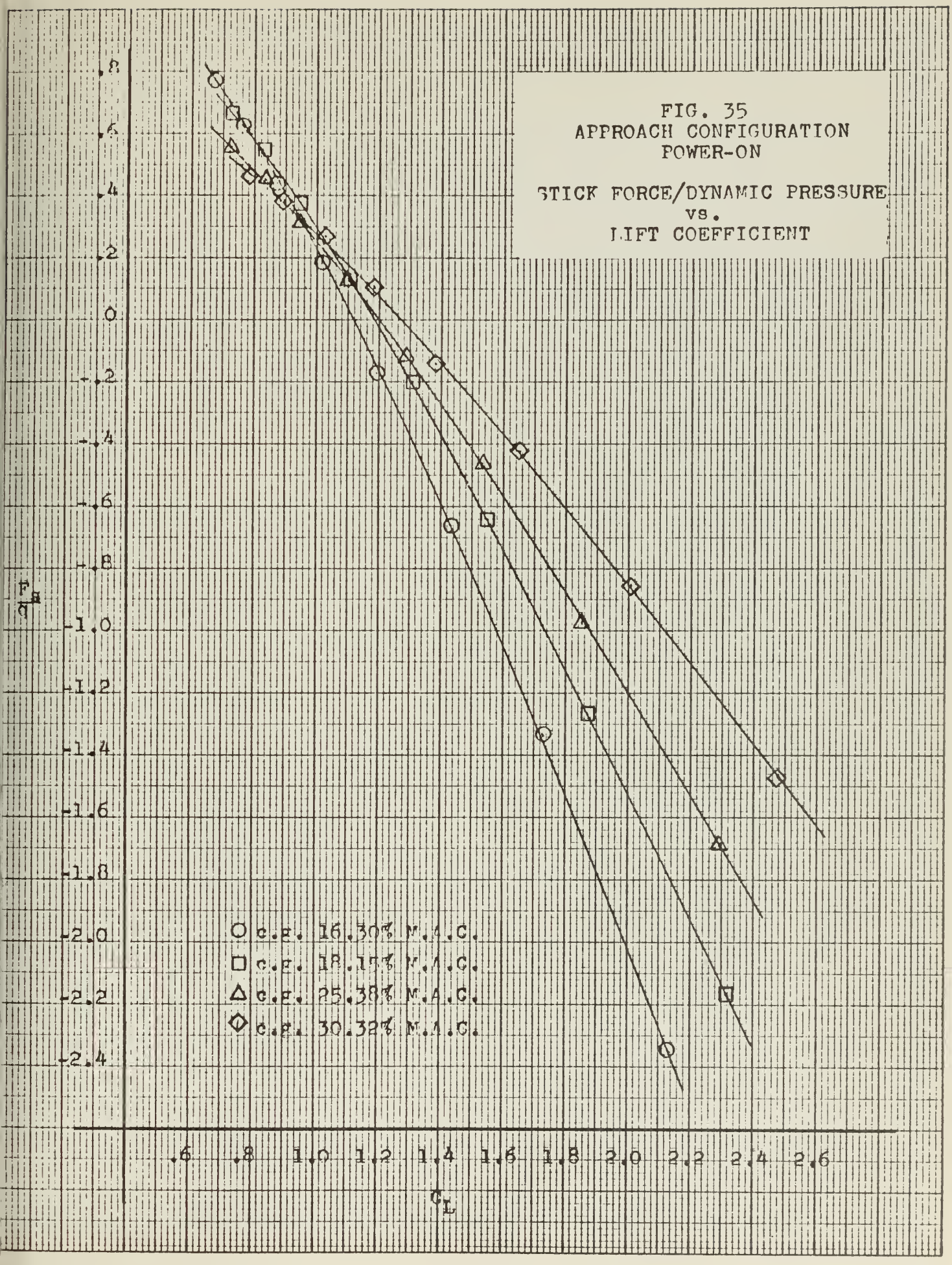
FIG. 35
APPROACH CONFIGURATION
POWER-ON
STICK FORCE/DYNAMIC PRESSURE
vs.
LIFT COEFFICIENT
.8
.6
.4
.2
0
-.2
-.4
-.6
-.8
-1.0
-1.2
-1.4
-1.6
-1.8
-2.0
-2.2
-2.4
Fs/q
○ c.g. 16.30% M.A.C.
□ c.g. 18.17% M.A.C.
△ c.g. 25.38% M.A.C.
◇ c.g. 30.32% M.A.C.
.6 .8 1.0 1.2 1.4 1.6 1.8 2.0 2.2 2.4 2.6
CL

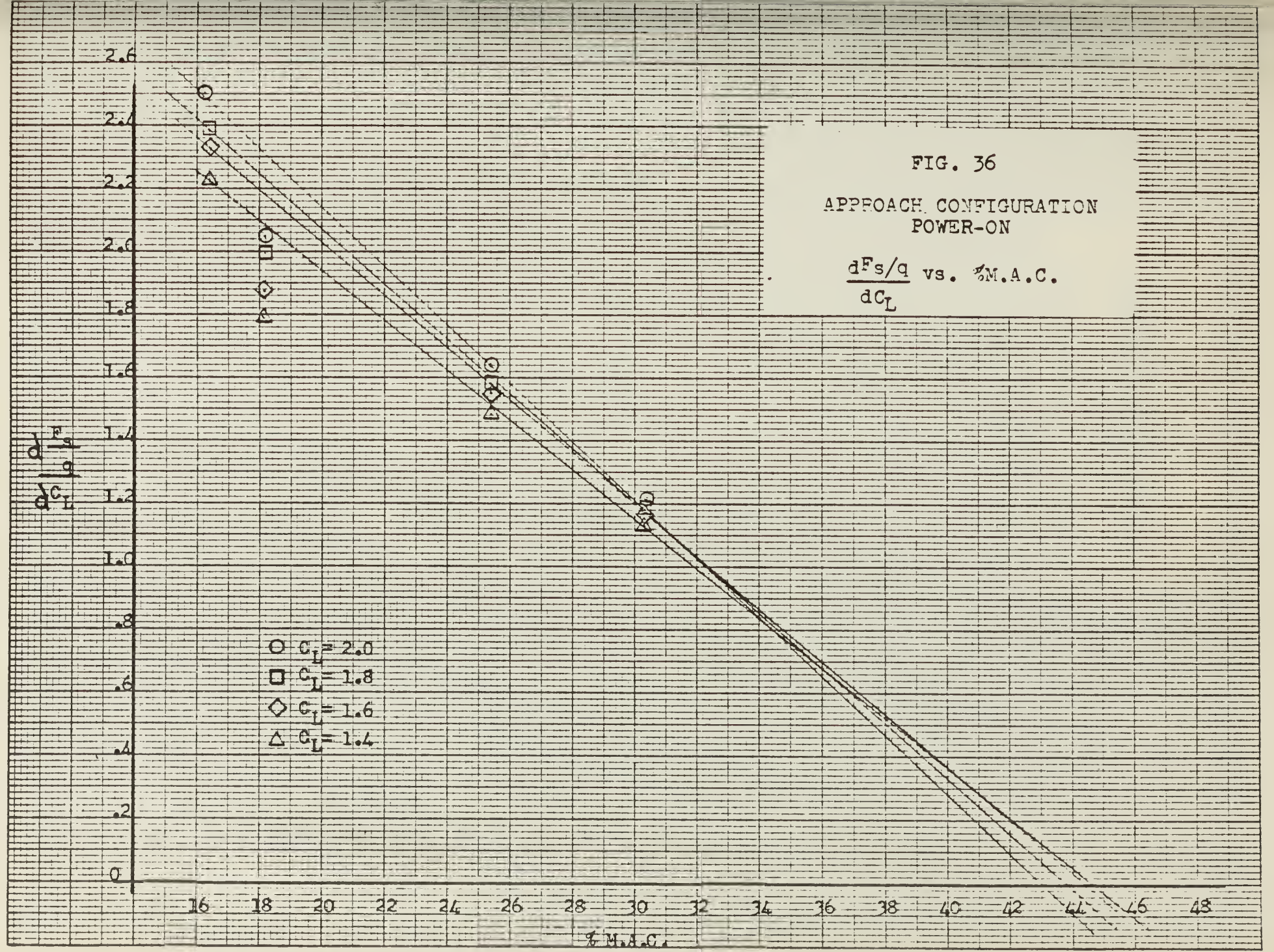
FIG. 36
APPROACH CONFIGURATION
POWER-ON
dFs/q / dCL vs. %M.A.C.
dFs/q / dCL
2.6
2.4
2.2
2.0
1.8
1.6
1.4
1.2
1.0
.8
.6
.4
.2
0
16
18
20
22
24
26
28
30
32
34
36
38
40
42
44
46
48
% M.A.C.
CL= 2.0
CL= 1.8
CL= 1.6
CL= 1.4

FIG. 37

FLIGHT TEST DATA
APPROACH CONFIGURATION
POWER-OFF

STICK FORCE vs. AIRSPEED

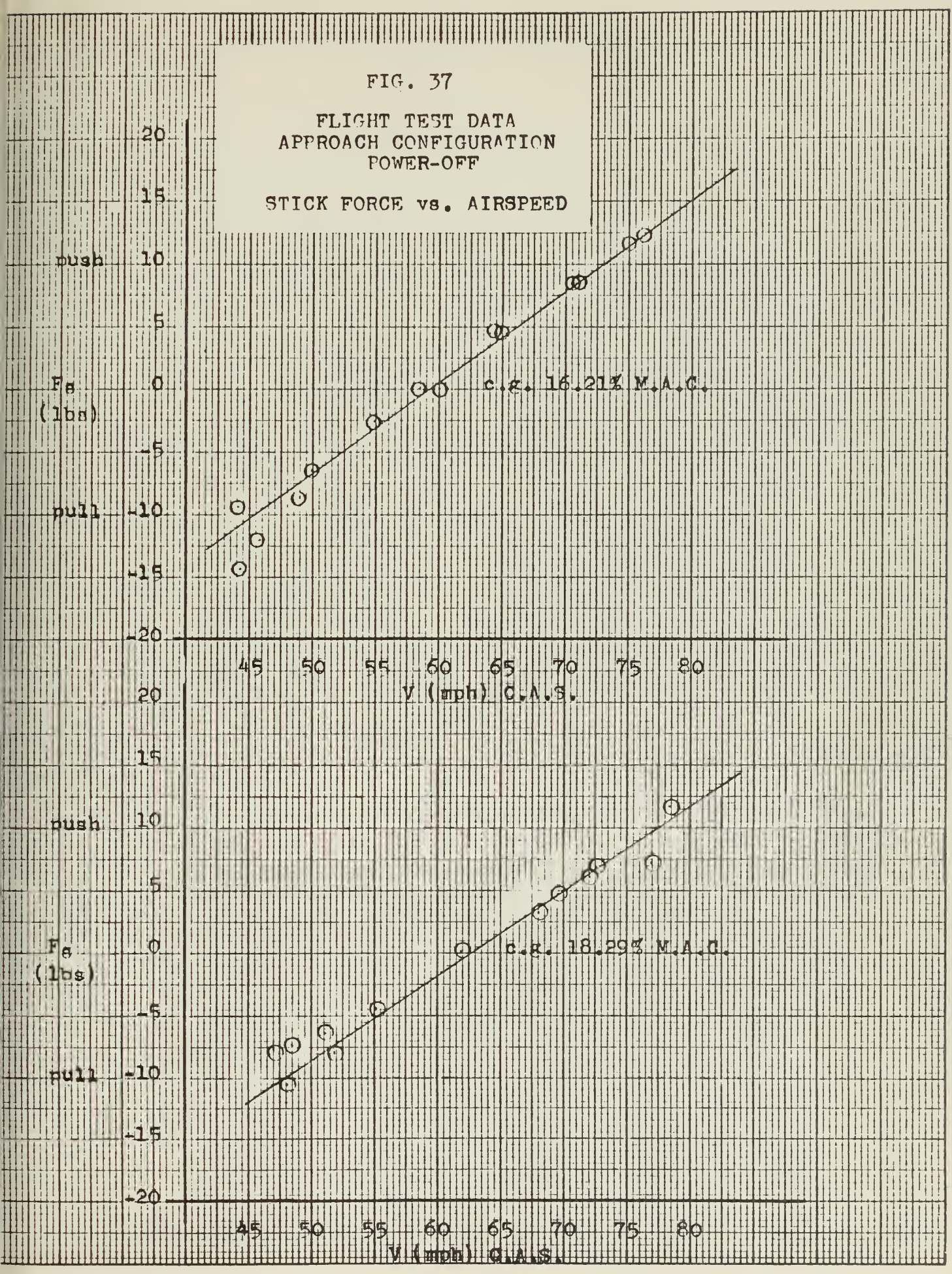

FIG. 37

FLIGHT TEST DATA
APPROACH CONFIGURATION
POWER-OFF

STICK FORCE vs. AIRSPEED

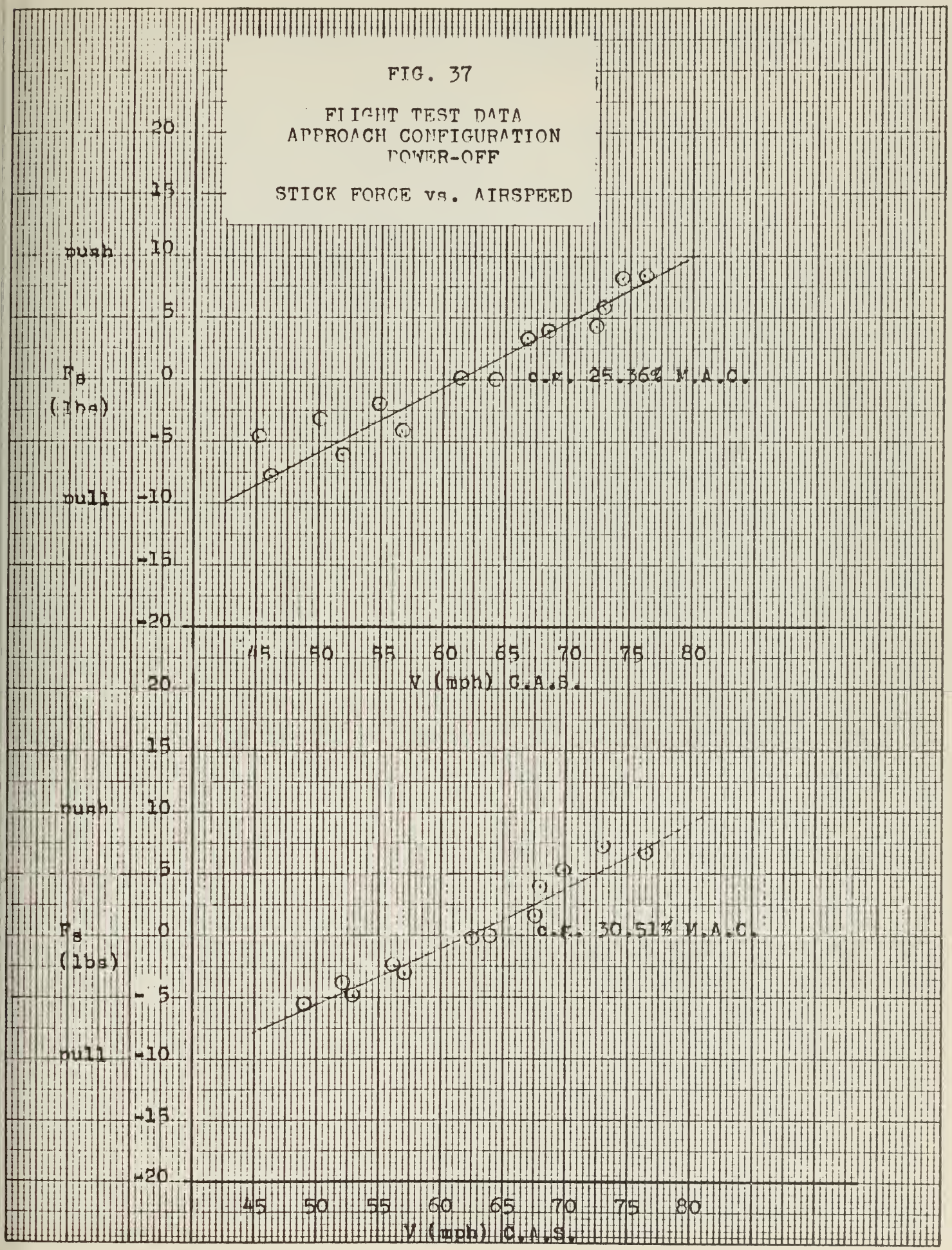

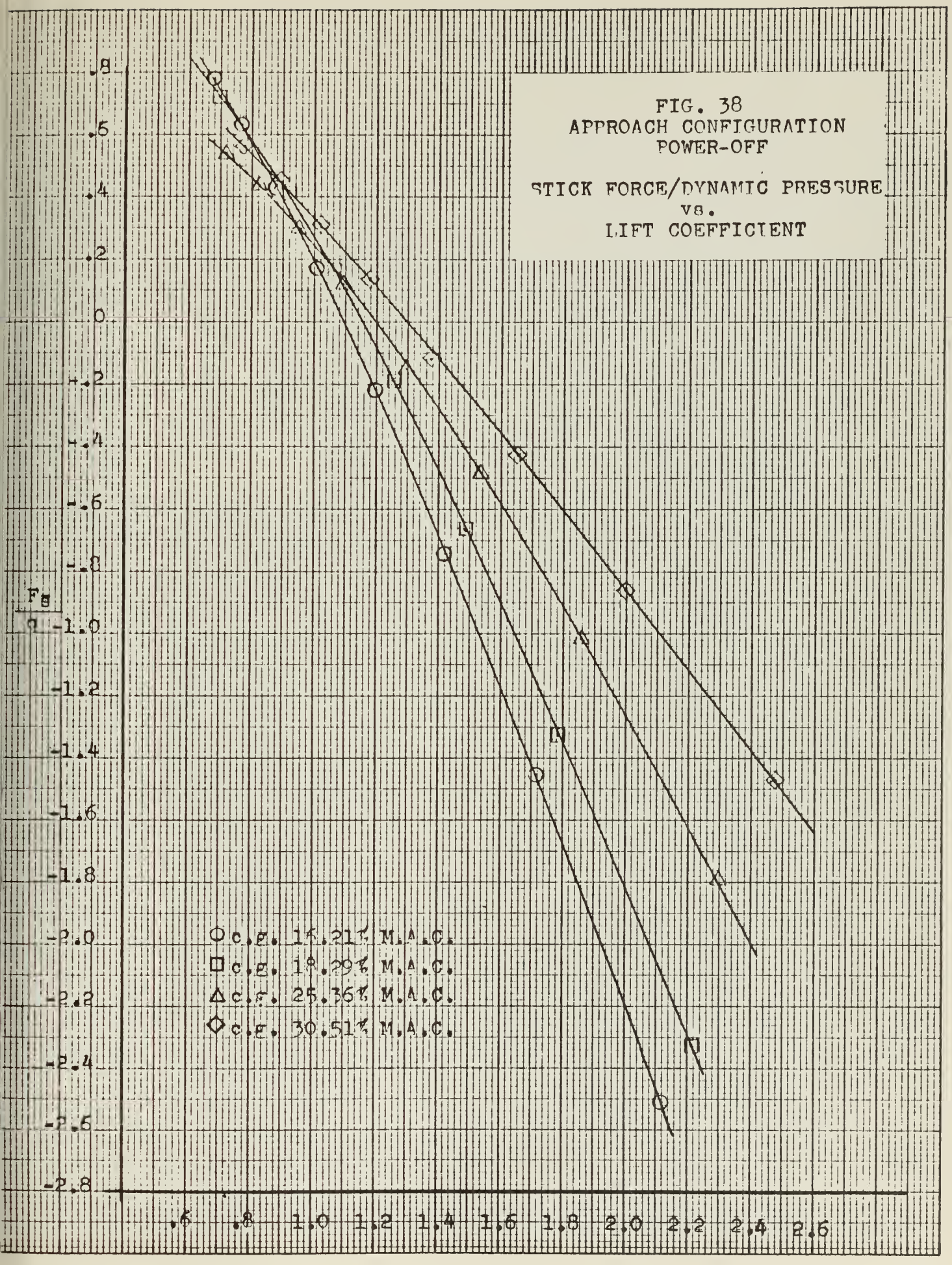
FIG. 38
APPROACH CONFIGURATION
POWER-OFF
STICK FORCE/DYNAMIC PRESSURE
vs.
LIFT COEFFICIENT
Fe/q
.8
.6
.4
.2
0
-.2
-.4
-.6
-.8
-1.0
-1.2
-1.4
-1.6
-1.8
-2.0
-2.2
-2.4
-2.6
-2.8
.6
.8
1.0
1.2
1.4
1.6
1.8
2.0
2.2
2.4
2.6
○ c.g. 14.21% M.A.C.
□ c.g. 18.29% M.A.C.
△ c.g. 25.36% M.A.C.
◇ c.g. 30.51% M.A.C.

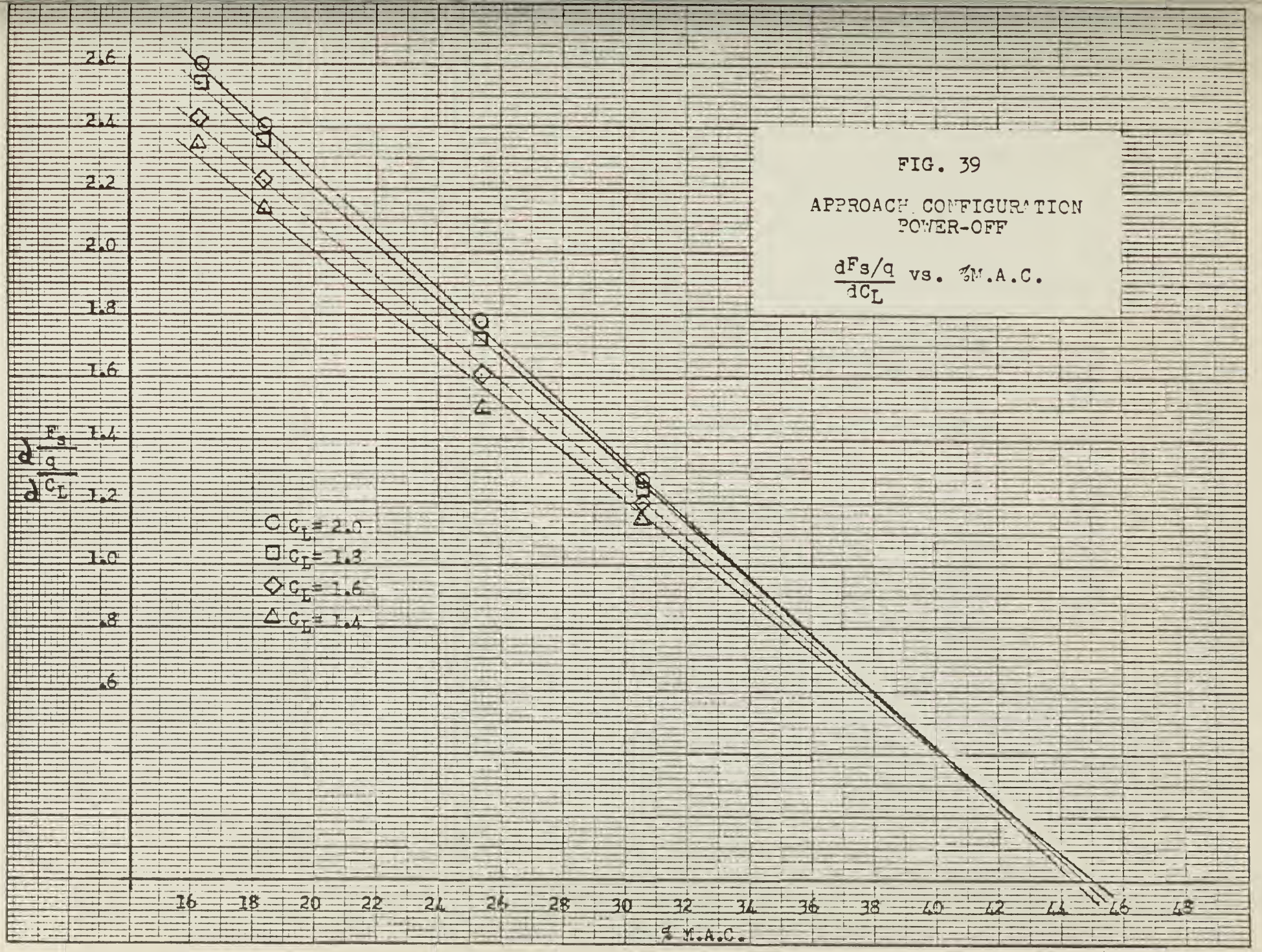
FIG. 39
APPROACH CONFIGURATION
POWER-OFF
$\frac{dFs/q}{dC_L}$ vs. %M.A.C.
$\frac{d\frac{F_s}{q}}{dC_L}$
2.6
2.4
2.2
2.0
1.8
1.6
1.4
1.2
1.0
.8
.6
○ C_L = 2.0
□ C_L = 1.8
◇ C_L = 1.6
△ C_L = 1.4
16 18 20 22 24 26 28 30 32 34 36 38 40 42 44 46 48
% M.A.C.

FIG. 40

NEUTRAL POINT SUMMARY
APPROACH CONFIGURATION

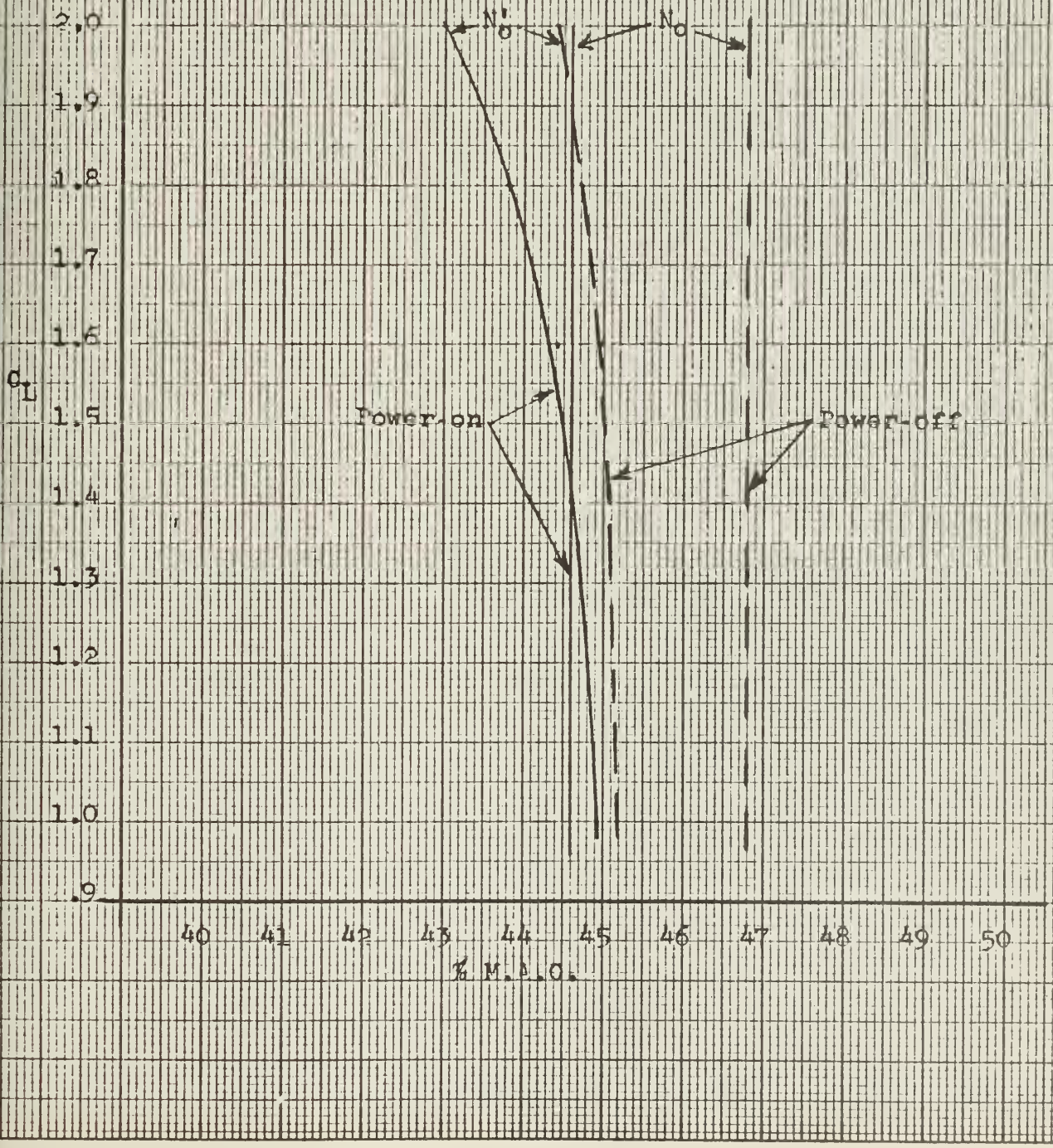

FIG. 41
FLIGHT TEST DATA
CRUISE CONFIGURATION
POWER-ON
ELEVATOR ANGLE
vs.
NORMAL ACCELERATION

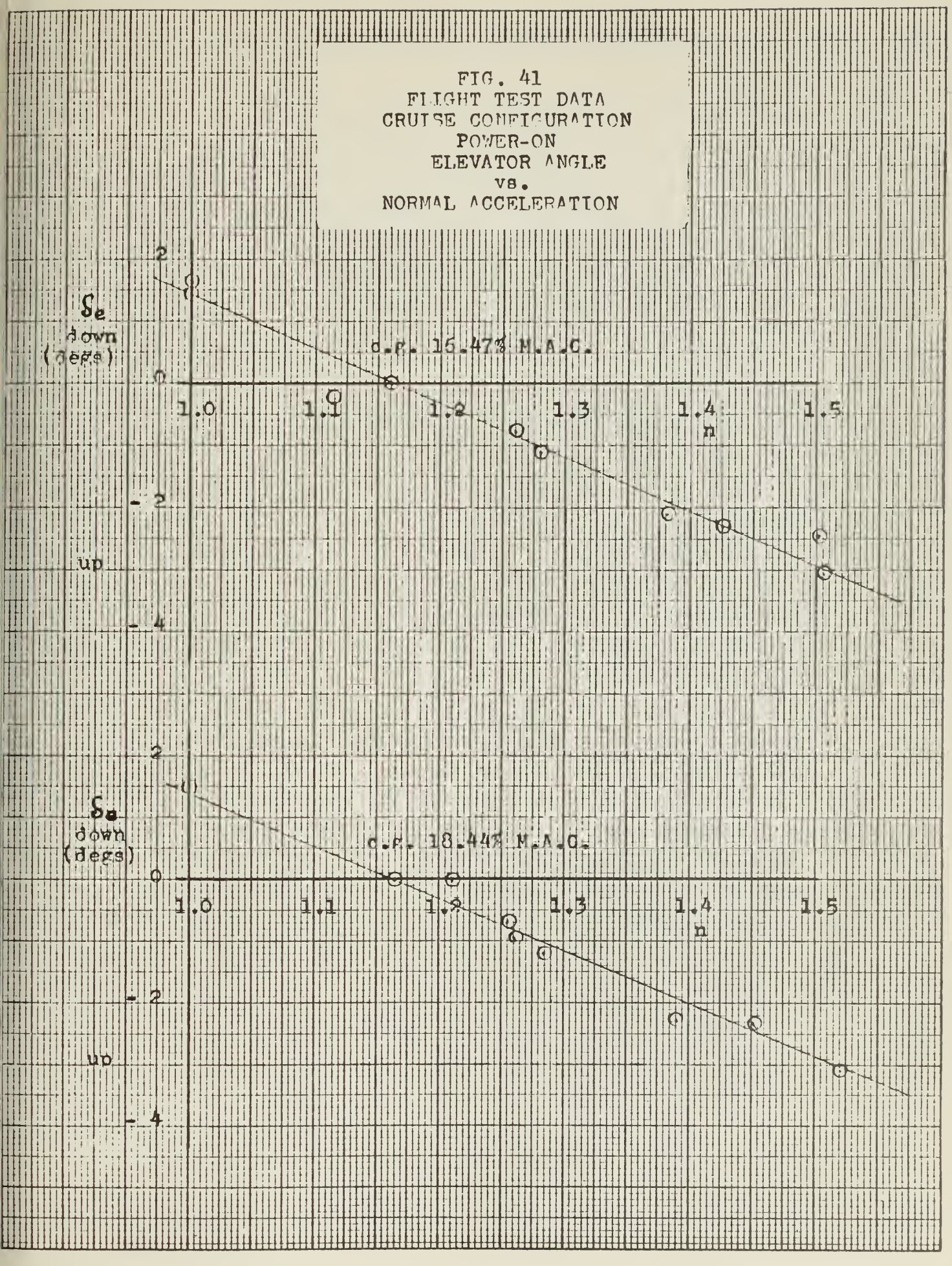

FIG. 41
FLIGHT TEST DATA
CRUISE CONFIGURATION
POWER-ON
ELEVATOR ANGLE
vs.
NORMAL ACCELERATION

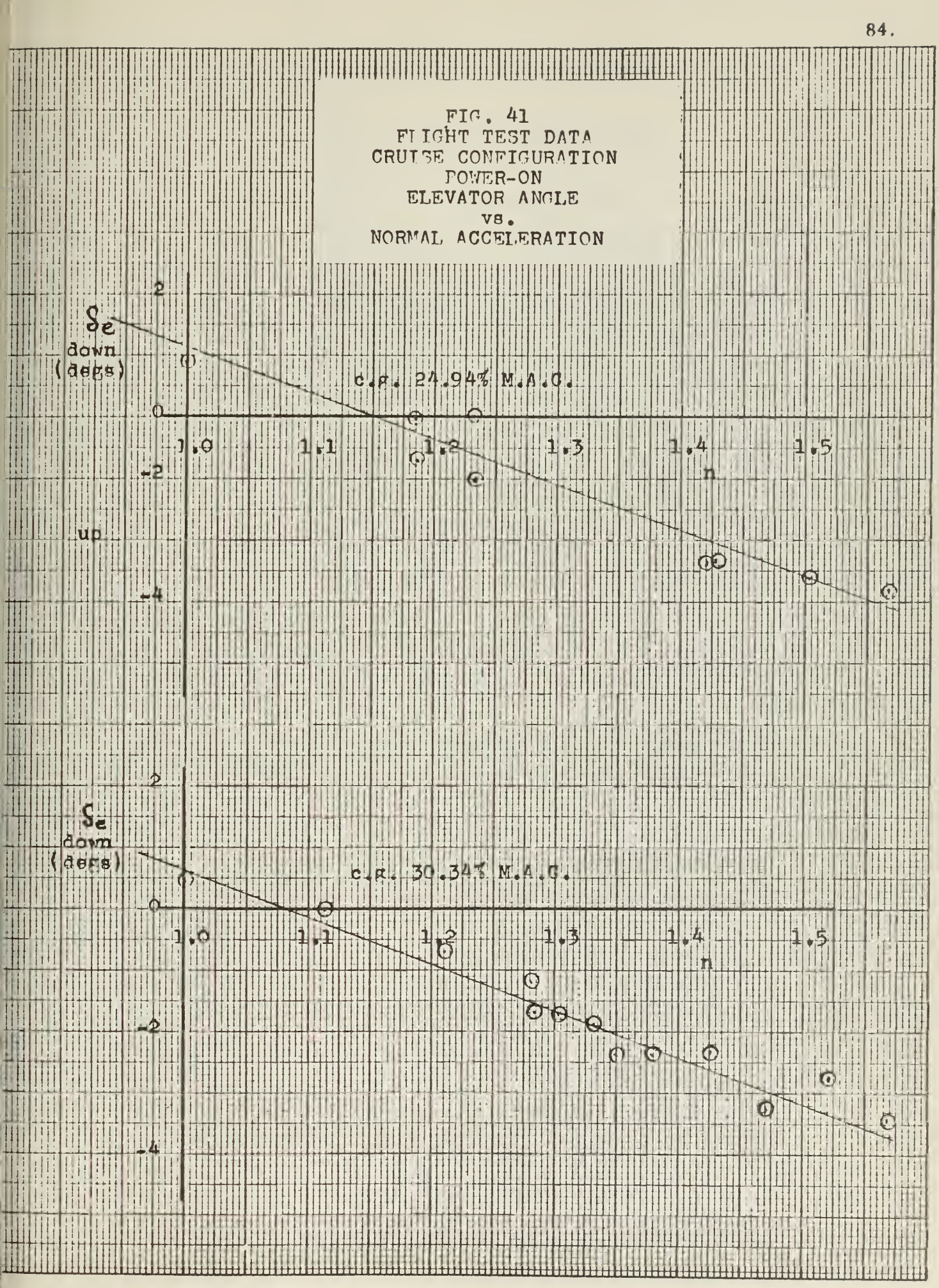

FIG. 42
CRUISE CONFIGURATION
POWER-ON

ELEVATOR ANGLE
vs.
NORMAL LIFT COEFFICIENT

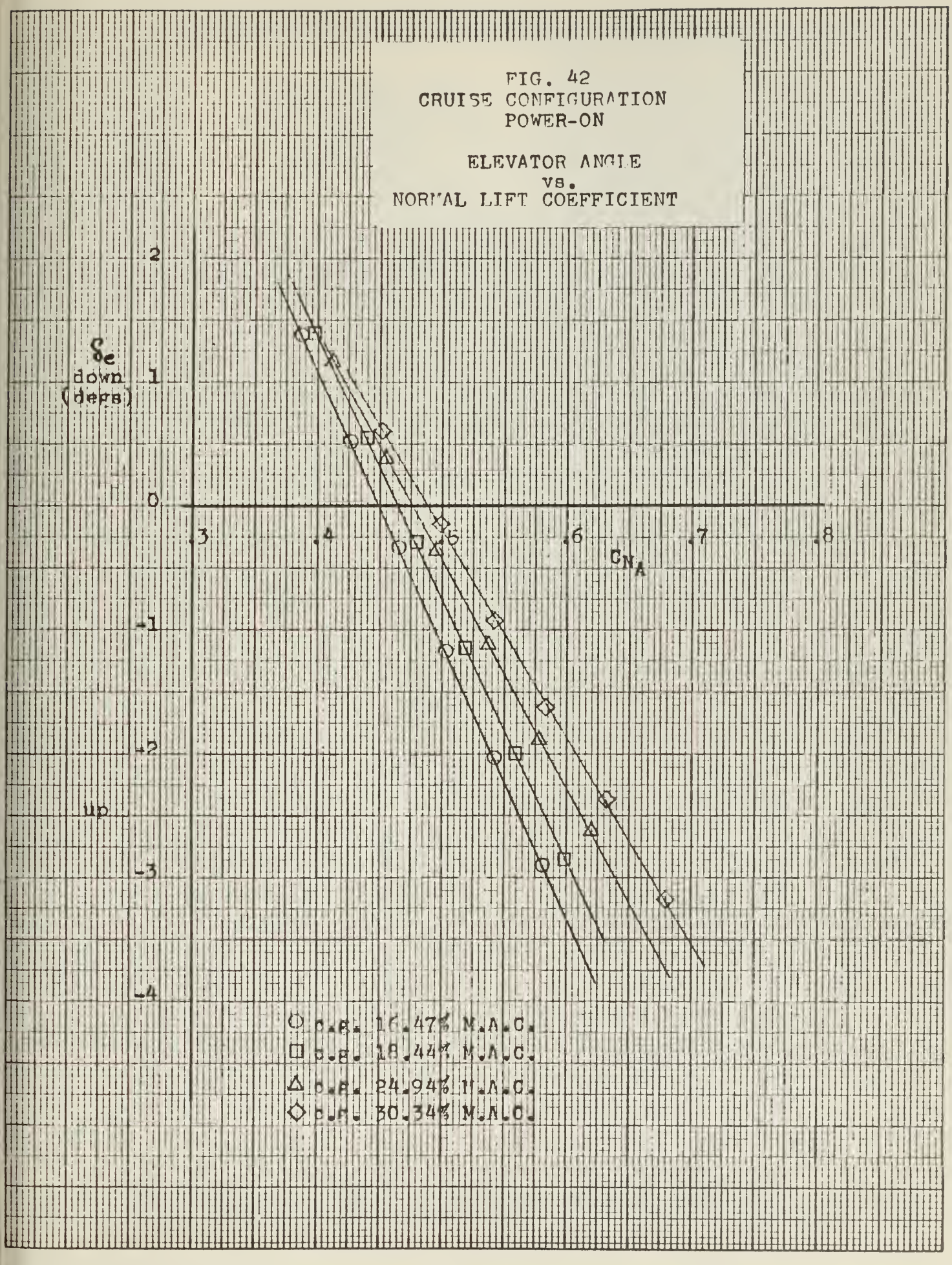

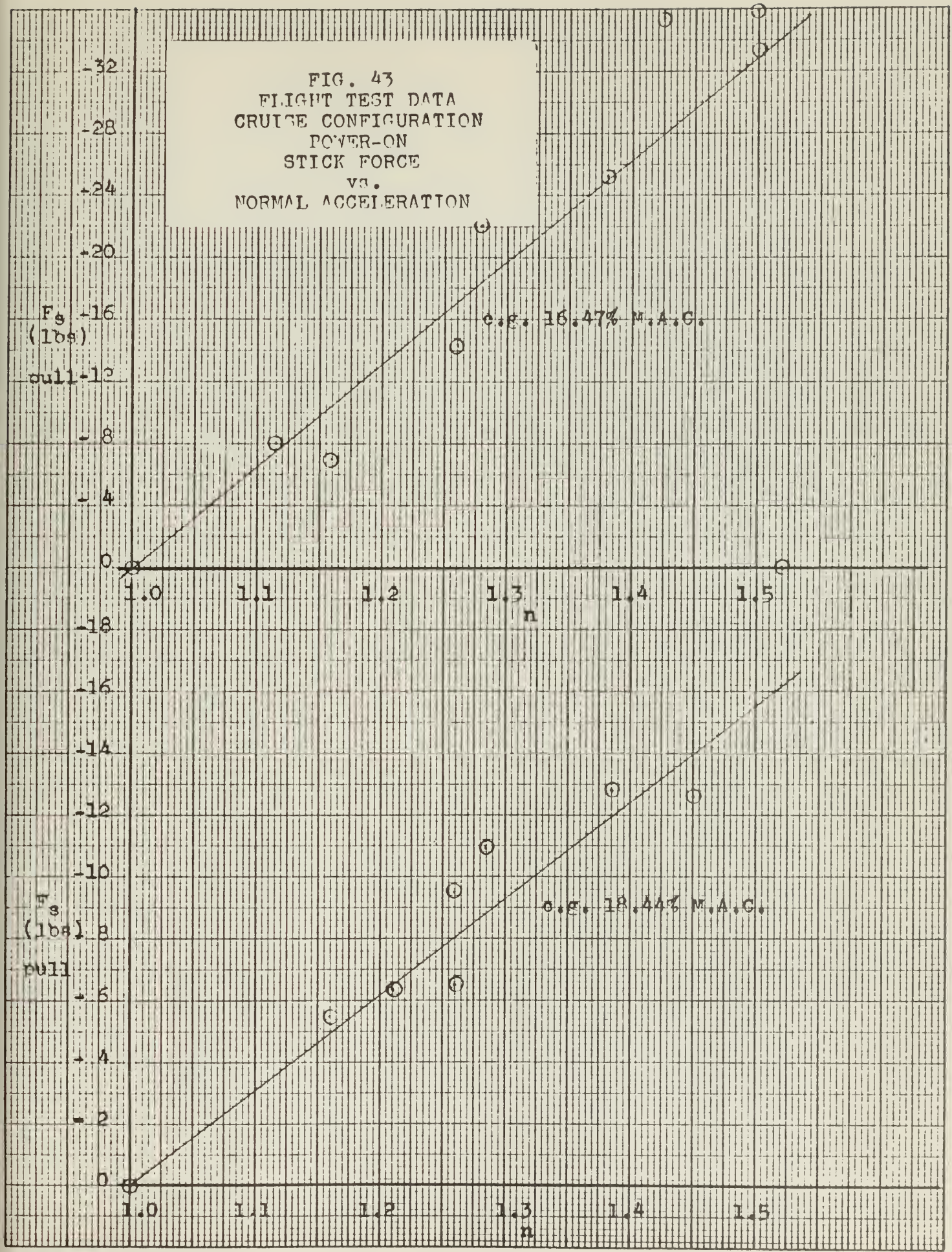
FIG. 43
FLIGHT TEST DATA
CRUISE CONFIGURATION
POWER-ON
STICK FORCE
VS.
NORMAL ACCELERATION
Fs (lbs) pull
-32
-28
-24
-20
-16
-12
- 8
- 4
0
1.0
1.1
1.2
1.3
1.4
1.5
n
c.g. 16.47% M.A.C.
Fs (lbs) pull
-18
-16
-14
-12
-10
- 8
- 6
- 4
- 2
0
1.0
1.1
1.2
1.3
1.4
1.5
n
c.g. 18.44% M.A.C.

FIG. 43
FLIGHT TEST DATA
CRUISE CONFIGURATION
POWER-ON
STICK FORCE
vs.
NORMAL ACCELERATION

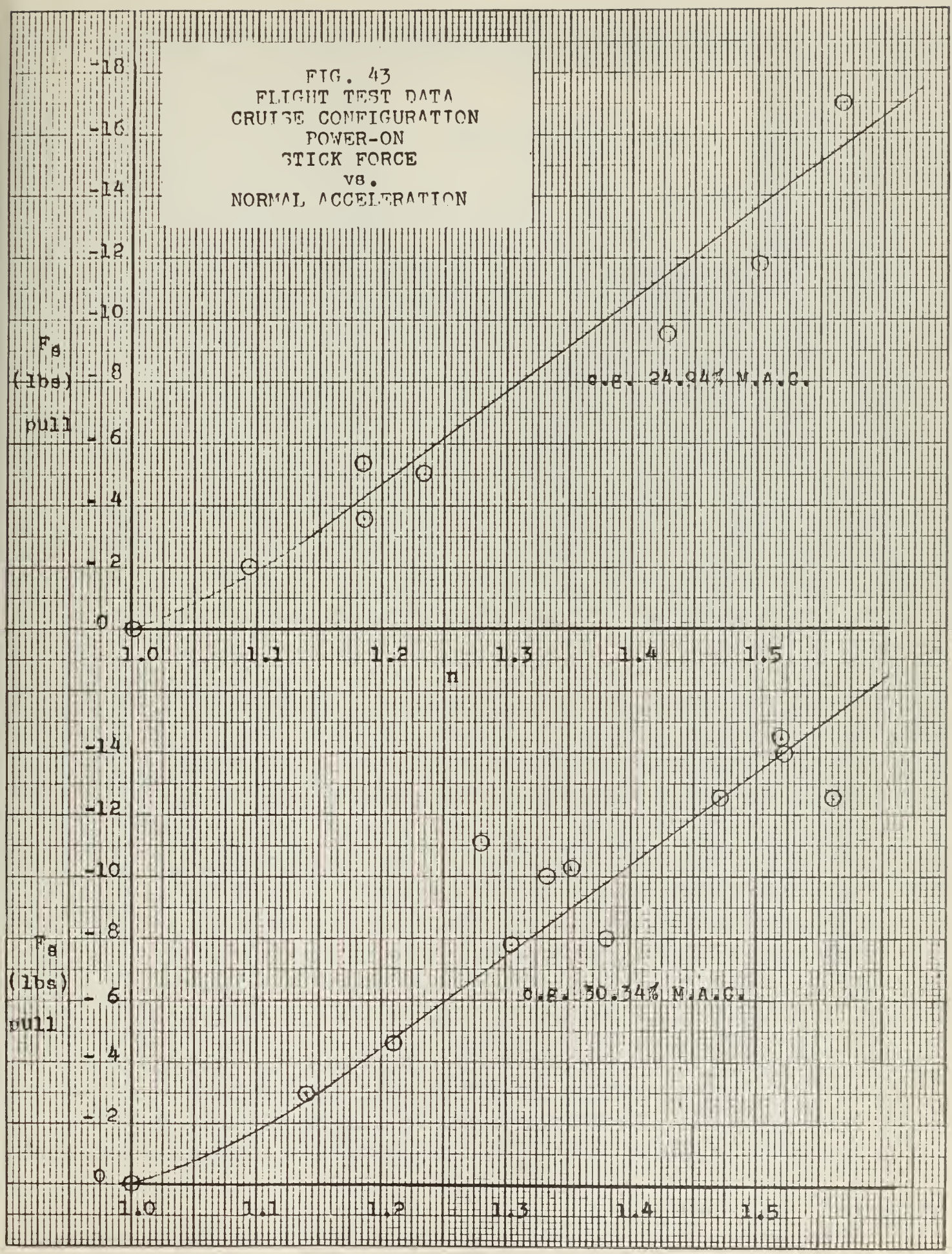

FIG. 44
CRUISE CONFIGURATION
POWER-ON

STICK FORCE/DYNAMIC PRESSURE
vs.
LIFT COEFFICIENT

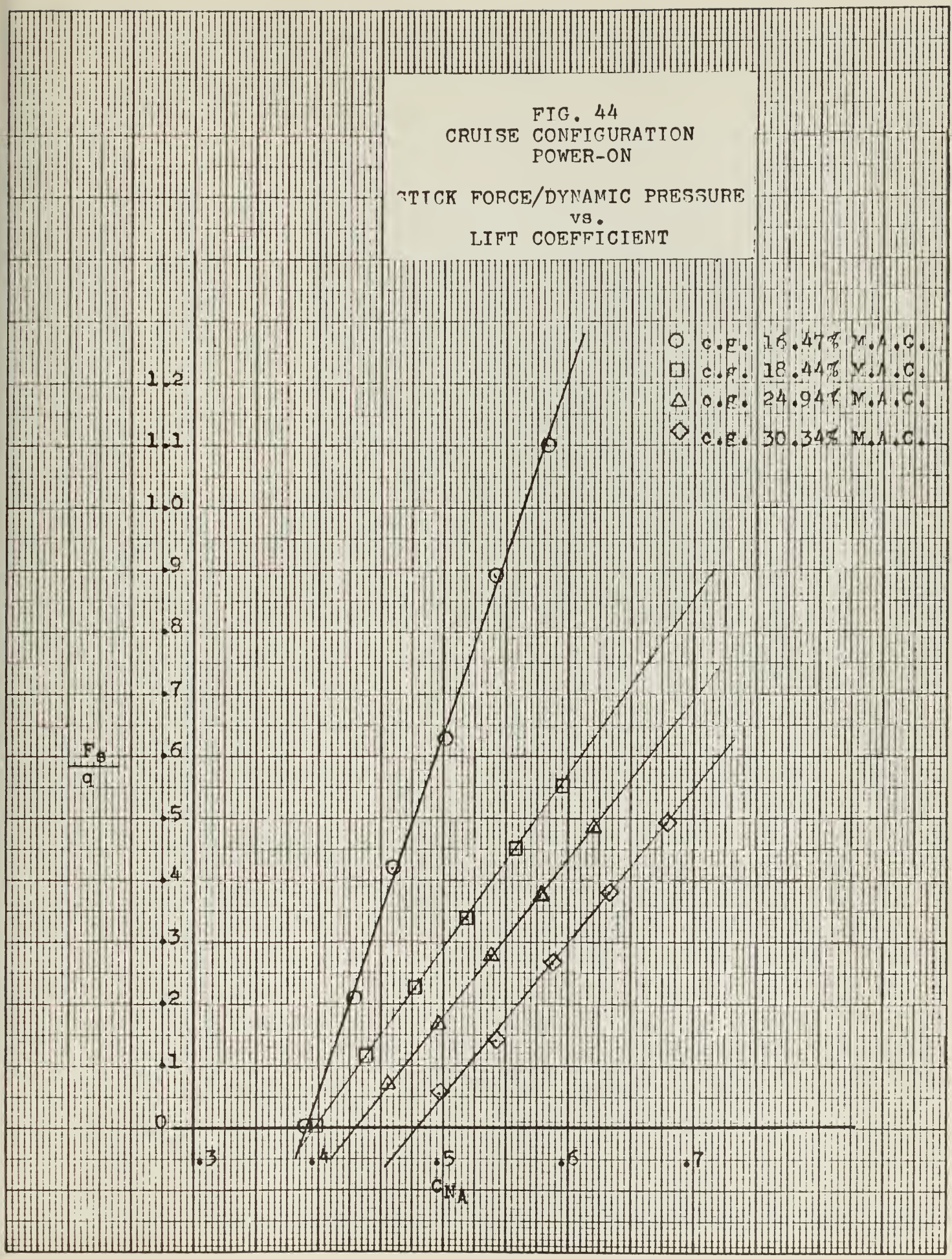

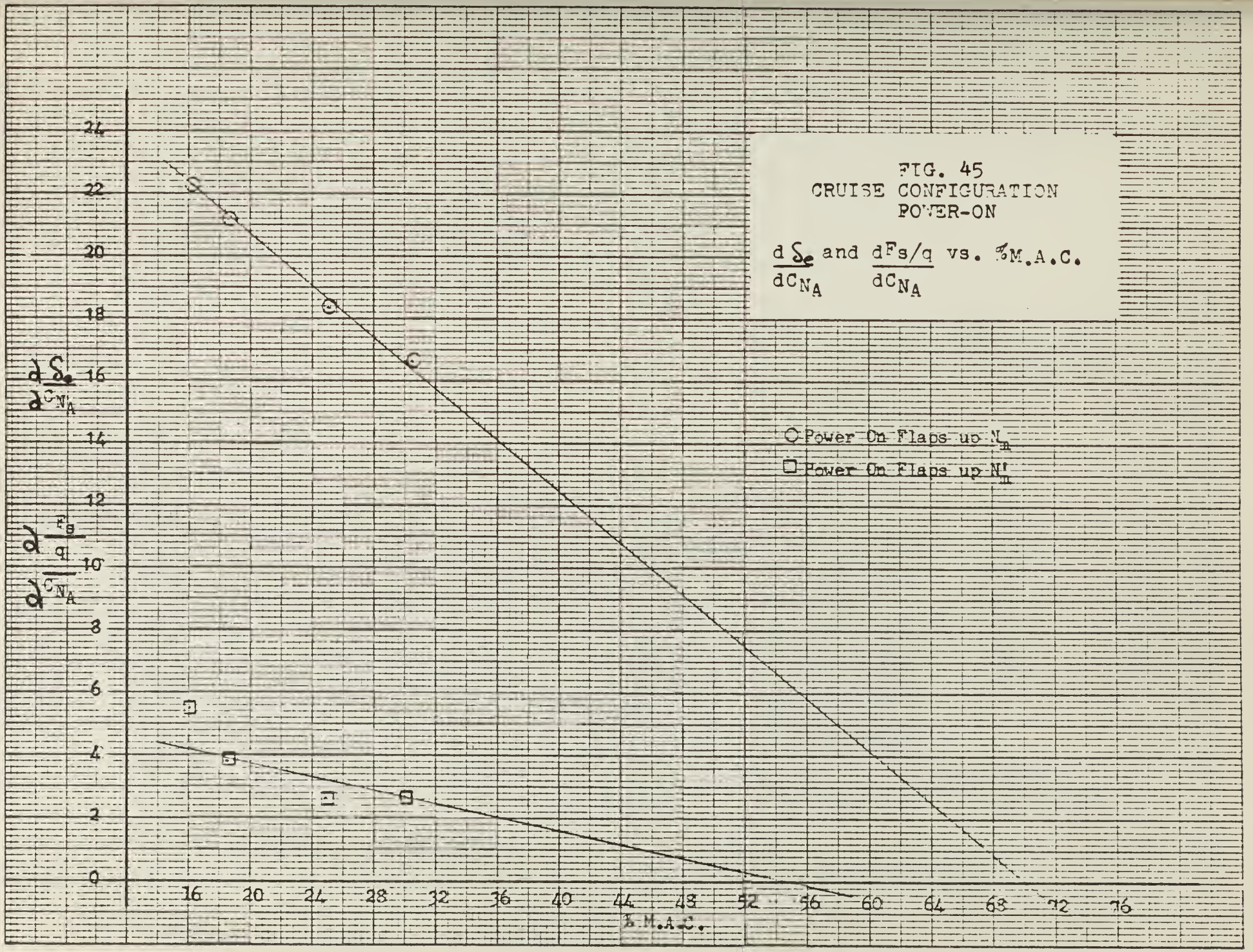
FIG. 45
CRUISE CONFIGURATION
POWER-ON
$\frac{d\delta_e}{dC_{N_A}}$ and $\frac{dF_s/q}{dC_{N_A}}$ vs. %M.A.C.
Power On Flaps up N_{II}
Power On Flaps up N'_{II}
$\frac{d\delta_e}{dC_{N_A}}$
$\frac{d\frac{F_s}{q}}{dC_{N_A}}$
24
22
20
18
16
14
12
10
8
6
4
2
0
16
20
24
28
32
36
40
44
48
52
56
60
64
68
72
76
% M.A.C.

FIG. 46

MANEUVER POINT SUMMARY
CRUISE CONFIGURATION

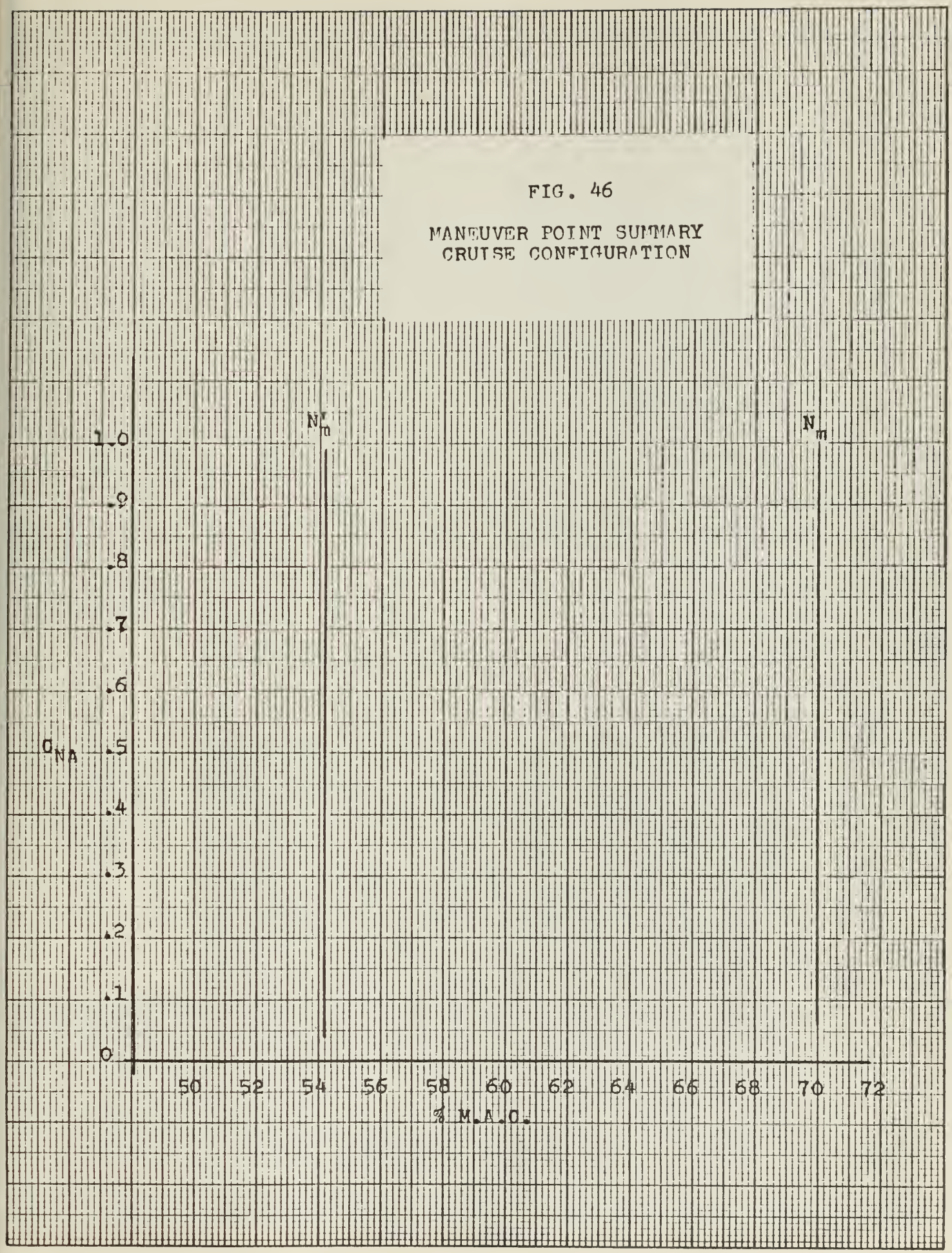

FIG. 47
FLIGHT TEST DATA
ROLL RATE
vs.
TOTAL AILERON ANGLE

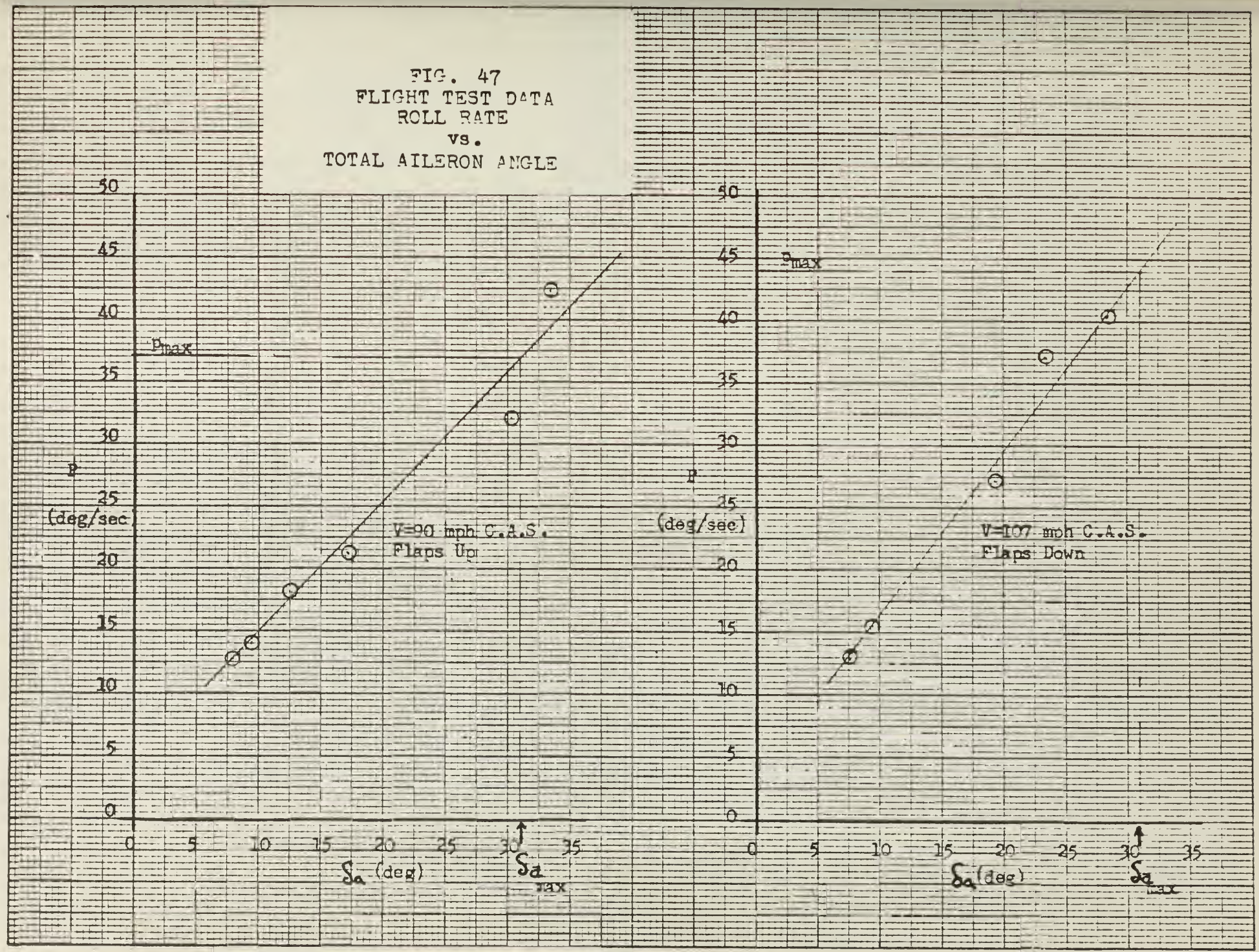

FIG. 47
FLIGHT TEST DATA
ROLL RATE
vs.
TOTAL AILERON ANGLE

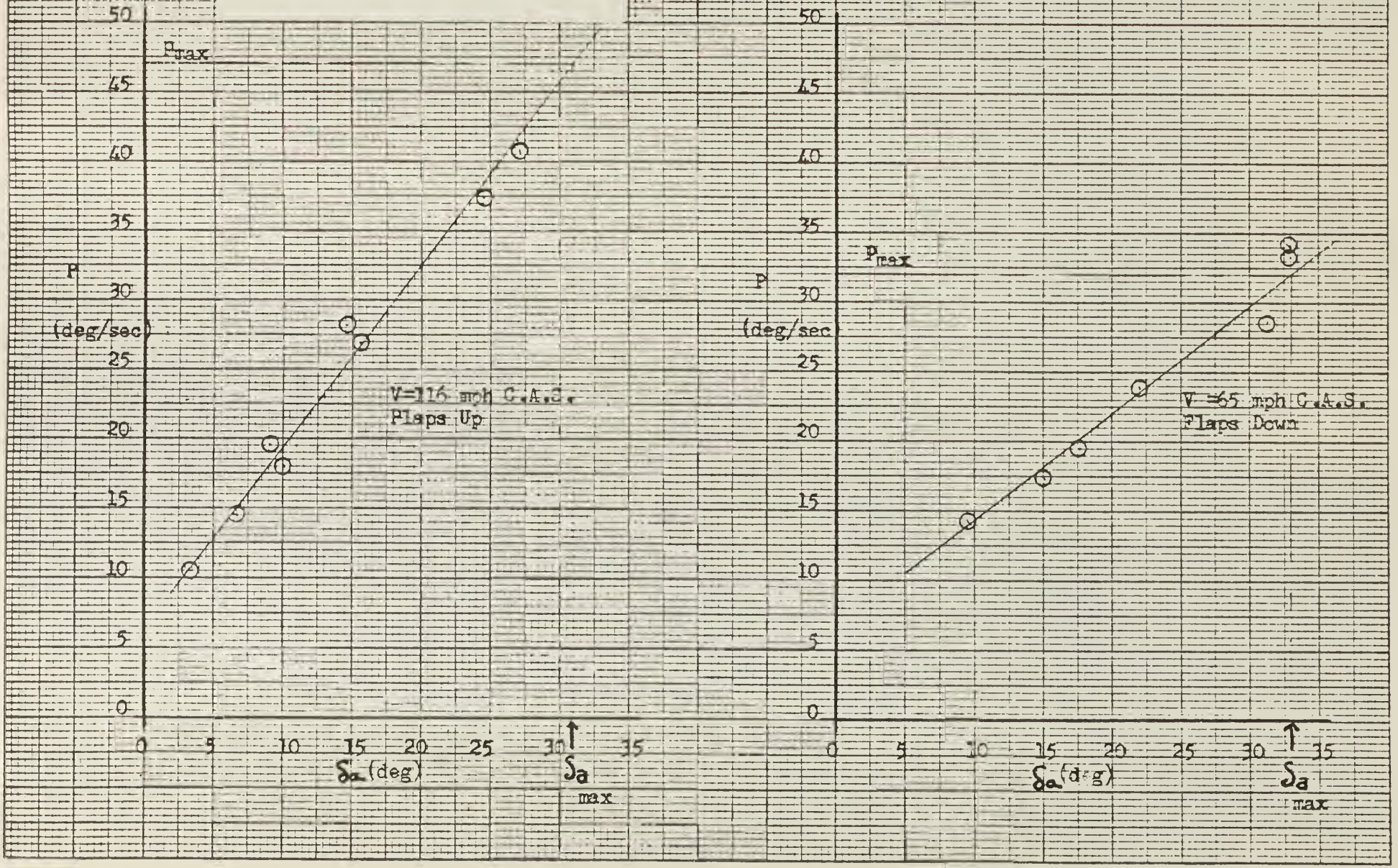

FIG. 48

SUMMARY OF
LATERAL PERFORMANCE

p, $\frac{pb}{2V}$, and δ_a vs. AIRSPEED

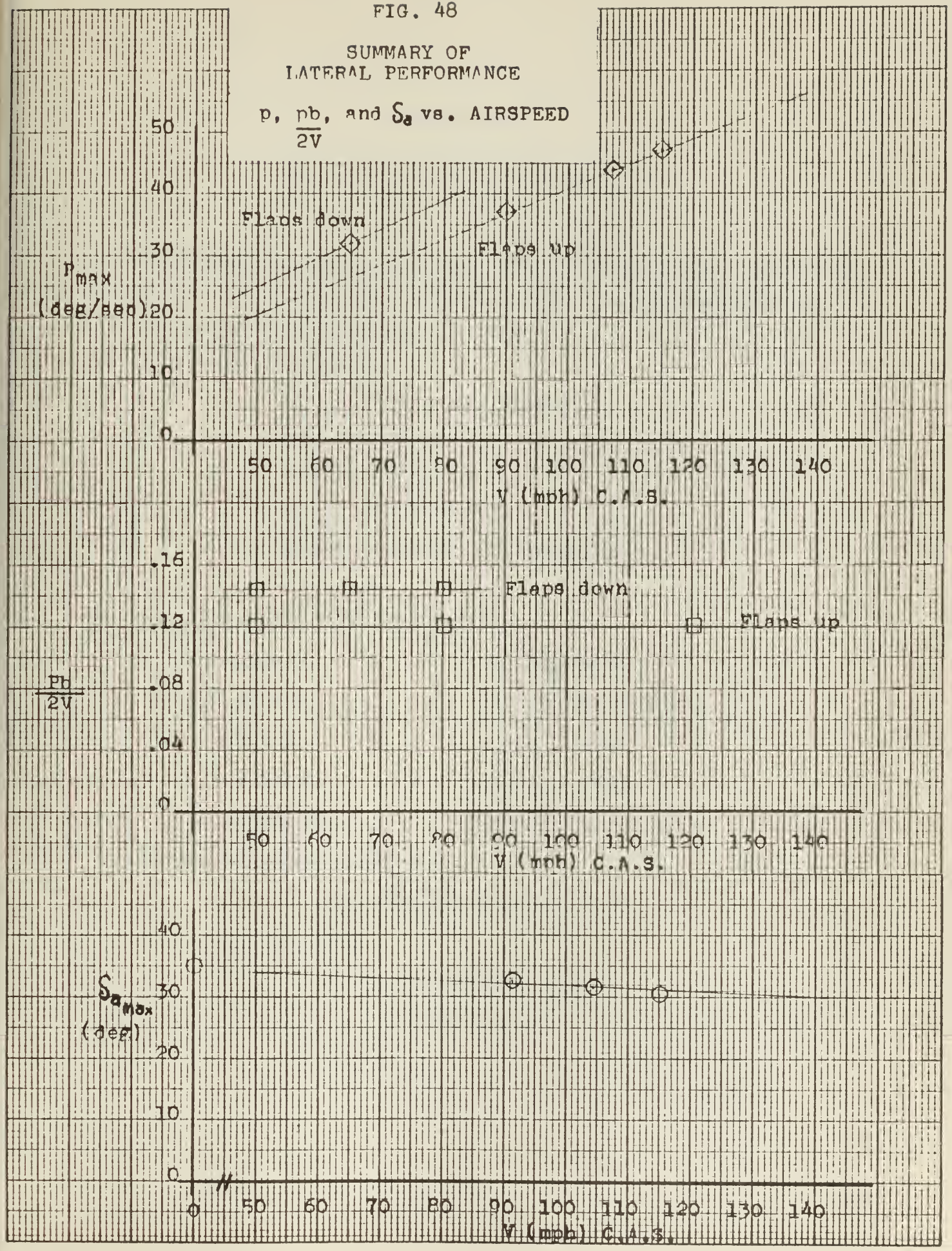

APPENDIX A

Theoretical Analysis Calculations

I. The following calculations are based upon the "Heli-Porter's" specifications (Table I), assumed values taken from Fig. 3, actual flight test conditions, and analytical procedures found in Ref. 7.

A. Flight Test Conditions:

$V_{(CAS)}$ = 105 mph = 154 fps.

Alt. = 8,000 ft.

Weight = 3593 lbs.

$x_{c.g.}$ = 25.2% M.A.C.

Power condition = 60% rated power

n = 1.5 g

B. Assumed values taken from Fig. 3:

z_a = 2.00 ft.

L_f = 30.0 ft.

h = 0.5 ft.

l_p = 9.222 ft.

x_1 = 7.652 ft.

x_2 = 9.222 ft.

$l_t = 21.208 - 6.234\, x_{c.g.}$

$c_b / c_f = .250$

$c_a / c_w = .200$

elevator gap = $.001 c_t$

C. Assumed Theoretical Values:

e, Oswald efficiency factor, = .75

$\eta_p = 85\%$

$\eta_t = 85\,(1 + 8T_c / \pi)$ Ref. 9 mod.

$C_{ma.c.} = -0.060$ Ref. 11

$\beta = 20^{o}$ @ .75R

II. The stick-fixed neutral point, N_o, are equal to:

$$N_o = x_{c.g.} - \left.\frac{dC_m}{dC_L}\right|_{Fixed}$$

A. Stick-fixed Neutral Point, Power-on.

$$N_{o\ \text{Power on}} = x_{c.g.} - \frac{x_a}{c_w} - C_{L_w}\left[\frac{2}{\pi e AR_w} - \frac{.035}{a_{w_o}}\right]\frac{z_a}{c_w} - \frac{dC_{m_{a.c.}}}{dC_L}$$

$$- \frac{K_f w_f L_f}{S_w c_w a_w} - \frac{dT_c}{dC_L}\frac{2 D_p{}^2 h}{S_w c_w} - \frac{dC_{N_p}}{dC_L}\frac{\ell_p S_p}{S_w c_w}$$

$$+ \frac{a_t}{a_w}\bar{V}\left[1 - \frac{d\epsilon}{d\alpha} - \frac{d\epsilon_p}{d\alpha}\right]\eta_t + C_{L_t}\bar{V}\frac{d\eta_t}{dC_L}$$

B. Stick-fixed Neutral Point, Power-off.

$$N_{o\ \text{Power off}} = x_{c.g.} - \frac{x_a}{c_w} - C_{L_w}\left[\frac{2}{\pi e AR_w} - \frac{.035}{a_{w_o}}\right]\frac{z_a}{c_w} - \frac{dC_{m_{a.c.}}}{dC_L}$$

$$- \frac{K_f w_f L_f}{S_w c_w a_w} - \left(\frac{dC_N}{d\alpha}\right)_{PT_c=0}\frac{d\beta}{d\alpha}\frac{\ell_p S_p}{S_w c_w a_w} - \frac{a_t \bar{V} \eta_t}{a_w .07}\left(\frac{dC_N}{d\alpha}\right)_{PT_c=0}\frac{d\beta}{d\alpha}$$

$$+ \frac{a_t}{a_w}\bar{V}\left[1 - \frac{d\epsilon}{d\alpha}\right]\eta_t$$

1. The wing lift coefficient was determined from

$$C_{L_w} = \frac{2W}{\rho_o V_{(CAS)}{}^2 S_w} = \frac{2 \times 3593}{.002378 \times (154)^2 \times 306.7}$$

$$C_{L_w} = .417$$

The slope of the wing and tail lift curves were calculated from

$$a_w = \frac{a_o}{1 + \frac{r\, a_o}{\pi\, AR_w}} = \frac{2\pi}{1 + \frac{1 \times 2\pi}{\pi \times 7.96}}$$

$$a_w = 5.022 \text{ per rad.} = .0876 \text{ per deg.}$$

$$a_t = \frac{2\pi}{1 + \frac{1 \times 2\pi}{\pi \times 4.285}}$$

$$a_t = 4.283 \text{ per rad.} = .07475 \text{ per deg.}$$

where a_o is the two-dimensional lift curve slope and r is the end plate correction which is equal to 1.0 for an airfoil without end plates. Figs. 5-6 Ref. 7.

2. The tail volume was determined from

$$\overline{V} = \frac{S_t\, \ell_t}{S_w\, c_w} = \frac{65.343 \times (21.208 - 6.234 \times .252)}{306.7 \times 6.229}$$

$$\overline{V} = .672$$

3. The engine's thrust coefficient, T_c, was determined from

$$T_c = \frac{550\ \text{Bhp}\ \eta_p\ C_{L_w}^{3/2}\ \rho^{1/2}}{(2\ W/S)^{3/2}\ (D_p)^{1/2}}$$

$$= \frac{550 \times (.60 \times 325) \times .85 \times (.417)^{3/2} \times (.001869)^{1/2}}{\left(\frac{2 \times 3593}{306.7}\right)^{3/2} \times (7.75)^{1/2}}$$

$$T_c = .156$$

where the propeller efficiency, η_p, was assumed equal to .85 and the Bhp was taken as 60% of rated power at 3,000 rpm.

The variation of T_c with C_L is

$$\frac{dT_c}{dC_L} = \frac{3}{2} \frac{Bhp\, \eta_p\, 550\, C_L^{1/2}\, \rho^{1/2}}{(2\, W/S)^{3/2}\, (D_p)^{1/2}}$$

$$= \frac{3 \times (.60 \times 3.25) \times .85 \times 550 \times (.417)^{1/2} \times (.001869)^{1/2}}{2\, (2 \times \frac{3593}{306.7})^{3/2}\, (7.75)^{1/2}}$$

$$\frac{dT_c}{dC_L} = .559$$

4. The rate of change of downwash with respect to α was determined from

$$\frac{d\varepsilon}{d\alpha} = \frac{114.6\, a_w}{\pi\, AR_w} = \frac{114.6 \times .0876}{\pi \times 7.96}$$

$$\frac{d\varepsilon}{d\alpha} = .401 \text{ per rad.}$$

The wing upwash parameter, $d\beta/d\alpha = 1.143$ was determined from Fig. 5.15 of Ref. 7 for $x_1/c_w = 1.23$.

The rate of change of downwash due to the propeller, $d\varepsilon_p/d\alpha$, is equal to

$$\frac{d\varepsilon_p}{d\alpha} = A + B' C_{Y'\psi_o}$$

where $A = .08$ and $B' = .26$ for $T_c = .156$ from Fig. 12 of Ref. 12. $C_{Y'\psi_o} = .14$ for an assumed value of $\beta = 20^o$ @ .75 R and a 3-bladed propeller from Fig. 2 of Ref. 12.

$$\frac{d\varepsilon_p}{d\alpha} = .08 + .26 \times .14$$

$$\frac{d\varepsilon_p}{d\alpha} = .1164$$

5. The power effect derivative, dC_{N_p}/dC_L, was determined from

$$\frac{dC_{N_p}}{dC_L} = \frac{dC_N}{d\alpha}\bigg|_p \frac{d\beta}{\frac{d\alpha}{a_w}} = .224 \times \frac{1.143}{5.022}$$

$$\frac{dC_{N_p}}{dC_L} = .0510$$

where $dC_N/d\alpha\ _p = f C_{Y'} \psi_o$. From Fig. 1 of Ref. 12 $f = 1.6$ for $T_c = .156$. Therefore, $dC_N/d\alpha\ _p = .224$.

6. The tail efficiency, η_t, was determined from the following relationships and assumptions:

$$\eta_t = .85 \left[1 + \frac{8T_c}{\pi}\right]$$

$$\eta_t = .85 \text{ for } T_c = 0$$

$$= 1.185 \text{ for } T_c = .156$$

The tail efficiency of $\eta_t = 1.185$ in the power-on configuration was felt to be slightly high and was modified as follows. A new tail efficiency, η_t^*, was assumed equal to

$$\eta_t^* = \eta_{t_{T_c=0}} + \left[\eta_{t_{T_c=.156}} - \eta_{t_{T_c=0}}\right] \frac{D_p}{b_t}$$

$$= .85 + [1.187 - .85] \frac{7.75}{16.733}$$

$$\eta_t^* = 1.006 \text{ for } T_c = .156$$

Based upon the above modification a $\eta_t^* = 1.00$ for the power-on configuration was felt justified.

The variation of η_t^* with respect to C_L is equal to

$$\frac{d\eta_t^*}{dC_L} = \frac{d}{C_L}\left[\eta_{t_{T_c=0}} + (\eta_{t_{T_c=.156}} - \eta_{t_{T_c=0}})\frac{D_p}{b_t}\right]$$

$$= \frac{.85 \times 8}{\pi}\frac{dT_c}{dC_L}\frac{D_p}{b_t} = \frac{.85 \times 8.0 \times .559 \times 7.75}{\pi \times 16.733}$$

$$\frac{d\eta_t^*}{dC_L} = .5604$$

7. The hinge-moment parameters, C_{h_α} and C_{h_δ}, for the elevator where determined from

$$C_{h_\alpha} = C_{h_\alpha}\frac{a_t}{a_o}$$

$$C_{h_\delta} = C_{h_\delta} + \tau_e (C_{h_\alpha} - C_{h_\alpha})$$

where the two-dimensional hinge-moment coefficients were determined from Fig. 144 of Ref. 8 for a NACA 0009 blunt nosed airfoil section, .001c gap, and $c_b/c_f = .250$. The elevator effectiveness, τ_e, was determined from Fig. 5-33 of Ref. 7 for $S_e/S_t = .34$.

$$C_{h_\alpha} = -.0053 \times \frac{4.283}{2\pi}$$

$$C_{h_\alpha} = -.0036$$

$$C_{h_\delta} = -.0075 + .53(-.0036 + .0053)$$

$$C_{h_\delta} = -.0066$$

8. The tail lift coefficient, C_{L_t}, was calculated by equating the moment equation of the aircraft equal to zero (trimmed flight) and solving for C_{L_t}.

$$C_{m_{a.c.}} = C_L \frac{x_a}{c_w} + C_D \frac{z_a}{c_w} + C_{m_{a.c.}} + C_{L_w} \left(\frac{dC_m}{dC_L}\right)_{Fuse}$$

$$+ C_{L_w} \left(\frac{dC_m}{dC_L}\right)_{Power} - C_{L_t} \bar{V} \eta_t = 0$$

$$C_{L_t} = \frac{1}{\bar{V} \eta_t} \{C_{m_{a.c.}} + C_{L_w} [\frac{x_a}{c_w} + \frac{K_f w_f^2 L_f}{S_w c_w a_w} + \frac{dT_c}{dC_L} \frac{2 D_p^2 h}{S_w c_w}$$

$$+ \frac{dC_{N_p}}{dC_L} \frac{\ell_p S_p}{S_w c_w}]\}$$

$$= \frac{1}{.672 \times 1.0} \{ - 0.06 + .417 [.002 + \frac{.012 \times (5.25)^2 \times 30}{306.7 \times 6.229 \times .0876}$$

$$+ \frac{.559 \times 2 \times (7.75)^2 \times .5}{306.7 \times 6.229} + \frac{.051 \times 9.222 \times \pi \times (7.75)^2}{306.7 \times 6.229 \times 4}]\}$$

$$C_{L_t} = - .03318$$

where $K_f = .012$ was determined from Fig. 5.16 of Ref. 7 for $x_2 / L_f = .307$.

9. The stick-fixed neutral points are equal to

a. Stick-fixed Neutral Point, Power-on.

$$N_o \Big|_{\substack{Power \\ on}} = x_{c.g.} - \frac{x_a}{c} - C_{L_w} [\frac{2}{\pi e AR_w} - \frac{.035}{a_{w_o}}] \frac{z_a}{c_w} - \frac{dC_{m_{a.c.}}}{dC_L}$$

$$- \frac{K_f w_f^2 L_f}{S_w c_w a_w} - \frac{dT_c}{dC_L} \frac{2 D_p^2 h}{S_w c_w} - \frac{dC_{N_p}}{dC_L} \frac{\ell_p S_p}{S_w c_w}$$

$$+ \frac{a_t}{a_w} \bar{V} [1 - \frac{d\varepsilon}{d\alpha} - \frac{d\varepsilon_p}{d\alpha}] \eta_t + C_{L_t} \bar{V} \frac{d\eta_t}{dC_L}$$

$$N_o\Big|_{\substack{\text{Power}\\ \text{on}}} = .252 - .002 - .417\left[\frac{2}{\pi \times .75 \times 7.96} - \frac{.035}{.0876}\right]\frac{2.00}{6.229}$$

$$- \frac{.012 \times (5.25)^2 \times 30}{306.7 \times 6.229 \times .0876} - \frac{.559 \times 2 \times (7.75)^2 \times .5}{306.7 \times 6.229}$$

$$- \frac{.051 \times 9.222 \times \pi \times (7.75)^2}{306.7 \times 6.229 \times 4} + \frac{4.283 \times .672}{5.022}\left[1 - .401 - .1164\right]1.0$$

$$+ (-.03318) \times .672 \times .5604$$

$$N_{o\ \substack{\text{Power}\\ \text{on}}} = .4649$$

b. Stick-fixed Neutral Point, Power-off.

$$N_o\Big|_{\substack{\text{Power}\\ \text{off}}} = x_{c.g.} - \left(\frac{dC_m}{dC_L}\right)_{\text{Wing}} - \left(\frac{dC_m}{dC_L}\right)_{\text{Fue}} - \left(\frac{dC_N}{d\alpha}\right)_{PT_c=0}\frac{d\beta}{d\alpha}\frac{\ell_p S_p}{S_w c_w a_w}$$

$$- \frac{a_t \bar{V} \eta_t}{a_w .07}\left(\frac{dC_N}{d\alpha}\right)_{PT_c=0}\frac{d\beta}{d\alpha} + \frac{a_t}{a_w}\bar{V}\left[1 - \frac{d\epsilon}{d\alpha}\right]\eta_t$$

$$N_o\Big|_{\substack{\text{Power}\\ \text{off}}} = .252 + .03721 - .05924 - \frac{.00235 \times 1.143 \times 9.222 \times \pi \times (7.75)^2}{306.7 \times 6.229 \times .0876 \times 4}$$

$$- \frac{4.283 \times .672 \times .85 \times .00235 \times 1.143}{5.022 \times .07} + \frac{4.283 \times .672}{5.022}\left[1 - .401\right].85$$

$$N_{o\ \substack{\text{Power}\\ \text{off}}} = .4963$$

C. The stick-free neutral points, N_o', are equal to

$$N_o' = N_o - \frac{dC_m}{dC_L}_{\substack{\text{Free}\\ \text{elevator}}}$$

where

$$\left.\frac{dC_m}{dC_L}\right|_{\substack{\text{Free}\\ \text{elevator}}} = \frac{C_{h_\alpha}\, a_t\, \bar{V}\, \eta_t\, \tau}{C_{h_\delta}\, a_w}\left[1 - \frac{d\epsilon}{d\alpha}\right]$$

$$= \frac{-.0036 \times 4.283 \times .672 \times .53}{-.0066 \times 5.022}\left[1 - .401\right]\eta_t$$

$$\left.\frac{dC_m}{dC_L}\right|_{\substack{\text{Free}\\ \text{elevator}}} = .09924\,\eta_t$$

1. Stick-free Neutral Point, Power-on.

$$N_o'\Big|_{\substack{\text{Power}\\ \text{on}}} = .4649 - .09924 \times 1.0$$

$$N_o'\Big|_{\substack{\text{Power}\\ \text{on}}} = .3657$$

2. Stick-free Neutral Point, Power-off.

$$N_o'\Big|_{\substack{\text{Power}\\ \text{off}}} = .4963 - .09924 \times .85$$

$$N_o'\Big|_{\substack{\text{Power}\\ \text{off}}} = .4119$$

D. The stick-fixed maneuver point, N_m, is equal to

$$N_m = N_o\Big|_{\substack{\text{Power}\\ \text{on}}} + \left.\frac{dC_m}{dC_L}\right|_{\substack{\text{Fixed}\\ \text{man.}}}$$

where

$$\left.\frac{dC_m}{dC_L}\right|_{\substack{\text{Fixed}\\ \text{man.}}} = \frac{-63\, g\, \ell_t\, p\, C_{m_\delta}}{2\tau\, W/S_w}\left[1+\frac{1}{n^2}\right]$$

and

$$C_{m_\delta} = -a_t\, V\, \eta_t\, \tau = -.07475 \times .672 \times 1.0 \times .53$$

$$C_{m_\delta} = -.02662$$

1. Stick-fixed Maneuver Point.

$$N_m = .4649 + \left\{\frac{-63 \times 32.2 \times 19.637 \times .001867 \times (-.02662)}{2 \times .53 \times 3593/306.7}\left[1+\frac{1}{1.5^2}\right]\right\}$$

$$N_m = .6952$$

2. The Stick-free Maneuver Point, N_m', is equal to

$$N_m' = N_o'\Big|_{\substack{\text{Power}\\ \text{on}}} + \left.\frac{dC_m}{dC_L}\right|_{\substack{\text{Free}\\ \text{man.}}}$$

$$= N_o'\Big|_{\substack{\text{Power}\\ \text{on}}} + \frac{57.3\, g\, \ell_t\, \rho\, C_{m_\delta}}{2\tau\,(W/S)\, C_{h_\delta}}\left[C_{h_\alpha} - \frac{1.1\, C_{h_\delta}}{\tau}\right]\left[1+\frac{1}{n^2}\right]$$

$$N_m' = .3657 + \frac{57.3 \times 32.2 \times 19.637 \times .001869 \times (-.02662)}{2 \times (3593/306.7) \times .53 \times (-.0066)}\left[-.0036 + \frac{1.1 \times .0066}{.53}\right]$$

$$\left[1+\frac{1}{1.5^2}\right]$$

$$N_m' = .6814$$

E. The helix angle, $pb/2V$, was determined from

$$\frac{pb}{2V} = \left[\frac{C_{\ell_\delta}}{\tau}\right] \frac{\tau_a \, \delta_a{}^{o} \, K}{114.6 \, C_{\ell_p}}$$

where

$C_{l_p} = .550$ from Fig. 9-14 of Ref. 7 for $\lambda = 1.0$ and $AR_w = 7.96$

$\tau_a = .43$ from Fig. 9-15 of Ref. 7 for $c_a / c_w = .2$

$K = .85$ from Fig. 9-16 of Ref. 7 for $\delta_a = 31.5^{o}$

$\frac{C_{\ell_\delta}}{\tau} = .65$ from Fig. 9-3 of Ref. 7 for .75% $b/2$, AR_w 7.96, and $\lambda = 1.0$

$$\frac{pb}{2V} = \frac{.65 \times .43 \times 31.5 \times .85}{114.6 \times .55}$$

$$\frac{pb}{2V} = .1188$$

SUMMARY OF RESULTS

A. Calculated Parameters

N_o	power-on	.4649
	power-off	.4963
N_o'	power-on	.3657
	power-off	.4119
N_m	power-on	.6952
N_m'	power-on	.6814
$\frac{pb}{2V}$	power-on	.1188

B. Associated Values

$C_{L_w} = .417$ $\quad a_w = 5.022$ per rad

$C_{L_t} = -.03318$ $\quad a_t = 4.283$ per rad

$\bar{V} = .672$ $\quad W/S = 11.715$ lbs/sq. ft.

$\frac{d\epsilon}{d\alpha} = .401$ $\quad \frac{d\epsilon_p}{d\alpha} = .1164$ $\quad \frac{d\beta}{d\alpha} = 1.143$

$T_c = .156$ $\quad C_{m_\delta} = -.02678$

$C_{h_\alpha} = -.0036$ $\quad C_{h_\delta} = -.0066$

SUMMARY OF RESULTS

A. Calculated Parameters

N_o	power-on	.4649
	power-off	.4963
N_o'	power-on	.3657
	power-off	.4119
N_m	power-on	.6952
N_m'	power-on	.6814
$\frac{pb}{2V}$	power-on	.1188

B. Associated Values

$C_{L_w} = .417$ $\quad a_w = 5.022$ per rad

$C_{L_t} = -.03318$ $\quad a_t = 4.283$ per rad

$\bar{V} = .672$ $\quad W/S = 11.715$ lbs/sq. ft.

$\frac{d\epsilon}{d\alpha} = .401$ $\quad \frac{d\epsilon_p}{d\alpha} = .1164$ $\quad \frac{d\beta}{d\alpha} = 1.143$

$T_c = .156$ $\quad C_{m_\delta} = -.02678$

$C_{h_\alpha} = -.0036$ $\quad C_{h_\delta} = -.0066$